Padova, October 25, 2022

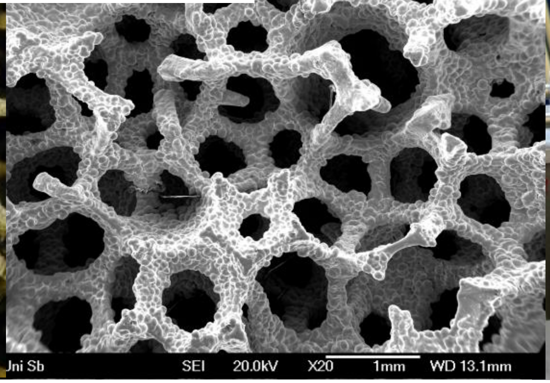

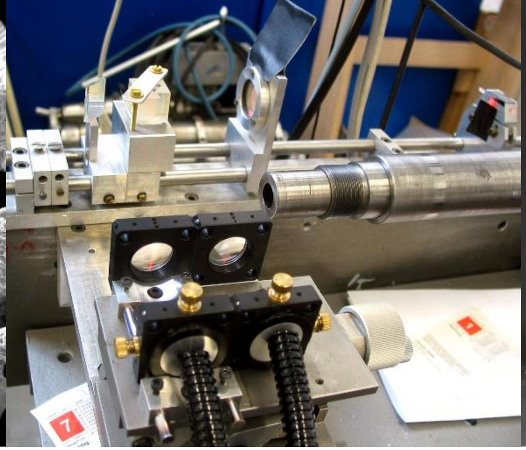

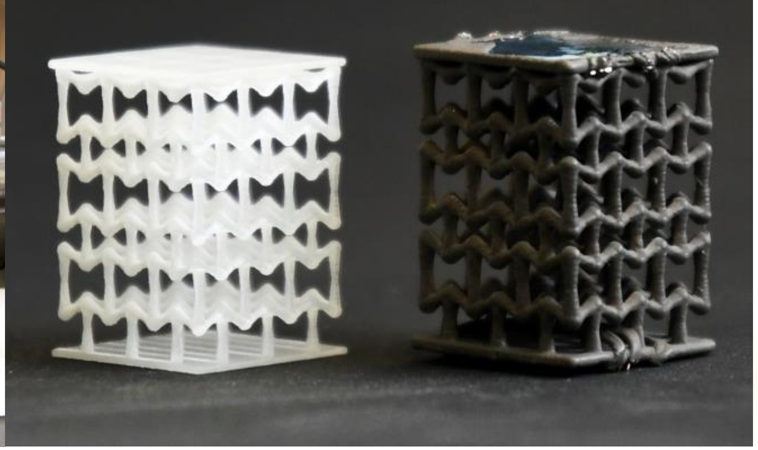

Preparation, Multiscale Mechanical Characterisation and Simulation of Hybrid Foams and Metamaterials

Prof. Dr.-Ing. Dr. rer. nat. Anne Jung

Saarland University
Applied Mechanics
AG Foams and Metamaterials

anne.jung@mx.uni-saarland.de

Cellular Materials – In General

Challenges in Materials Science

- Increased demand for materials and energy
- Increased requirements on material properties
- Resource efficiency
- Application-optimised and multifunctional materials

> "When modern man builds large load-bearing structures,
> he uses dense solids, steel, concrete, glass.
> When nature builds large load-bearing structures,
> she generally uses cellular materials: wood, bone, coral.
> There must be a good reason for it."
> (Michael F. Ashby, 1984)

www.hdmobilewalls.com/2018/l

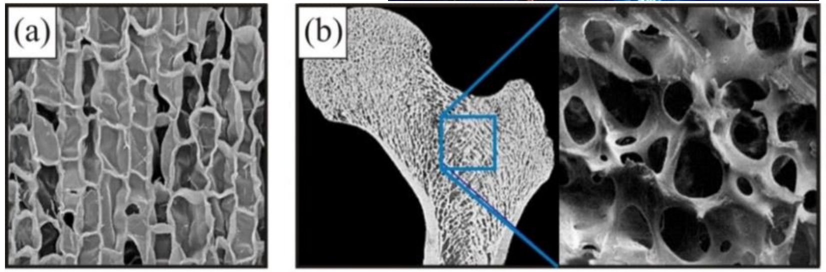

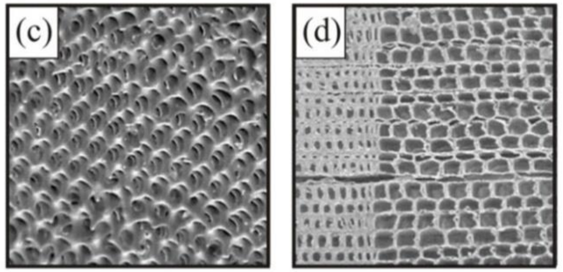

(a) corc
(b) bone
(c) sea star
(d) pine wood

Metal foams

= solid foams; artificial porous structures

Cellular Materials – In General

- Bio-inspired lightweight materials
- Stochastic 3D network
- Usually made of polymers
  or Al cast alloys
- Disadvantages: low strength, no multifunctionality

> ”When modern man builds large load-bearing structures,
> he uses dense solids, steel, concrete, glass.
> When nature builds large load-bearing structures,
> she generally uses cellular materials: wood, bone, coral.
> There must be a good reason for it.”
> (Michael F. Ashby, 1984)

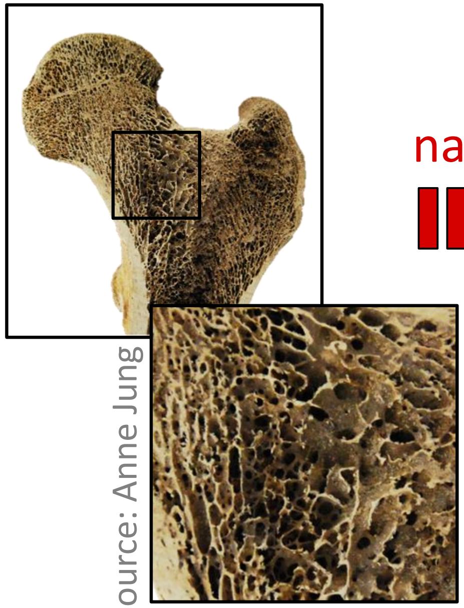

Source: Anne Jung

nature

engineering

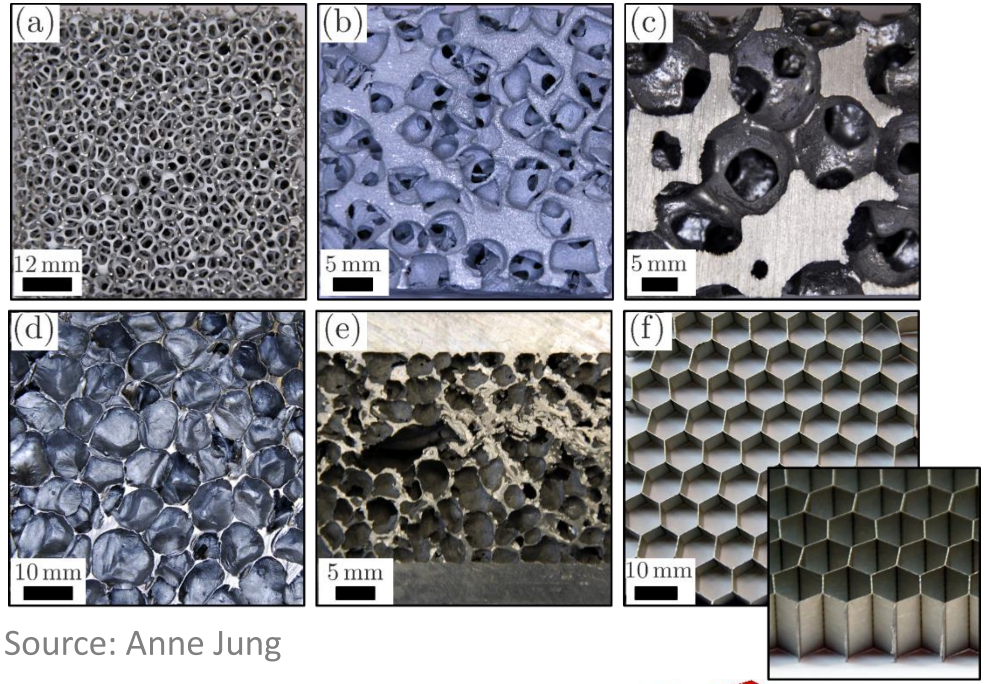

Source: Anne Jung

Universität des Saarlandes
Lehrstuhl für Technische Mechanik
AG Foams and Metamaterials
apl. Prof. Dr.-Ing. Dr. rer. nat. Anne Jung

Cellular Materials – Hierarchical Scales

Source: Anne Jung

nature

engineering

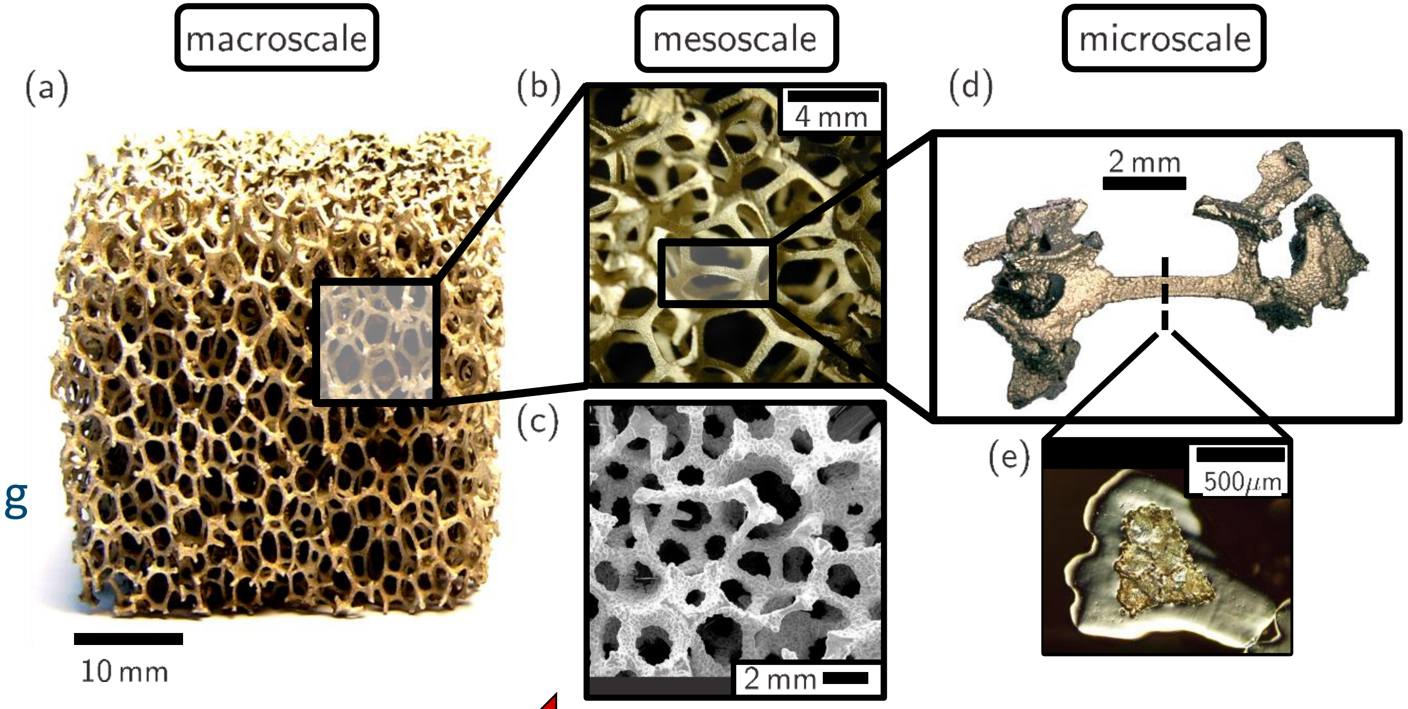

global behaviour ← local behaviour

Global properties are determined by:

- Microstructure
- Properties of the strut material
- Strut geometry

} experiments required on all scales

Cellular Materials – Applications

- **Lightweight construction:**
  High stiffness to weight ratio
- **Energy absorption:**
  Special stress-strain behaviour
- **Functional:**
  Large inner surface, EM shielding …

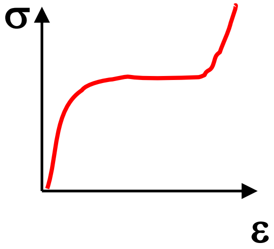

ideal **multifunctionality**

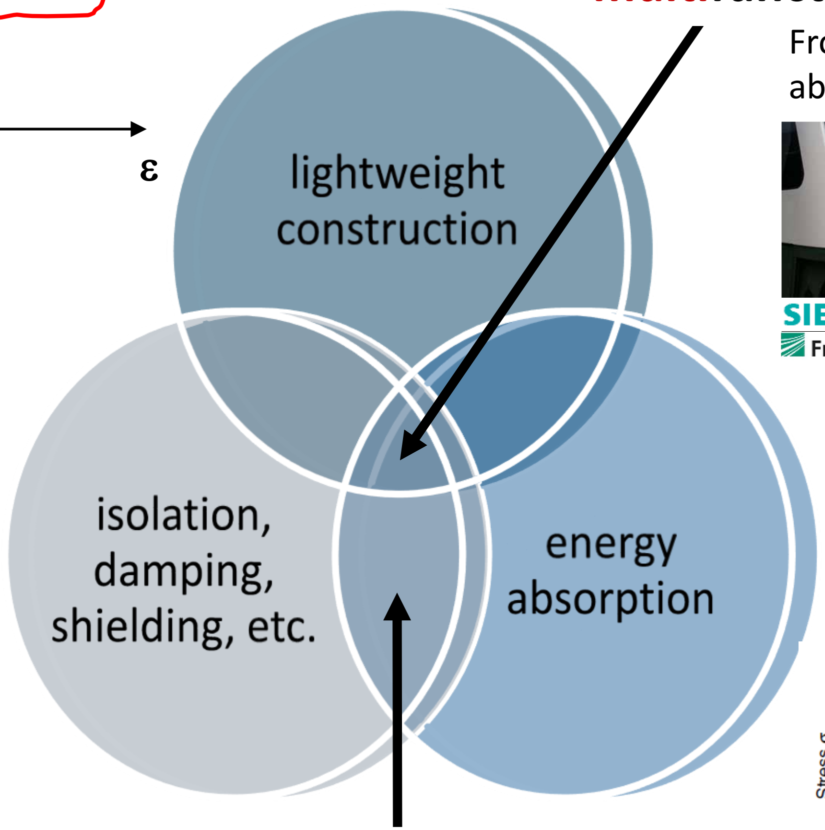

Frontal crash-absorber train

car - A-pillar

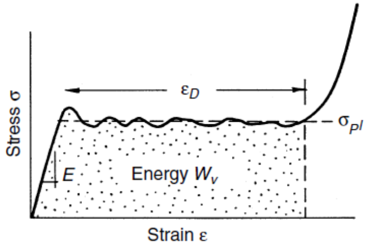

www.welt.de/wissenschaft/innovationen/

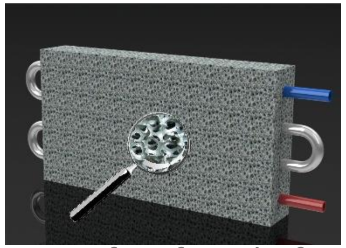

www.ifam.fraunhofer.de/

bifunctionality

Metamaterials

Metamaterials
(Greek Meta = beyond/above):

Mostly artificially produced materials that have properties that do not occur in naturally occurring materials.

Mechanical or structural metamaterials:

- Artificial structures with non-intuitive, unusual mechanical properties
- Properties depend mainly on special geometry
- material with programmable behaviour by varying and optimising the microstructure.

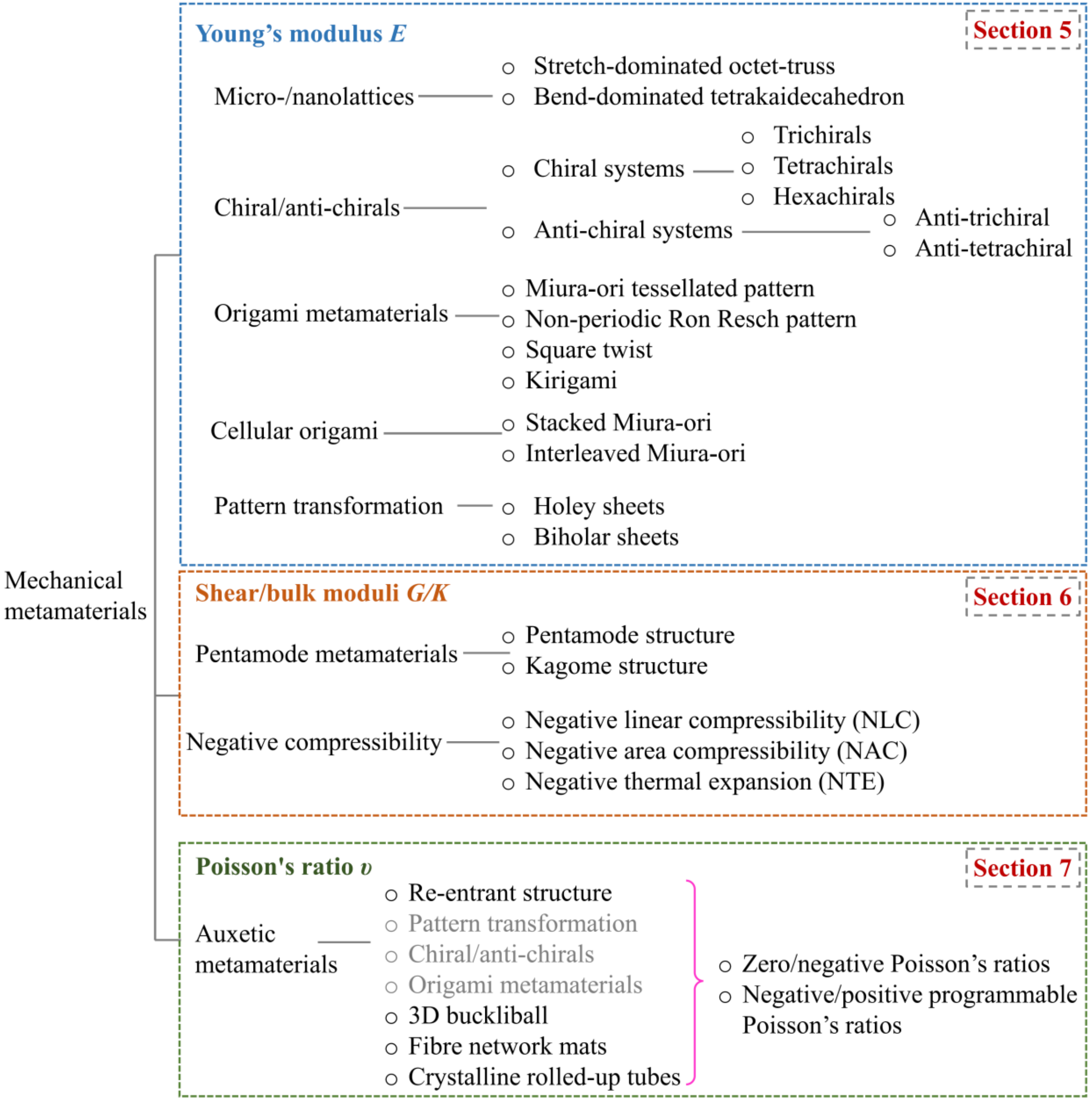

Fig. 2. Basic classification of mechanical metamaterials.

Universität des Saarlandes
Lehrstuhl für Technische Mechanik

X. Yu, J. Zhou, H. Liang, Z. Jiang, L. Wu
Mechanical metamaterials associated with stiffness, rigidity and compressibility: A brief review
Prog. Mater. Sci. 94, 114-173 (2018)

Metamaterials

Metamaterials
(Greek Meta = beyond/above):

Mostly artificially produced materials that have properties that do not occur in naturally occurring materials.

Strong structure-property-relationship

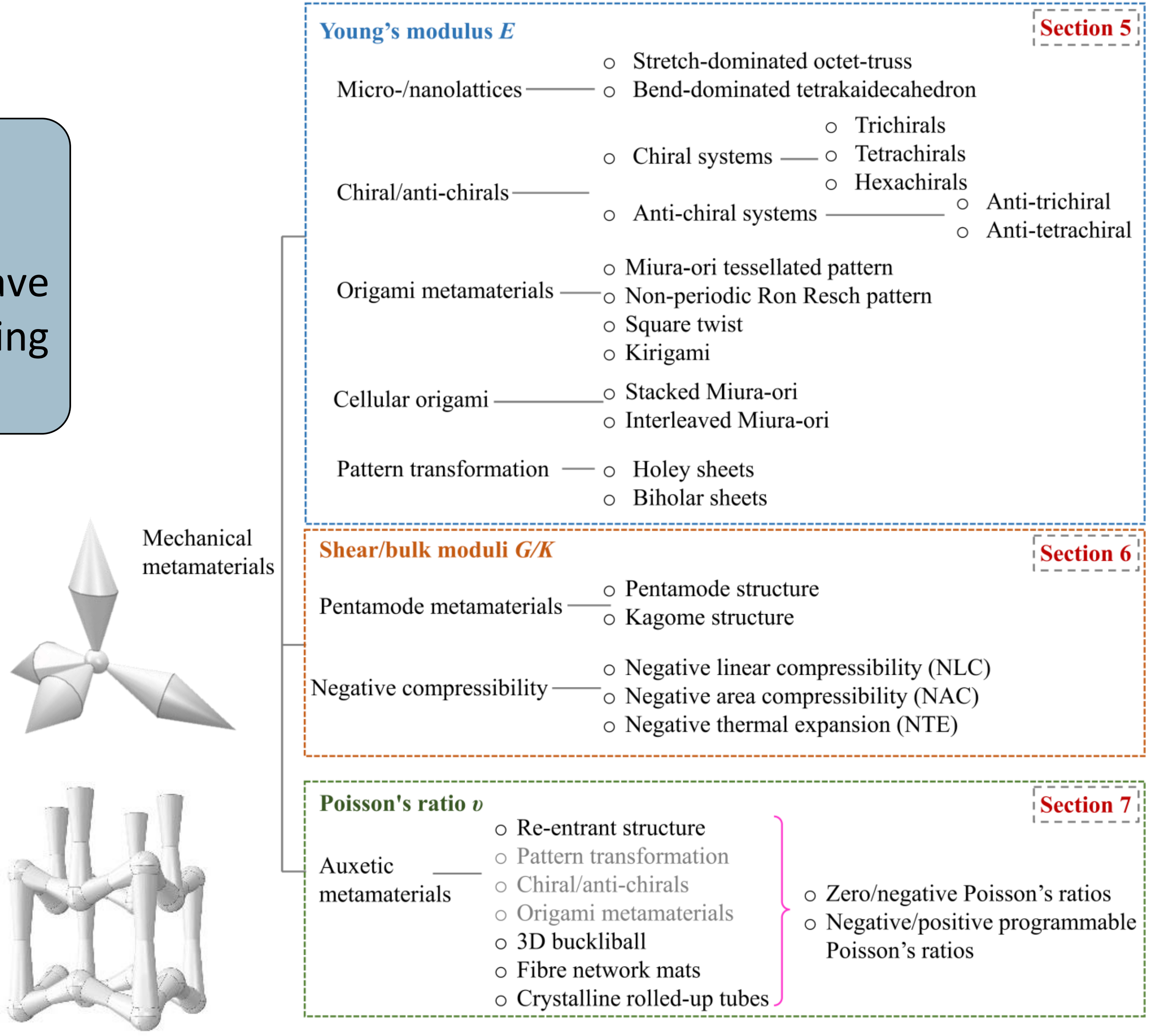

Fig. 2. Basic classification of mechanical metamaterials.

Universität des Saarlandes
Lehrstuhl für Technische Mechanik

X. Yu, J. Zhou, H. Liang, Z. Jiang, L. Wu
Mechanical metamaterials associated with stiffness, rigidity and compressibility: A brief review
Prog. Mater. Sci. 94, 114-173 (2018)

Cellular Materials – Auxetic Metamaterials

Auxetics

(greek: *auxetikos*
= "that which tends to increase“)

- When stretched, they become thicker perpendicular to the applied force.
- Negative Poisson’s ratio

$$\nu = -\frac{\varepsilon_2}{\varepsilon_1}$$

- **Application:**
  - Lightweight construction
  - Superior stiffness, energy absorption and toughness
  - Ideal for ballistic application

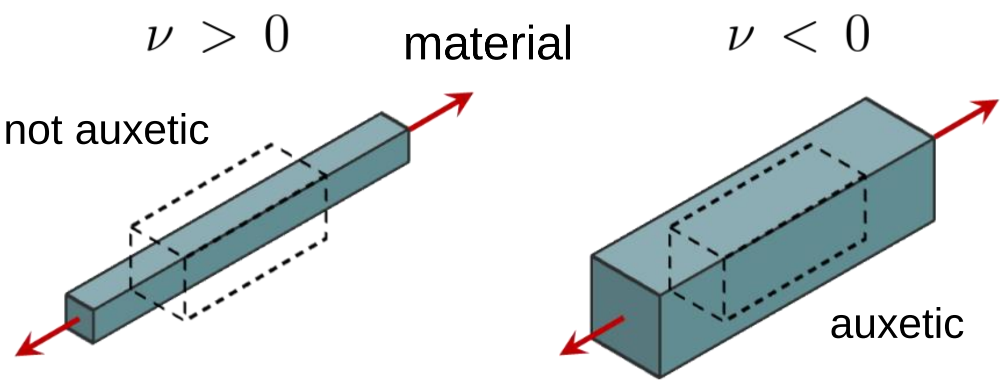

2D structur

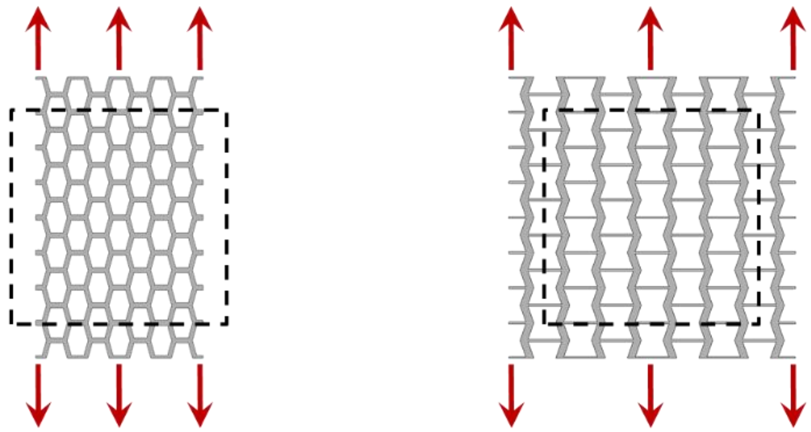

www.applied-auxetics.de

Cellular Materials – Auxetic Metamaterials

Auxetics

(greek: *auxetikos*
 = "that which tends to increase“)

- When stretched, they become thicker perpendicular to the applied force.
- Negative Poisson’s ratio

$$\nu = -\frac{\varepsilon_2}{\varepsilon_1}$$

- **Application:**
    - Lightweight construction
    - Superior stiffness, energy absorption and toughness
    - Ideal for ballistic application

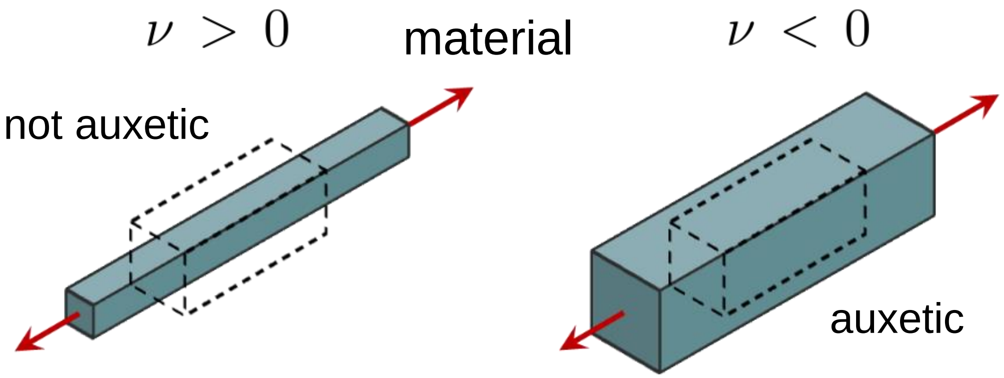

3D structur

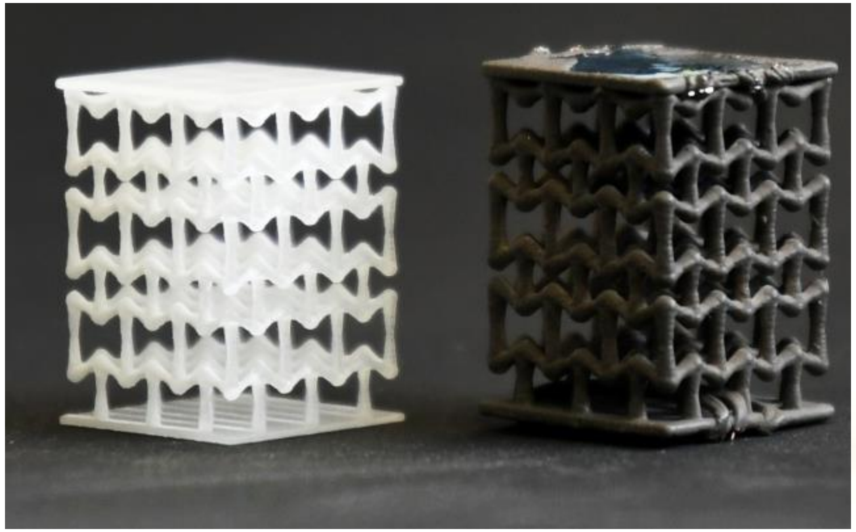

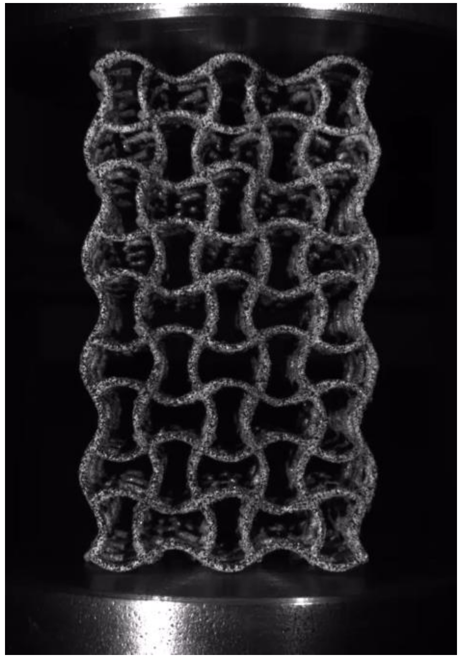

[Röhrig2021]

Investigated Materials – Cellular Hybrid Materials

Disadvantages of conventional Al or polymer foams: low strength, no multifunctionality ⇒ Ni/PU hybrid foams

cellular materials	nano materials (nano = Greek for gnome)	composite/coating
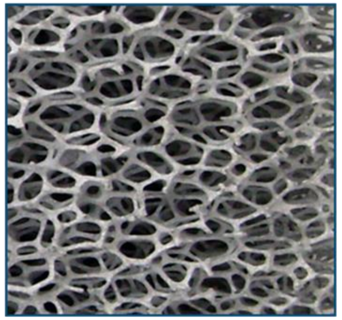	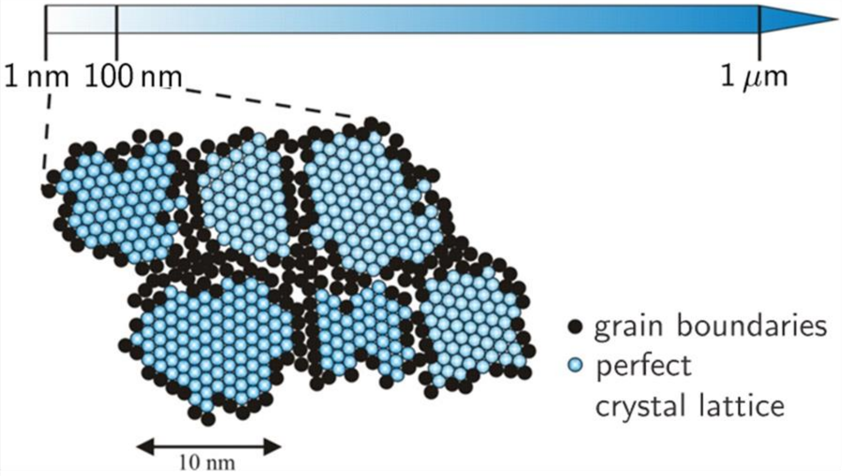	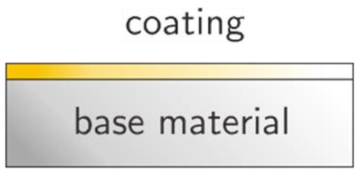
bionic lightweight materials	increasing strength by reduction in grain size	functional finishing

Hybrid Metal Foam

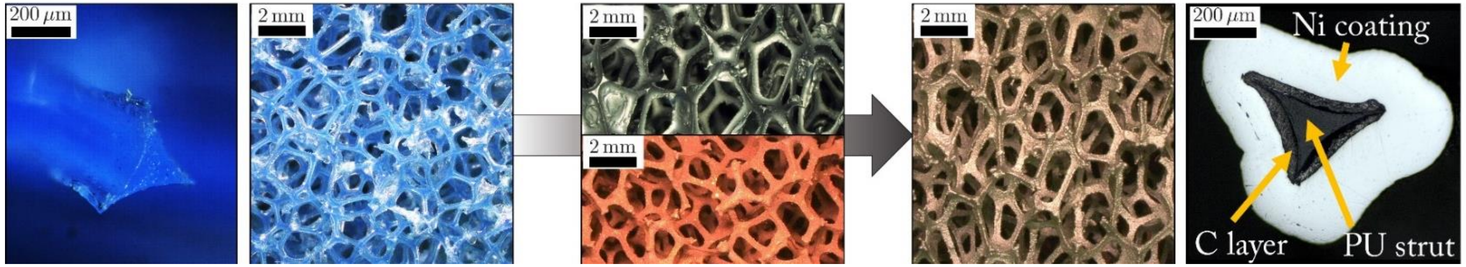

A. Jung & S. Diebels
Adv. Eng. Mater. 4, 532-541 (2016)

Hollistic Research Approach

- Synthesis
- Experimental characterisation
- Modelling
- Simulation

} performed on **all scales**

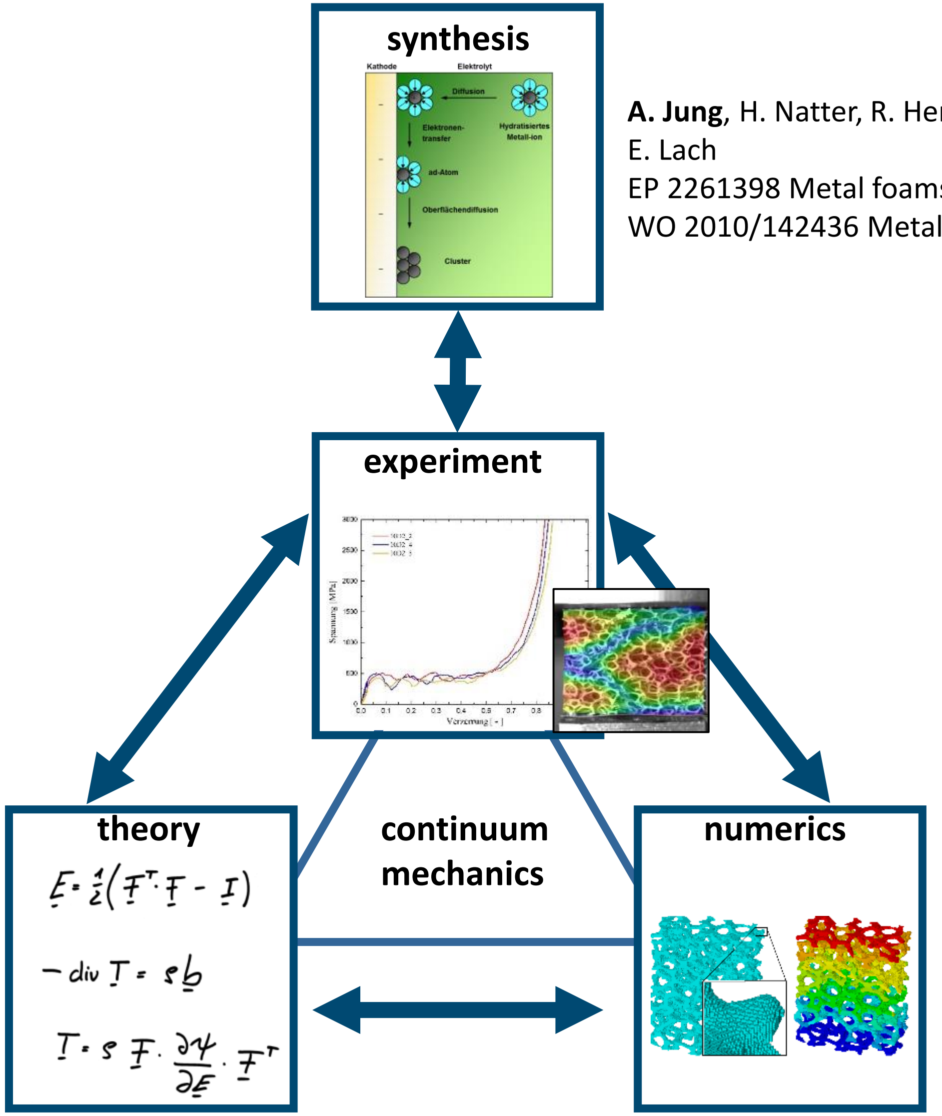

A. Jung, H. Natter, R. Hempelmann, E. Lach
EP 2261398 Metal foams
WO 2010/142436 Metal foams

Research topics

- **Electrochemical synthesis** of Ni/Al, Ni/PU hybrid foams, hybrid metamaterials, metal matrix composites
- **Dynamic and quasi-static** experimental and numerical characterisation of microheterogeneous on different scales
- **Multiaxial and micromechanical** characterisation
- Investigation of **localisation and damage**

Ni/PU Hybrid Foams

- Electrodeposition of nickel on polyurethane (PU) foam
- PU foam made electrically conductive by graphite or copper lacquer
- Strong mass transport limitation during electrodeposition
  $\Rightarrow$ Coating thickness inhomogeneities
- Metal/polymer composite foams

$$M^{z+} + z \cdot e^{-} \rightarrow M$$

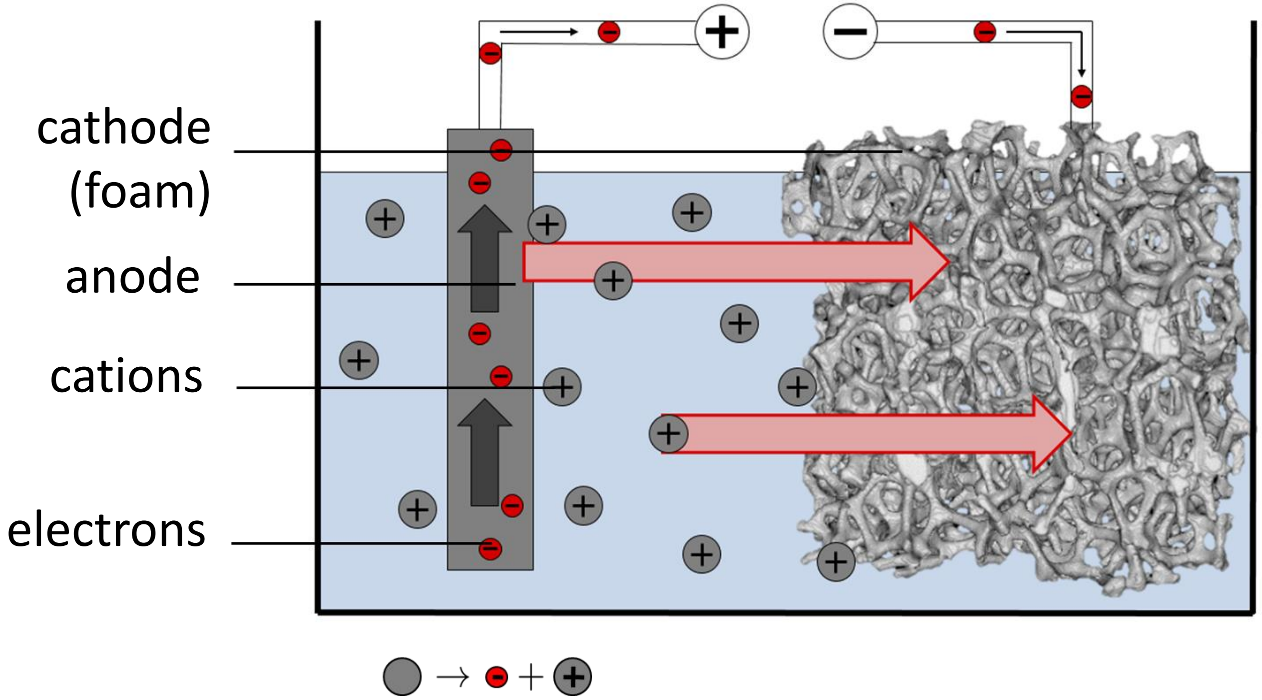

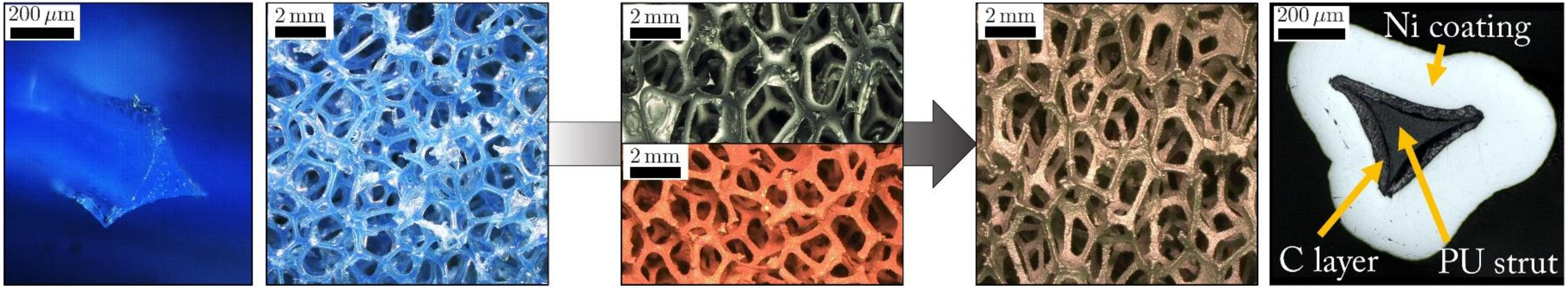

Universität des Saarlandes
Lehrstuhl für Technische Mechanik

A. Jung, H. Natter, R. Hempelmann, E. Lach
EP 2261398 Metal foams
WO 2010/142436 Metal foams

A. Jung & S. Diebels
Adv. Eng. Mater. 4, 532-541 (2016)

Mass Transport Limitations Electrodeposition

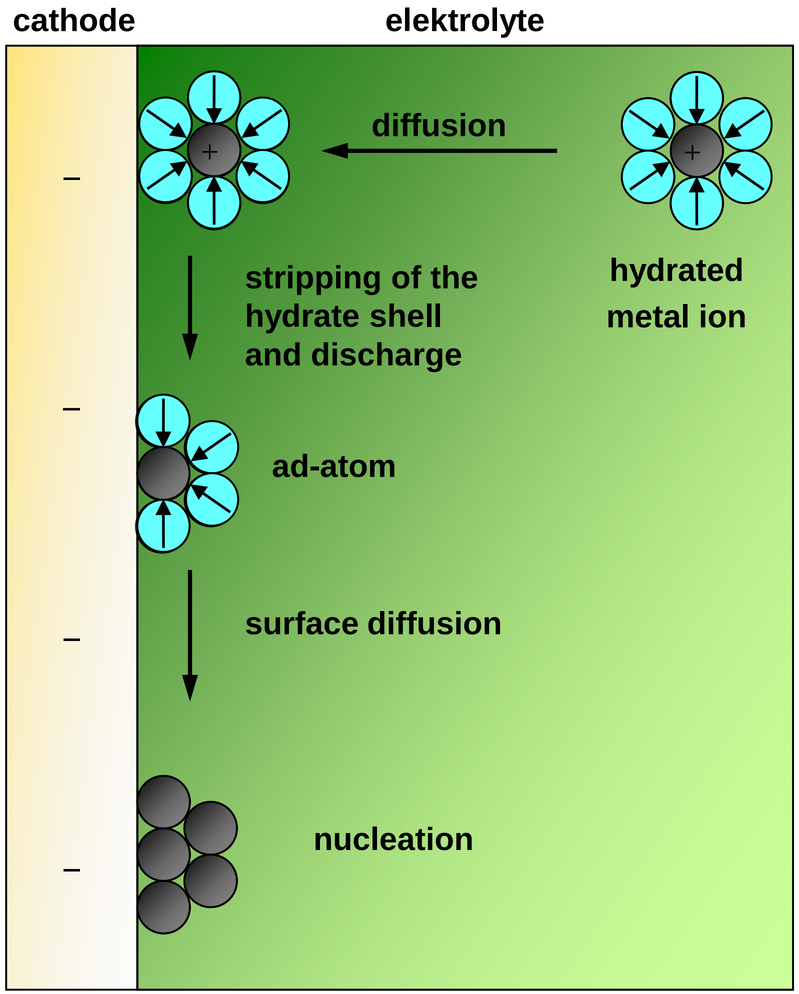

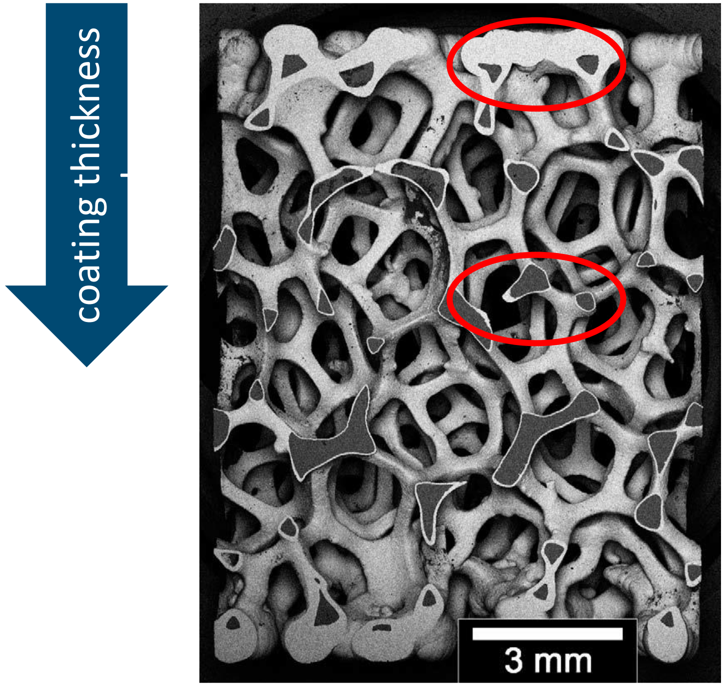

Bouwhuis et al. *Acta materialia*, *57*(14), 4046-4053.

- **Convection**
- **Diffusion**
- **Migration**

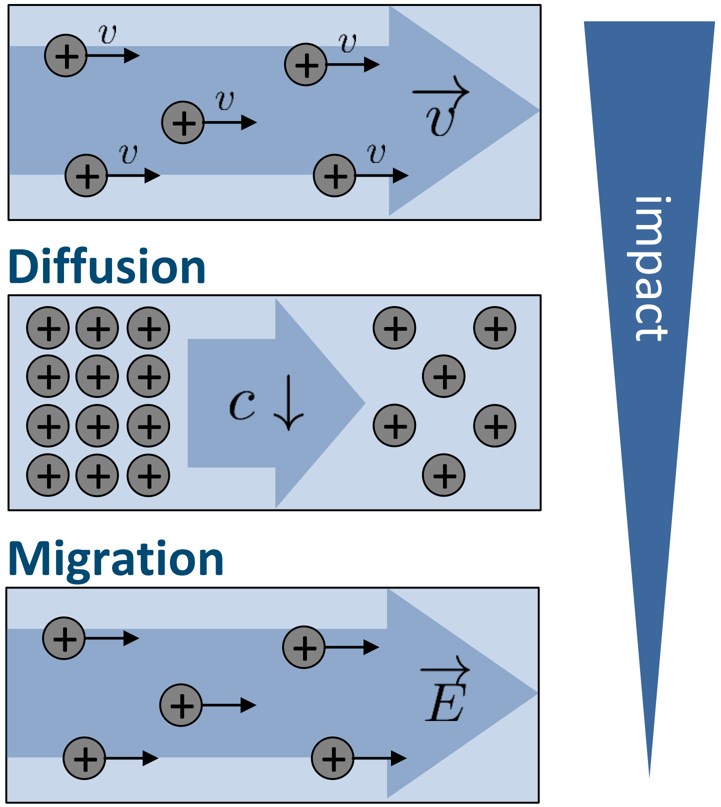

A. Jung, D. Klis, F. Goldschmidt
J. Magn. Magn. Mater. 378, 178-185 (2015)

AG Foams and Metamaterials
apl. Prof. Dr.-Ing. Dr. rer. nat. Anne Jung

Experimental Setup

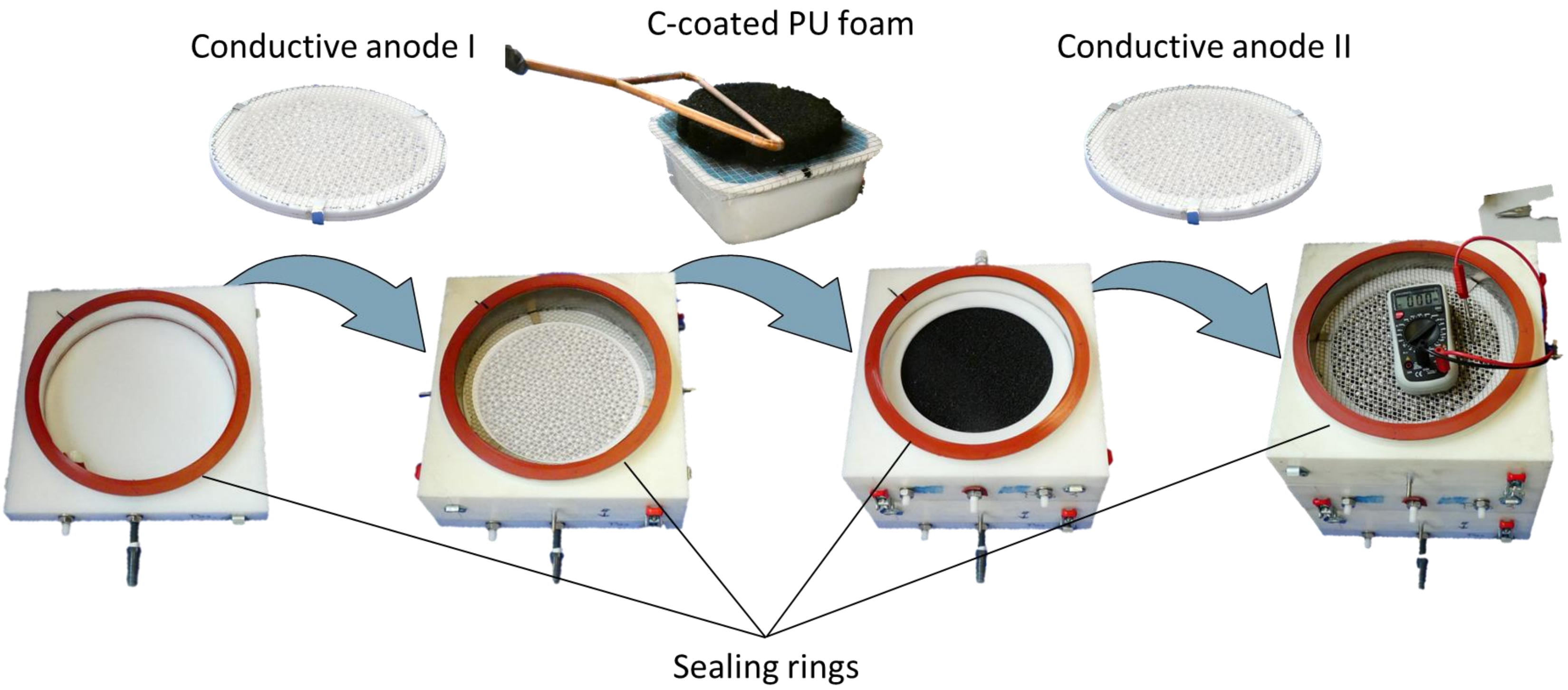

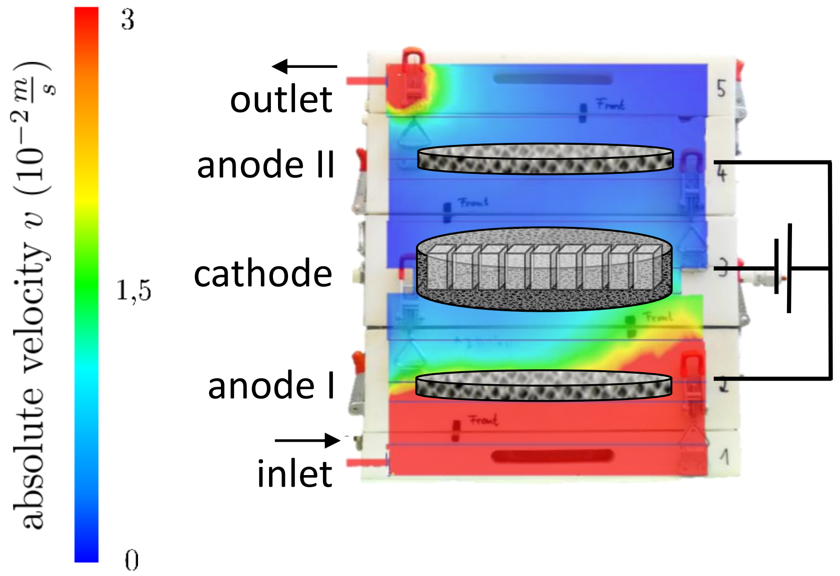

F. Kunz, **A. Jung**

Adv. Eng. Mater., https://doi.org/10.1002/adem.202200262 (2022)

Experimental Procedure

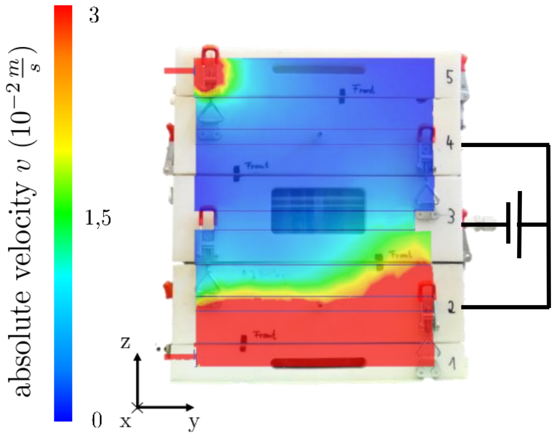

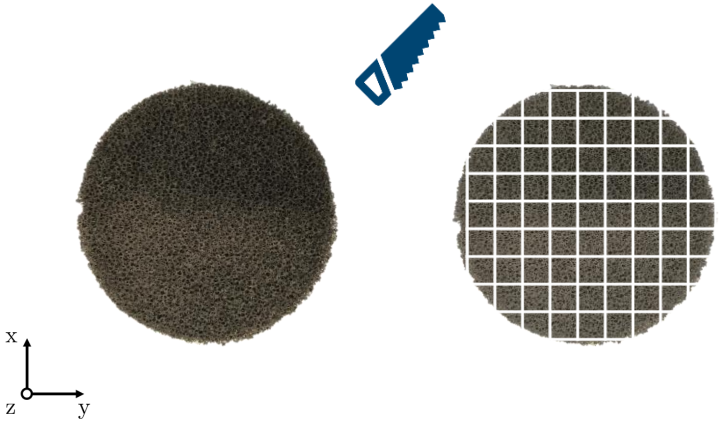

carbon coating

Flow controlled coating

preparation

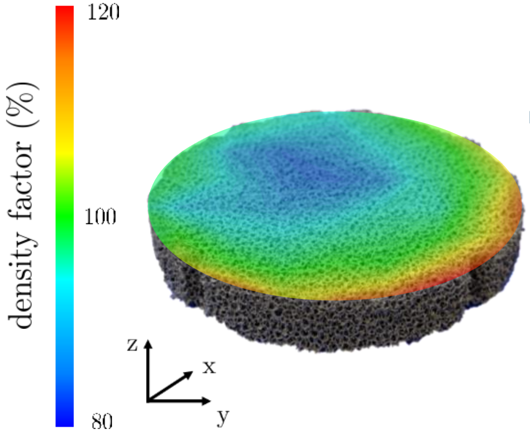

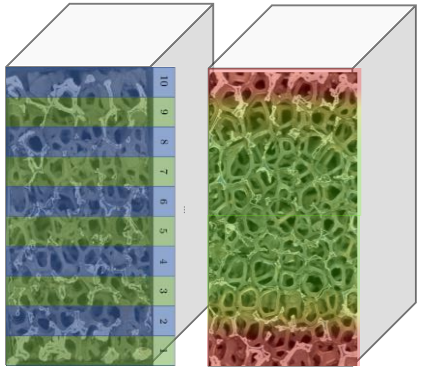

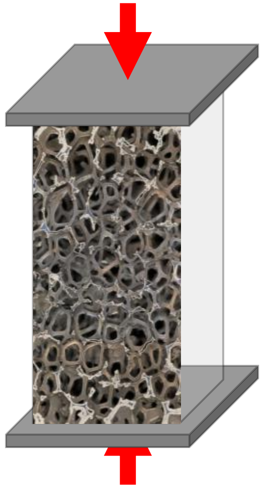

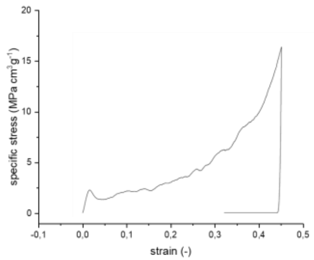

gravimetry

microscopy

compression tests

Universität des Saarlandes
Lehrstuhl für Technische Mechanik
AG Foams and Metamaterials
apl. Prof. Dr.-Ing. Dr. rer. nat. Anne Jung

Types of Coating Homogeneity Classification

Global

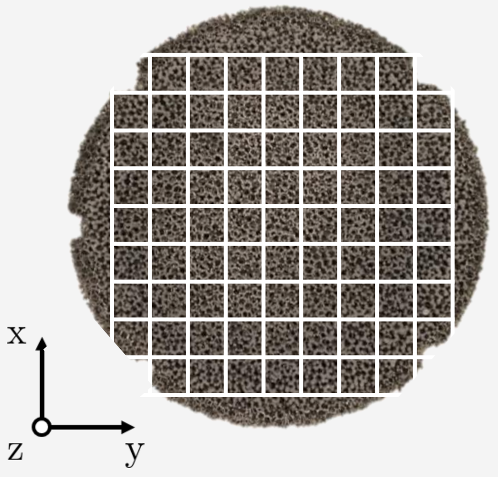

→ Foam plane distribution

→ x-y-distribution

Semi-global

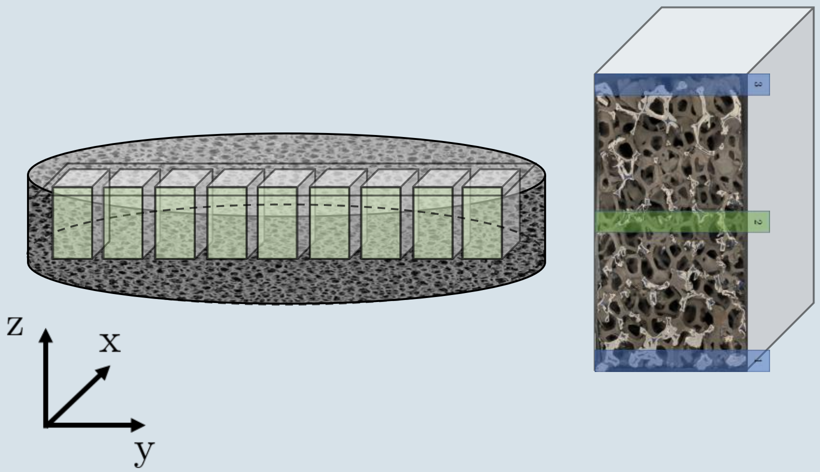

→ Coarse foam thickness distribution

→ y-z-distribution

Local

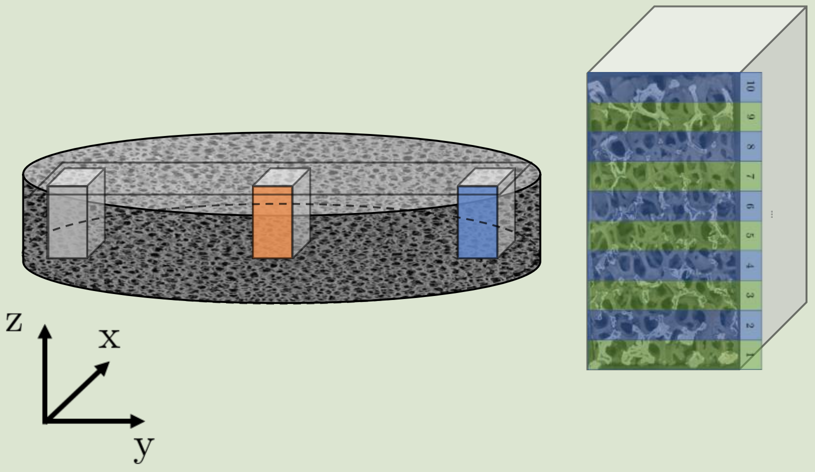

→ Fine foam thickness distribution

→ (y-)z-distribution

⇒ Investigation of the influences on the different distributions for different coating conditions

Global Homogeneity: Coating Thickness Distribution in Plane

- Density investigation of foam cuboids in plate

  ⇒ **Volumetric coating distribution**

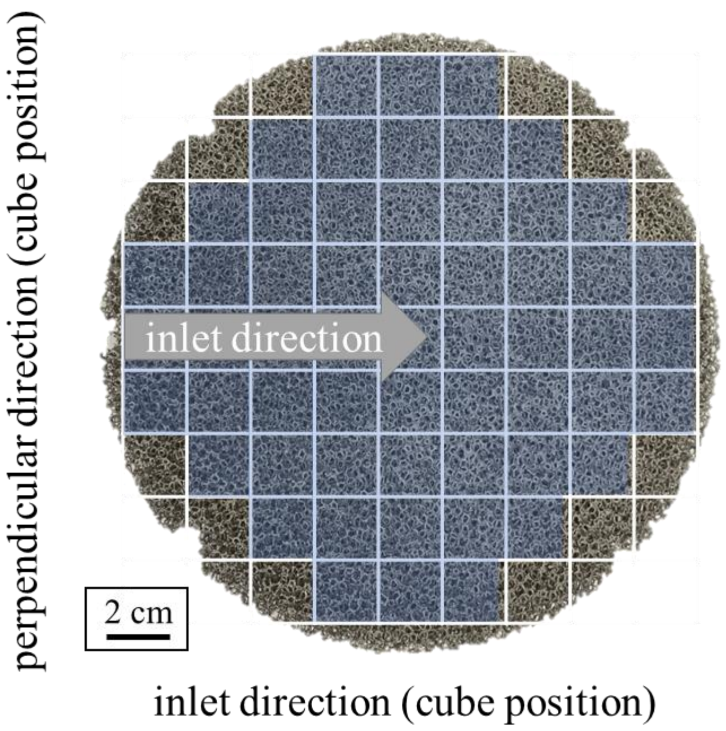

$$\text{density factor} = \frac{\text{local specimen density}}{\text{average specimen density}}$$

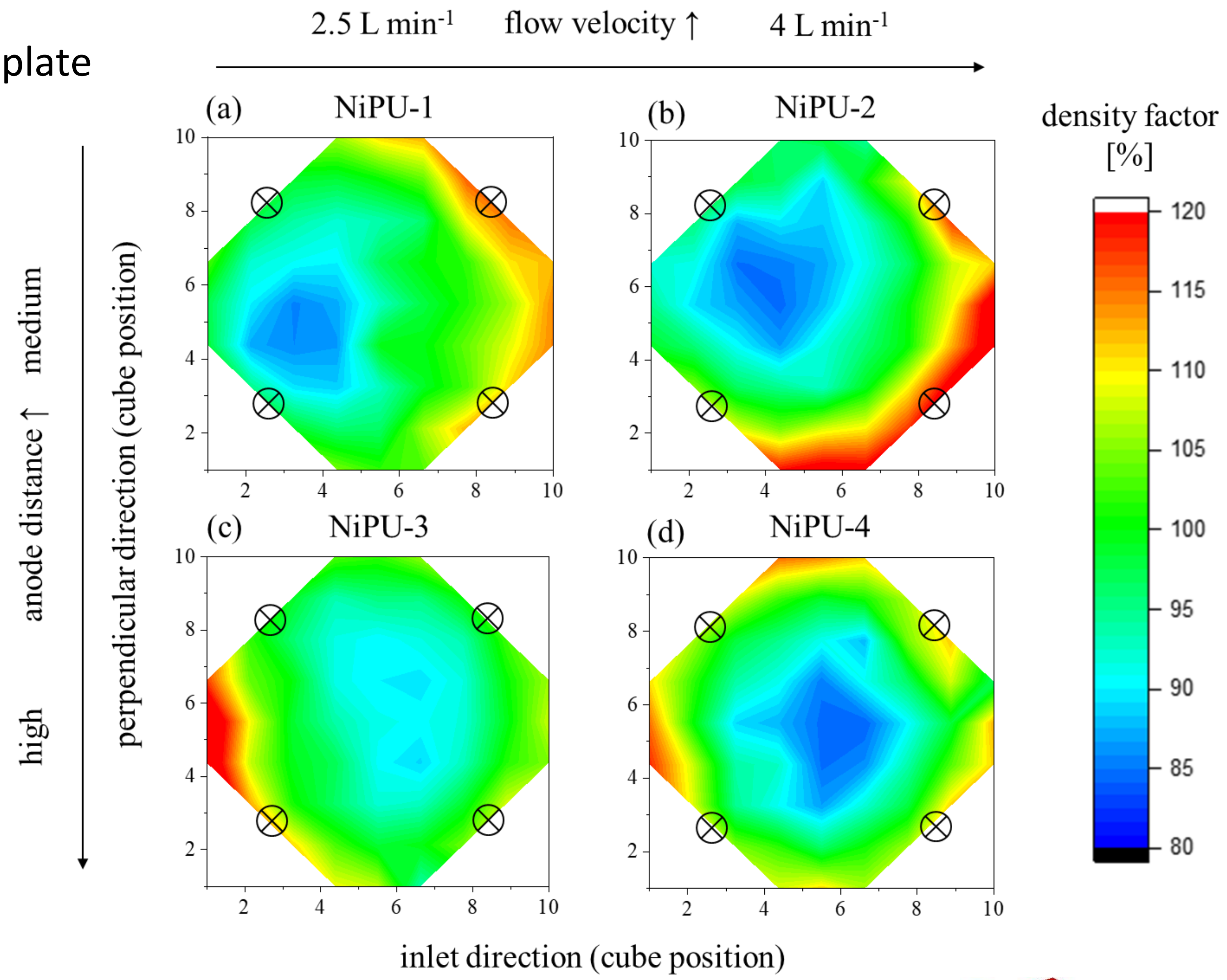

F. Kunz, **A. Jung**
Adv. Eng. Mater., https://doi.org/10.1002/adem.202200262 (2022)
AG Foams and Metamaterials
apl. Prof. Dr.-Ing. Dr. rer. nat. Anne Jung

Local Homogeneity: Coating Thickness Distribution

- Influence of coating parameters:
  - Flow velocity (convective mass transport)
    ⇒ Overcoating or coating reduction
  - Anode distance (electric field distribution)
    ⇒ Ionic migration
- Coating thickness depends on
  ⇒ Reactor position and foam thickness

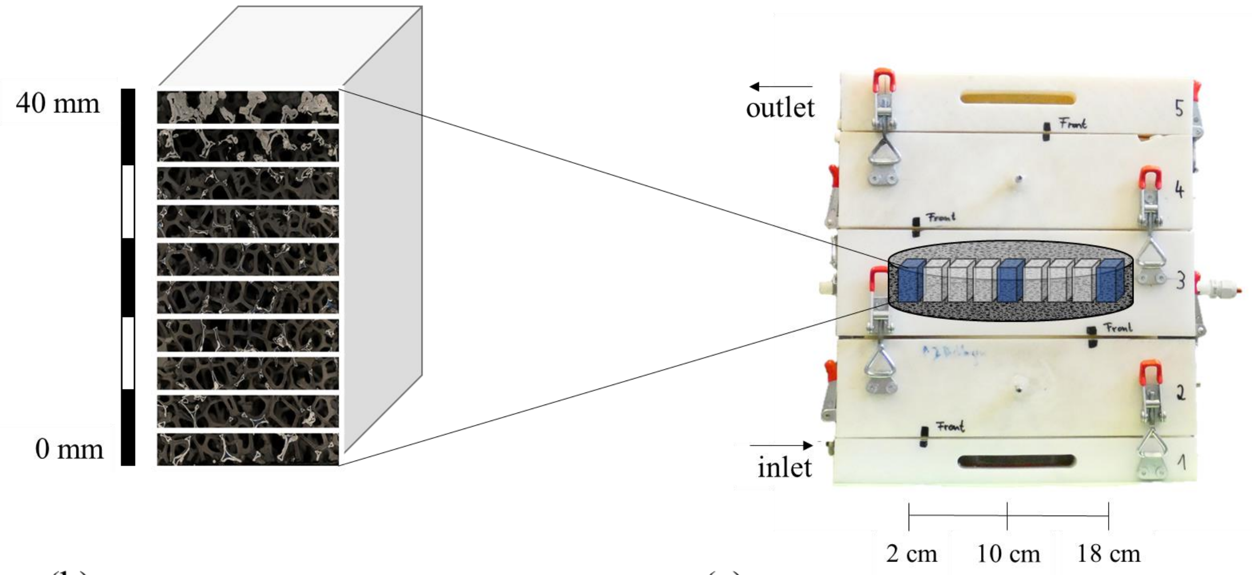

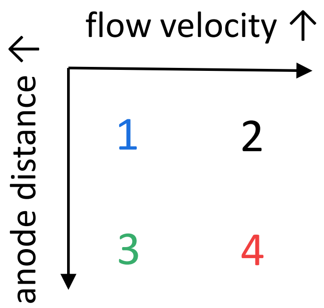

5 – minimal flow

6 – central connection

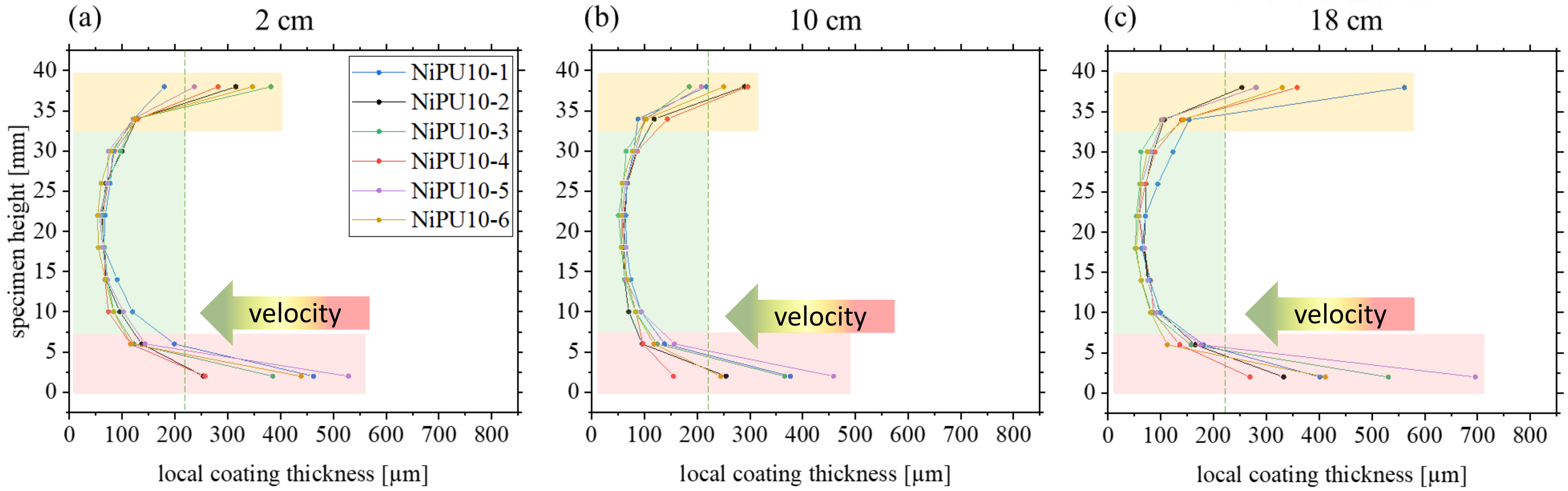

F. Kunz, **A. Jung**
Adv. Eng. Mater., https://doi.org/10.1002/adem.202200262 (2022)

AG Foams and Metamaterials
apl. Prof. Dr.-Ing. Dr. rer. nat. Anne Jung

Scanning Magnetometry Measurements

- **Portal Scanning Unit**
  - 650 mm x 650 mm surface measurements
  - 210 mm cylindric specimen
  - Scattering fields → 3 x ∅ specimen

- **LabVIEW® Controlling System**
  - Adaptive step size: Precision ↑ + accuracy ↑
  - Scanning modes: Line-/ plane-/ volume-scan
  - Microscopic stitching: LabVIEW® + Fiji®
  - Magnetisation measurement T-compensated
    - Accuracy of the Hall probe: ± 0,01 mT
    - Temperature coefficient -0,04 %/°C

    But: T-induced magnetisation shift of probe

    ⇒ Compensation with parallel measurement

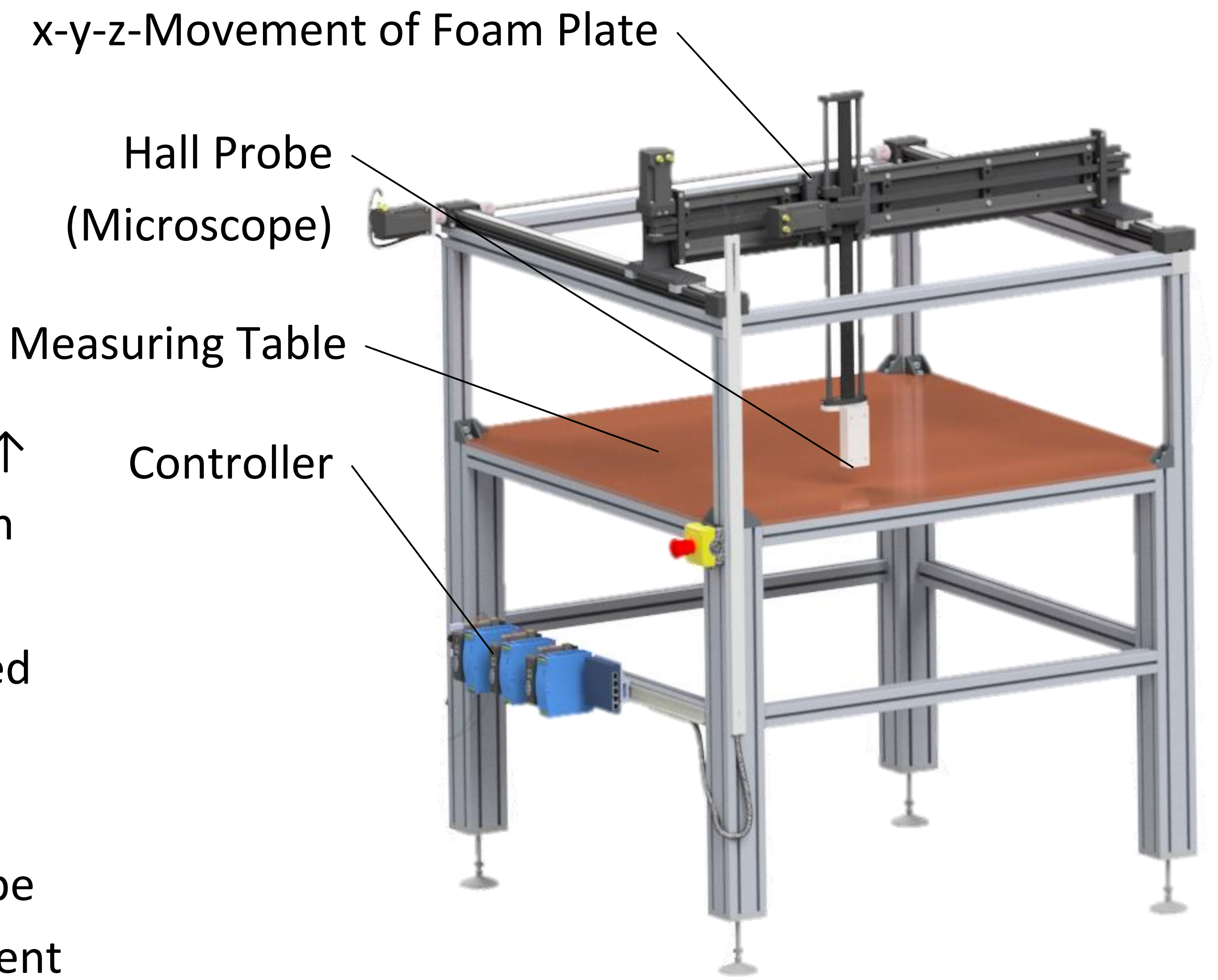

Ferromagnetic Properties of Ni/PU Hybrid Foams

- Saturating magnetic field strength?
- Vibrant sample magnetometry

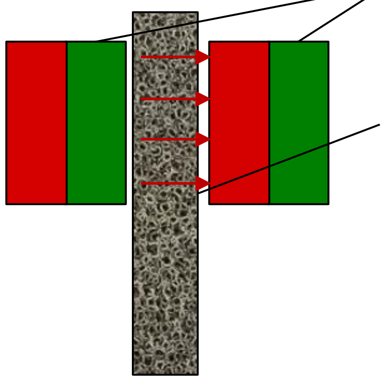

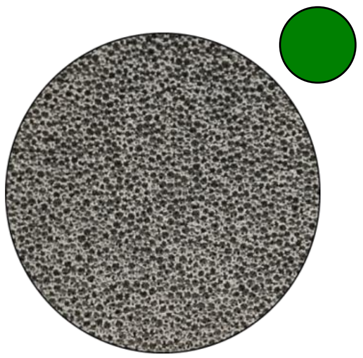

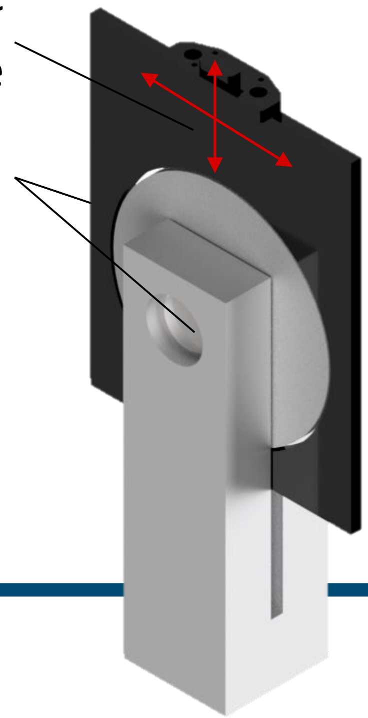

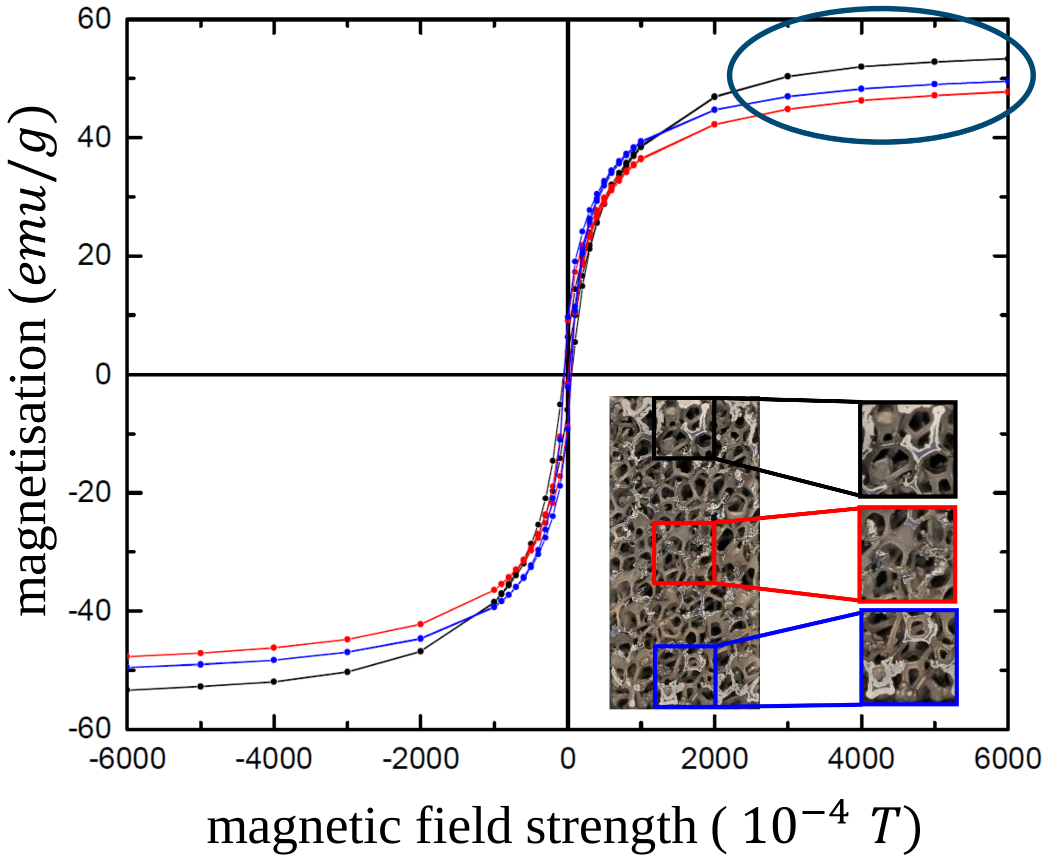

Measurement provided by H. Gao
Experimental Physics
Saarland University

Magnetisation Measurements in Hybrid Foams

- ∅ 70 mm x 10 mm (120 µm coating thickness)
- Produced in small scale reactor with known flow velocity distribution
- Magnetised through saturating magnetic field strength
- Magnetic field distribution shows spatial inhomogeneities

⇒ Overcoating is also represented in **gravimetry** (but error-prone at small scales)

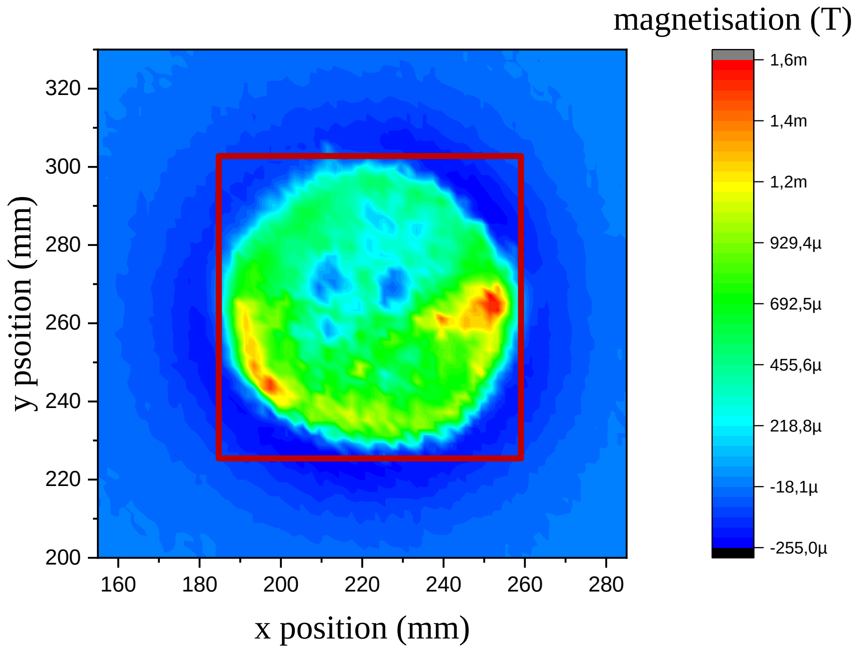

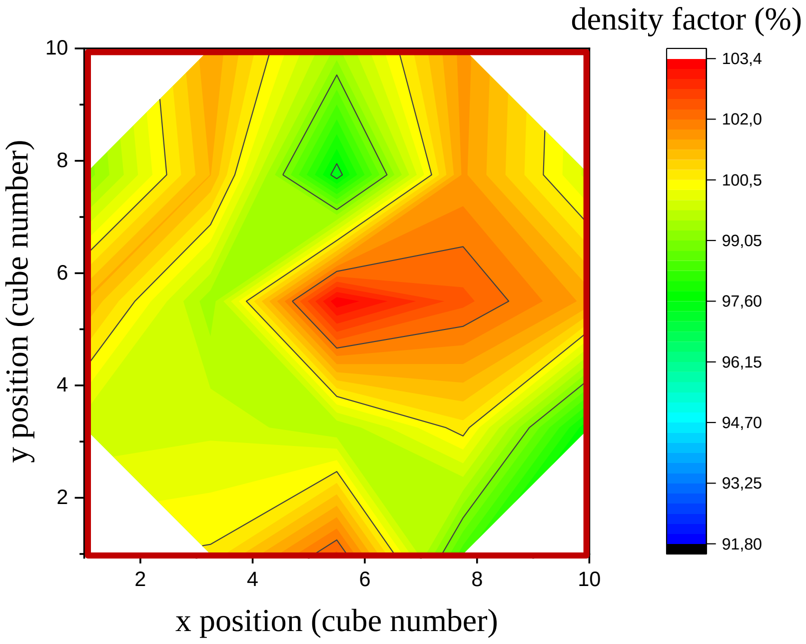

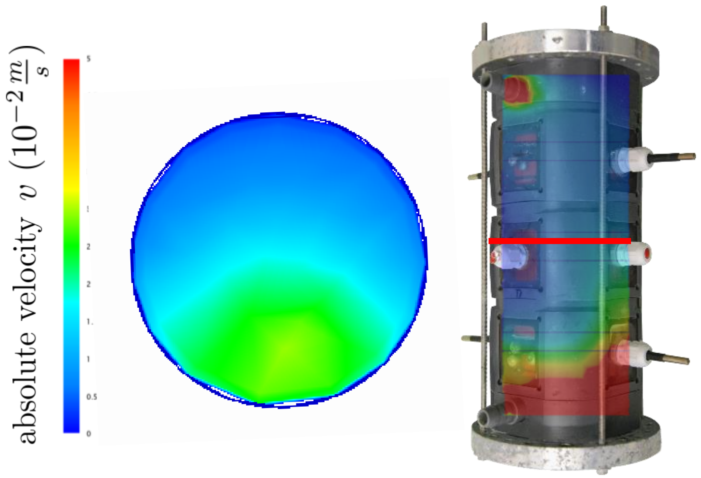

⇒ Further correlation necessary: Magnetometry & gravimetry & CT with bigger foams (MA Laura Lindner)

Structural and Experimental Characterisation

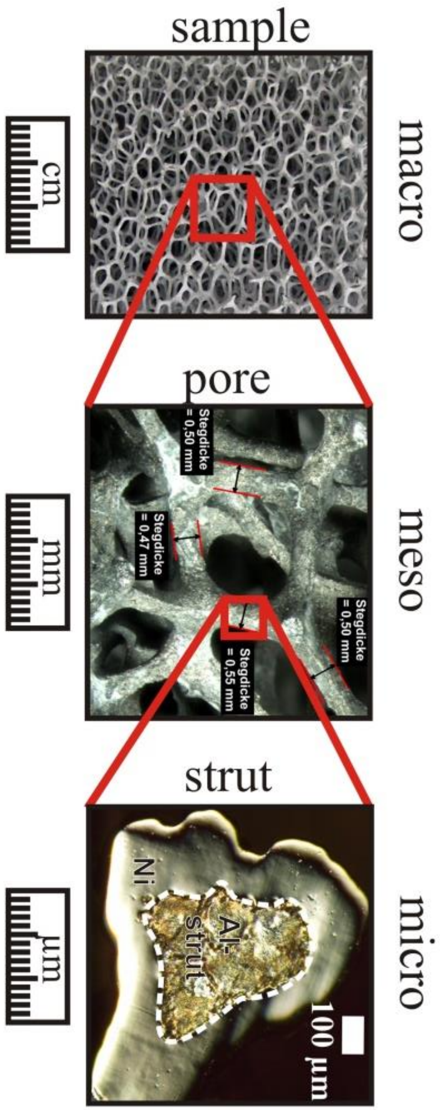

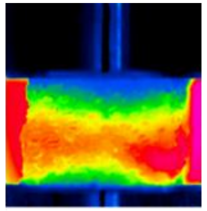

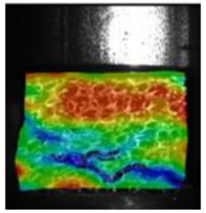

Macroscale

uni- and biaxiale material characterisation

- Compression/tensile tests + DIC
- Shear compression tests + DIC
- Pure torsion tests
- Compression-torsion/tension-torsion

- Drop weight tests + DIC
- SHPB tests + DIC
- Ballistic tests
- IR thermography

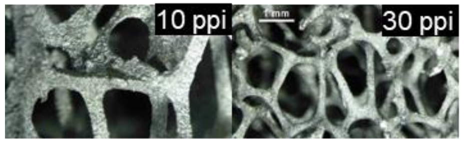

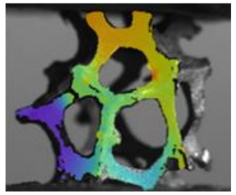

Mesoscale

- Optical microscopy
- X-ray CT, time-lapse µCT
- Photogrammetry
- Microcompression/microtensile (pore)

- Drop weight tests (pore)
- Gas gun tests (pore)
- DIC

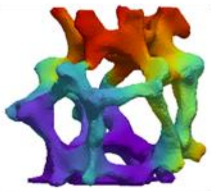

Microscale

- XRD
- EBSD
- Nano-/microindentation
- Microcompression/microtensile (strut) in-situ/ex-situ + DIC

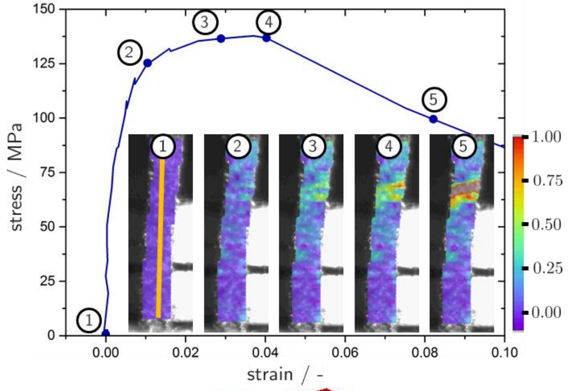

Macroscale

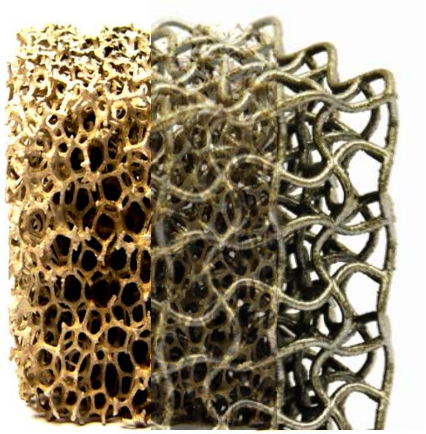

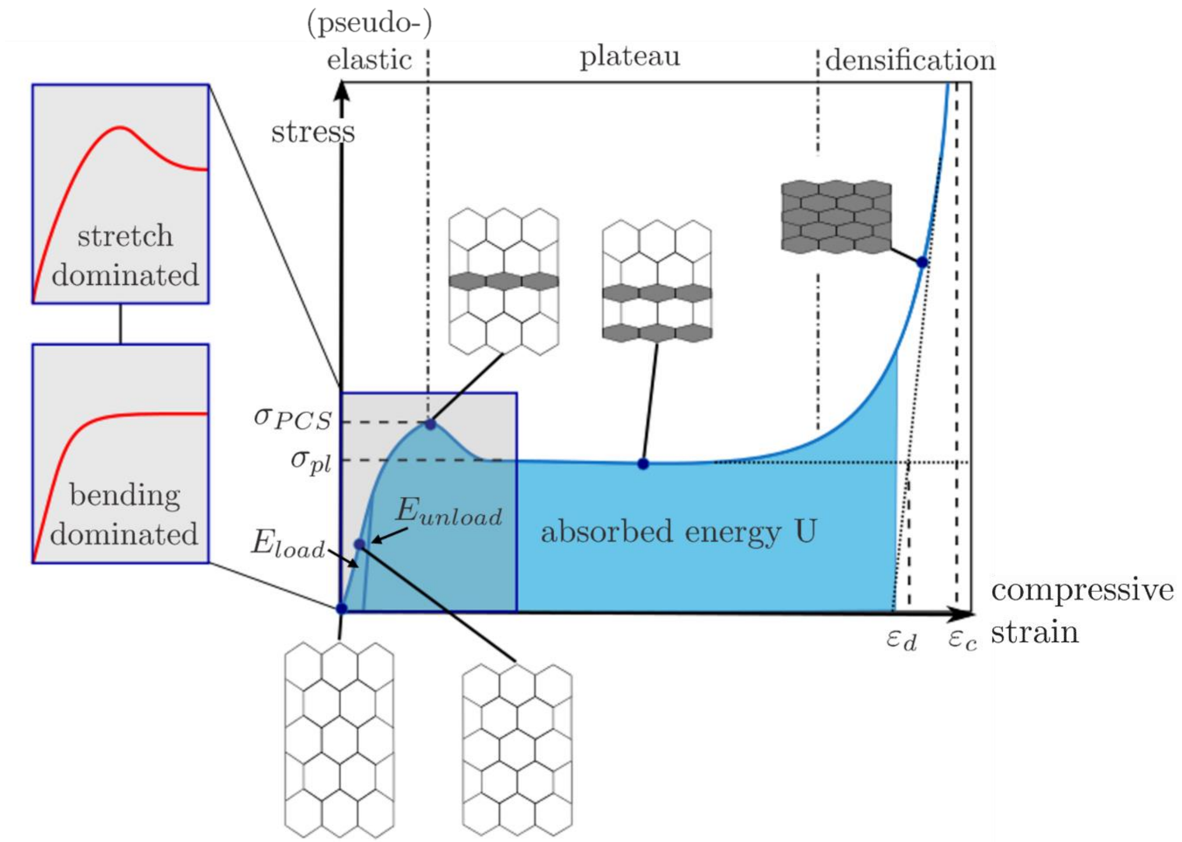

Universität des Saarlandes
Lehrstuhl für Technische Mechanik
AG Foams and Metamaterials
apl. Prof. Dr.-Ing. Dr. rer. nat. Anne Jung

Ni/Al Hybrid Foams – Coating Effect

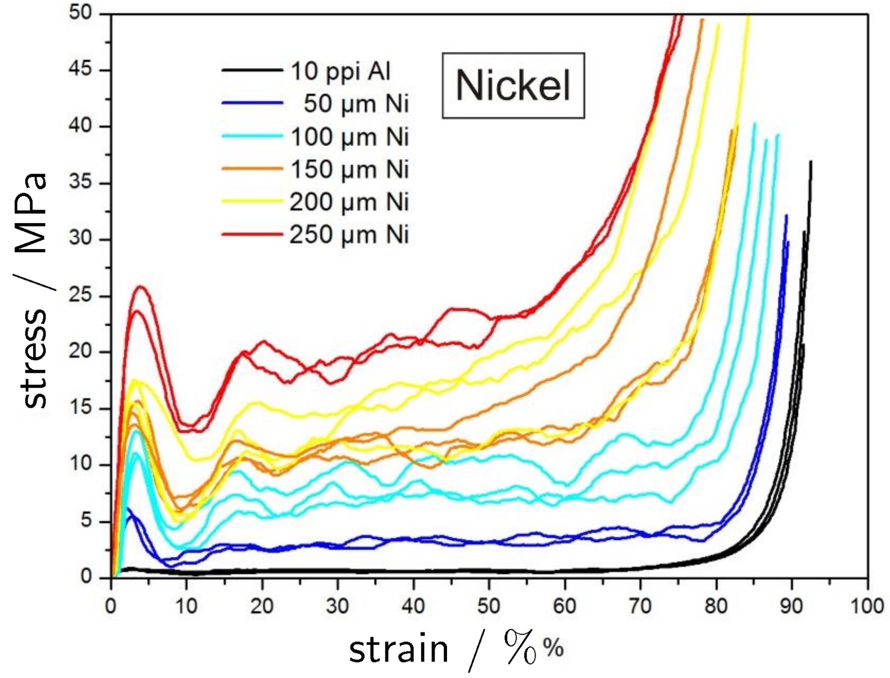

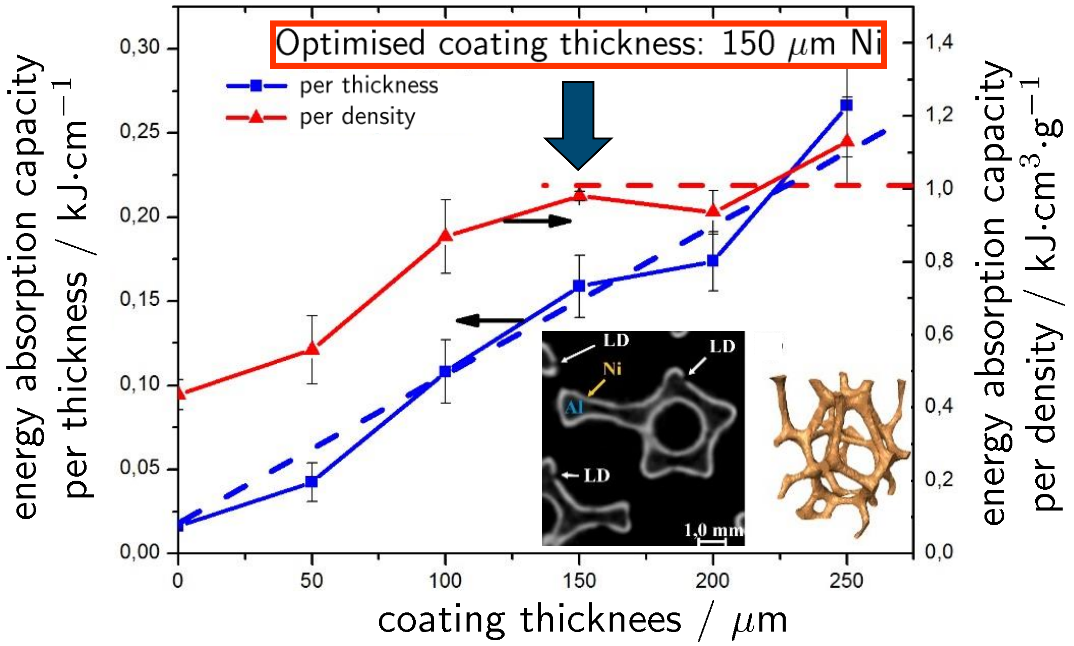

characteristic value	Al (10 ppi)	150 μm Ni (10 ppi)	enhancement factor
Young's modulus [MPa/kg]	6 806.45	23 739.42	3.5
plastic collapse stress [MPa/kg]	77.13	364.85	4.7
plateau stress [MPa/kg]	65.75	252.38	3.8
energy absorption capacity			
per thickness [kJ/cm]	0.017	0.158	9.6
per density [kJ cm^3/kg]	0.435	0.978	2.2

Strengthening of the outer fibre

$$F = \pi^2 \frac{E\,I}{s^2}$$

Ni coating $\Rightarrow$ ↑ stiffness, ↑ strength, ↑ energy absorption, ↑ mass

A. Jung, H. Natter, S. Diebels, E. Lach, R. Hempelmann
Adv. Eng. Mater. 13, (1-2), 23-28 (2011)

AG Foams and Metamaterials
apl. Prof. Dr.-Ing. Dr. rer. nat. Anne Jung

Ni/Al Hybrid Foams – Functionally Graded Foams

- Euro NCAP crash test: 55 km/h
- No energy absorption below
- Not enough energy absorption for higher speeds

⇒ Functionally graded foam as **passively controllable energy absorber**

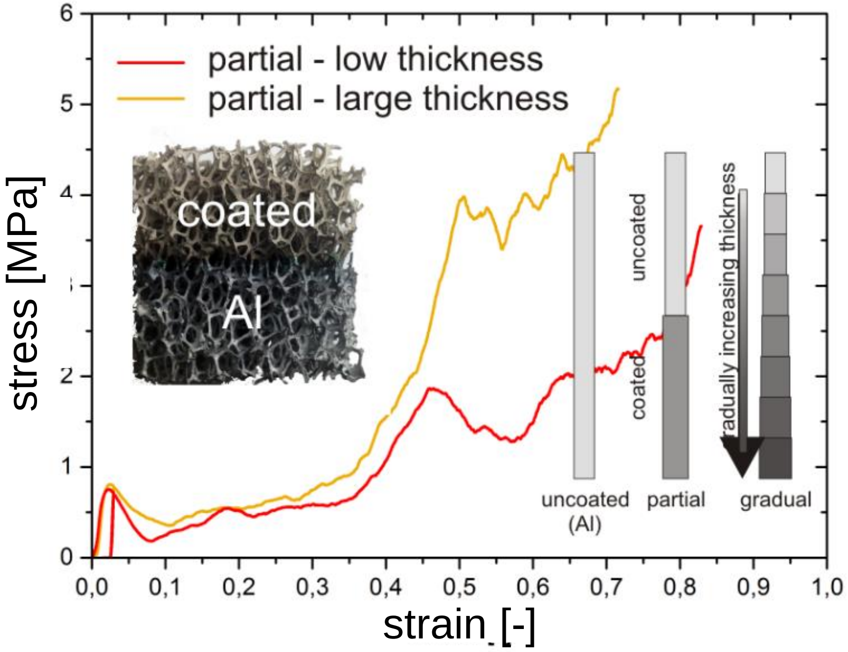

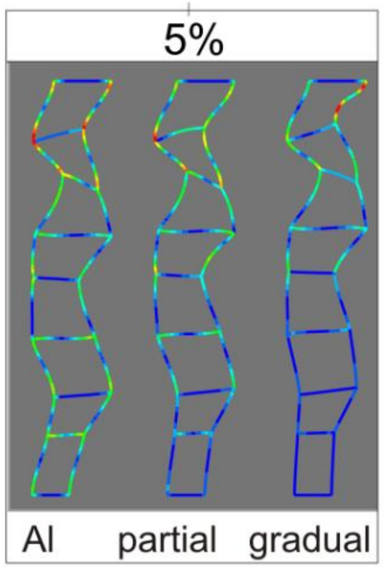

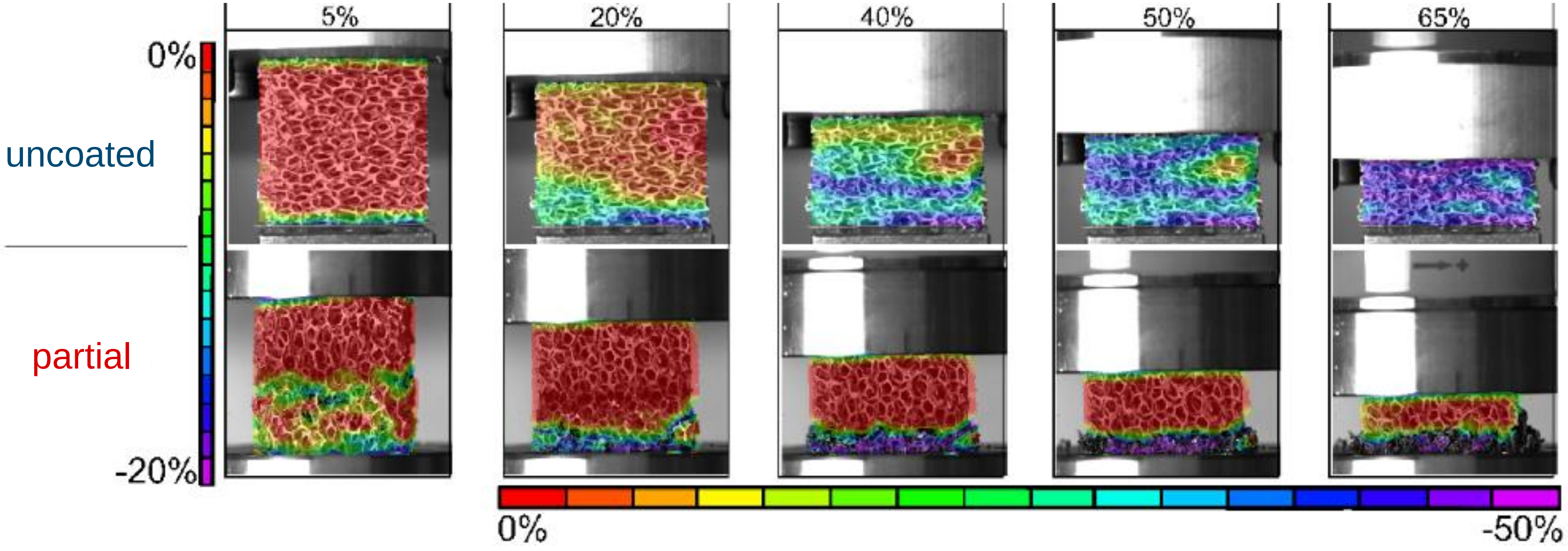

A. Jung, L.A.A. Beex, S. Diebels, S.P.A. Bordas
Mater. Des. 87, 36-41 (2015)

Full-Field Thermomechanical Analysis of Cellular Materials – Setup

- Uniaxial compression tests
  Instron ElectroPuls 10000®
- Strain rates: 0.025 – 0.250 s^{-1}

Additional speckle pattern on struts

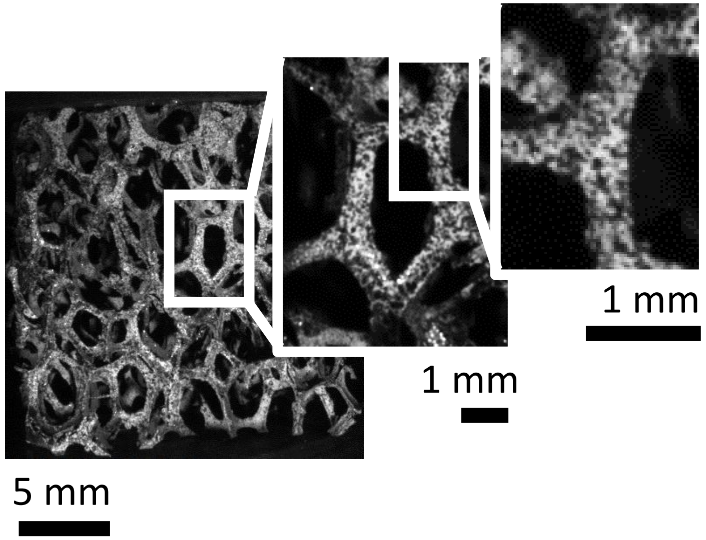

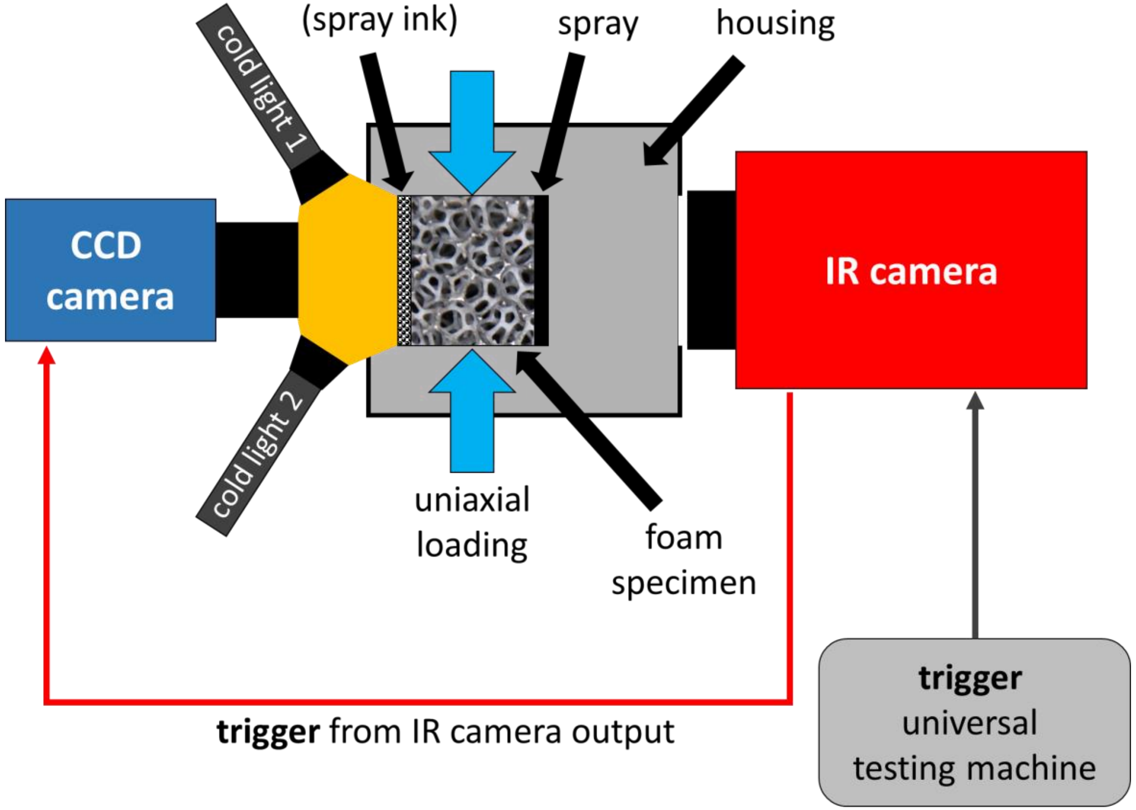

- CCD camera: Manta G235B, Ltd. AVT
- IR camera: ImageIR 9360, Infratec GmbH

A. Jung, S. Bronder, S. Diebels, M. Schmidt, S. Seelecke
Mater. Des. 160, 363-370 (2018)

AG Foams and Metamaterials
apl. Prof. Dr.-Ing. Dr. rer. nat. Anne Jung

Thermographic Analysis of Strain-rate Effects

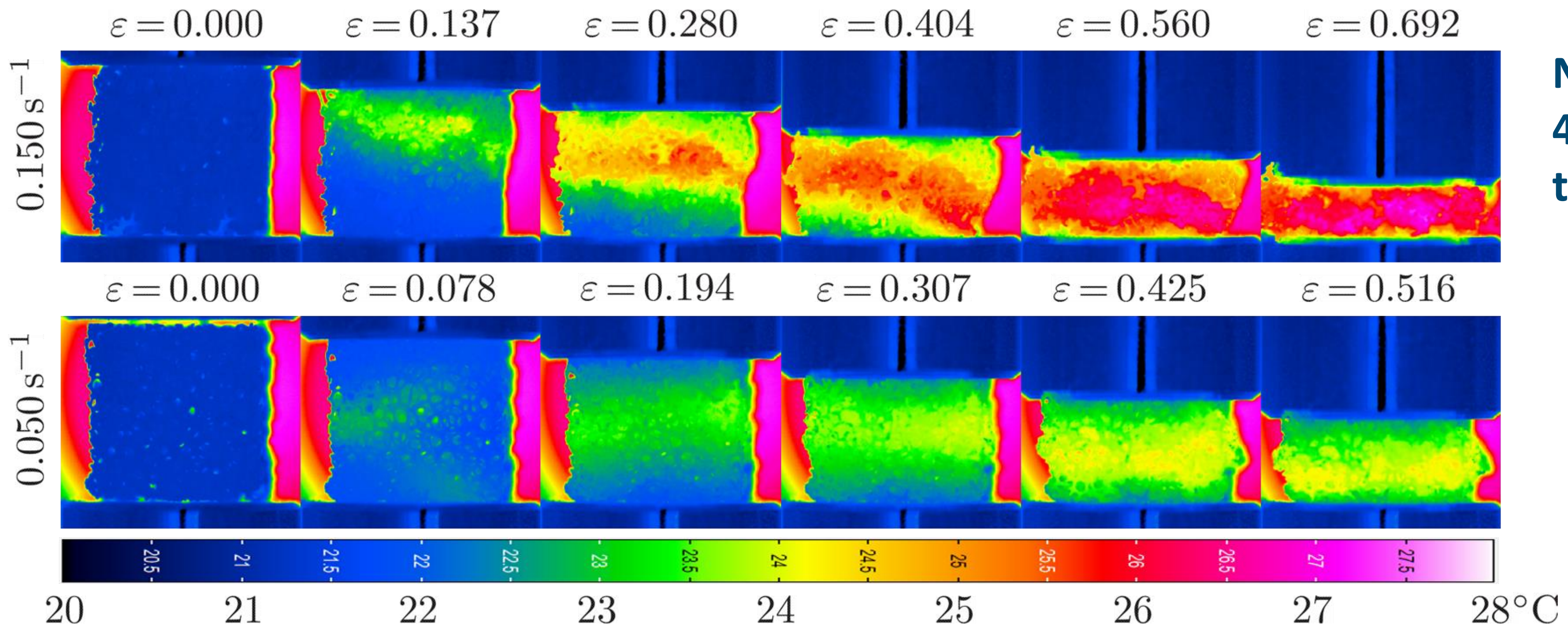

Ni/Al foams
40 µm coating thickness

A. Jung, S. Bronder, S. Diebels, M. Schmidt, S. Seelecke
Mater. Des. 160, 363-370 (2018)

Thermographic Analysis of Strain-rate Effects

Increasing temperature change with:

- Increasing strain rates
- Increasing Ni coating thickness
- Al → Ni

- Al → 40 µm Ni: factor of 2.5
- Al → 120 µm Ni: factor of 4.0

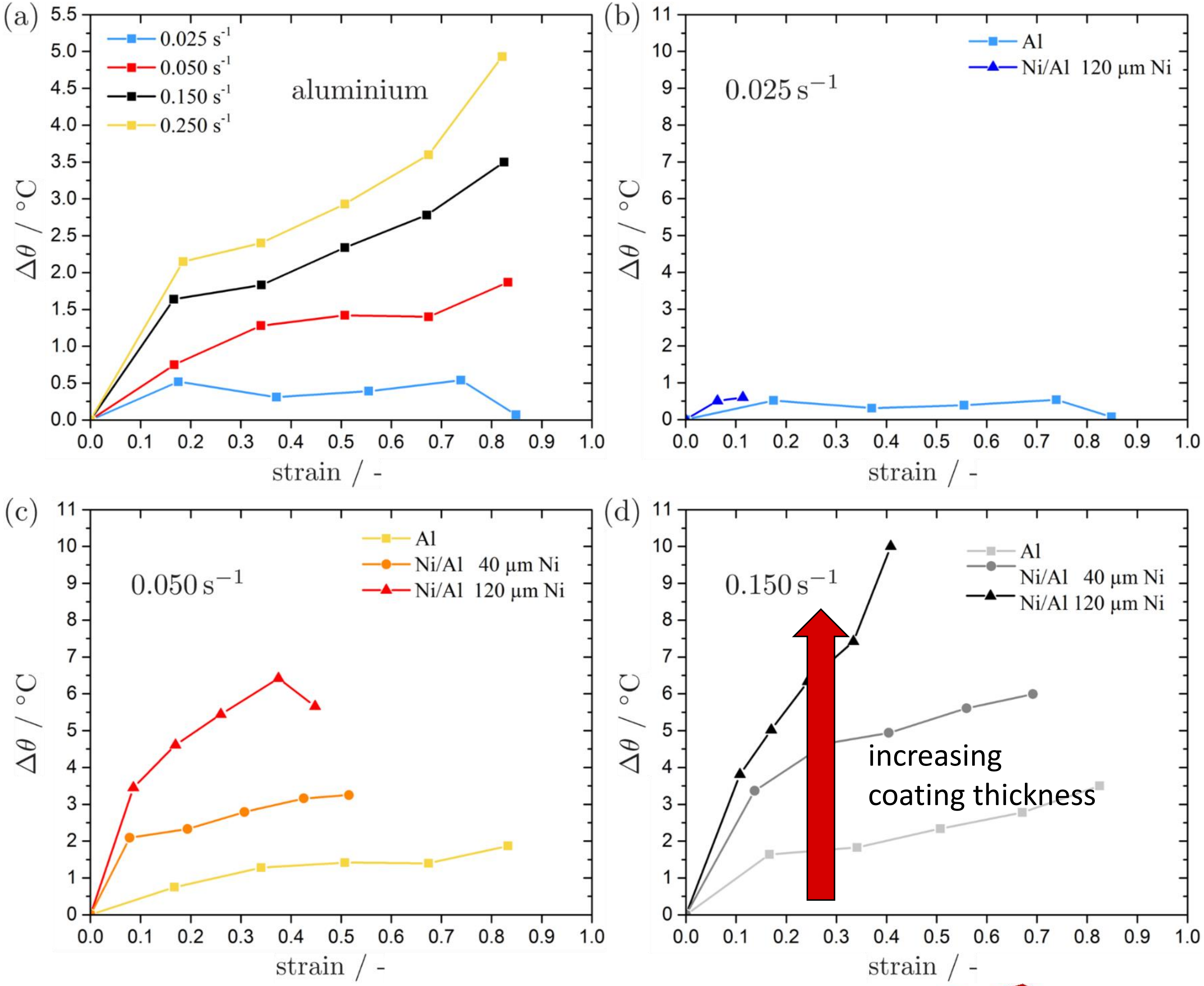

A. Jung, S. Bronder, S. Diebels, M. Schmidt, S. Seelecke
Mater. Des. 160, 363-370 (2018)

AG Foams and Metamaterials
apl. Prof. Dr.-Ing. Dr. rer. nat. Anne Jung

Deformation Analysis by Thermography and DIC

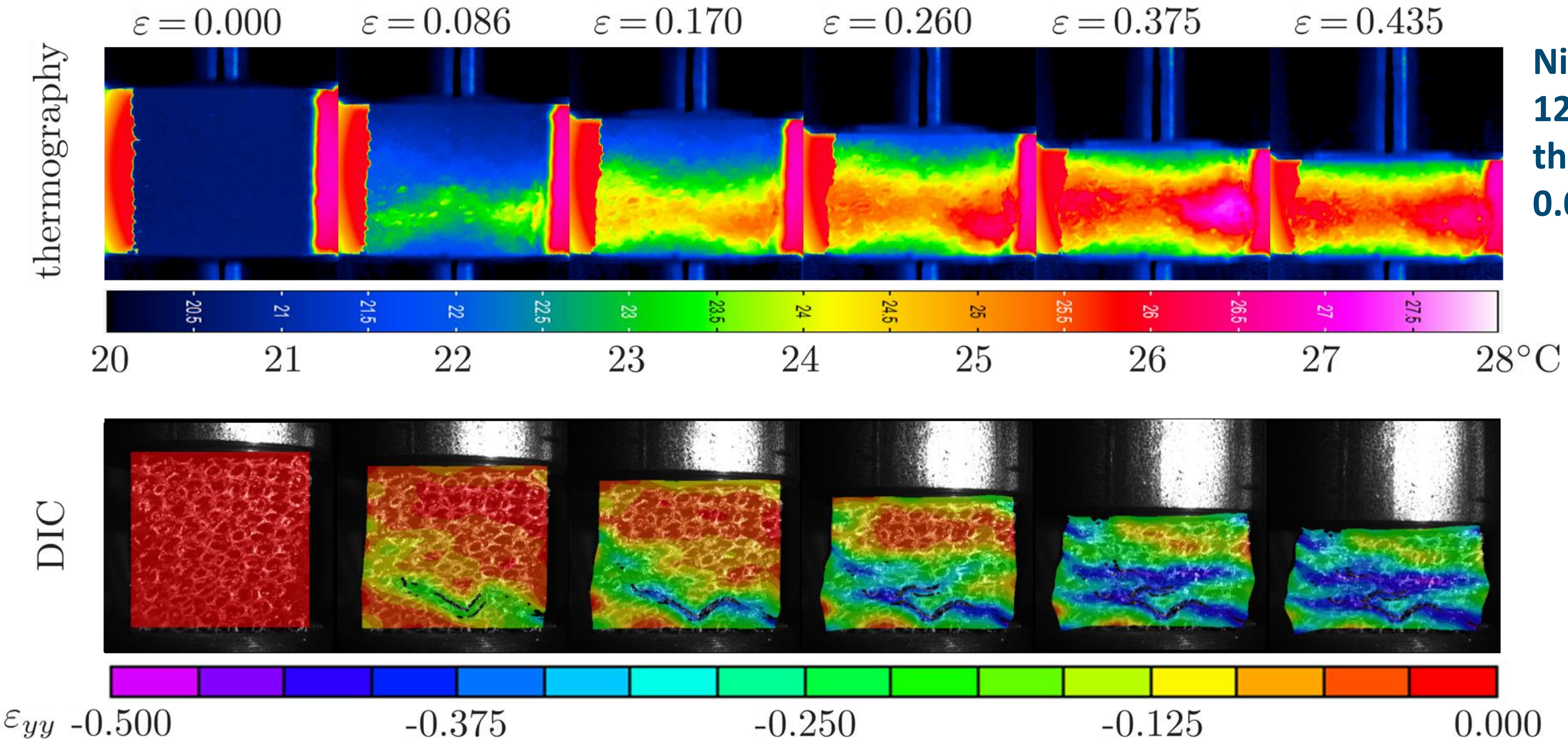

Ni/Al foams
120 µm coating thickness
0.050 s^{-1}

A. Jung, S. Bronder, S. Diebels, M. Schmidt, S. Seelecke
Mater. Des. 160, 363-370 (2018)

Automated Correlation of Thermography and UV-DIC

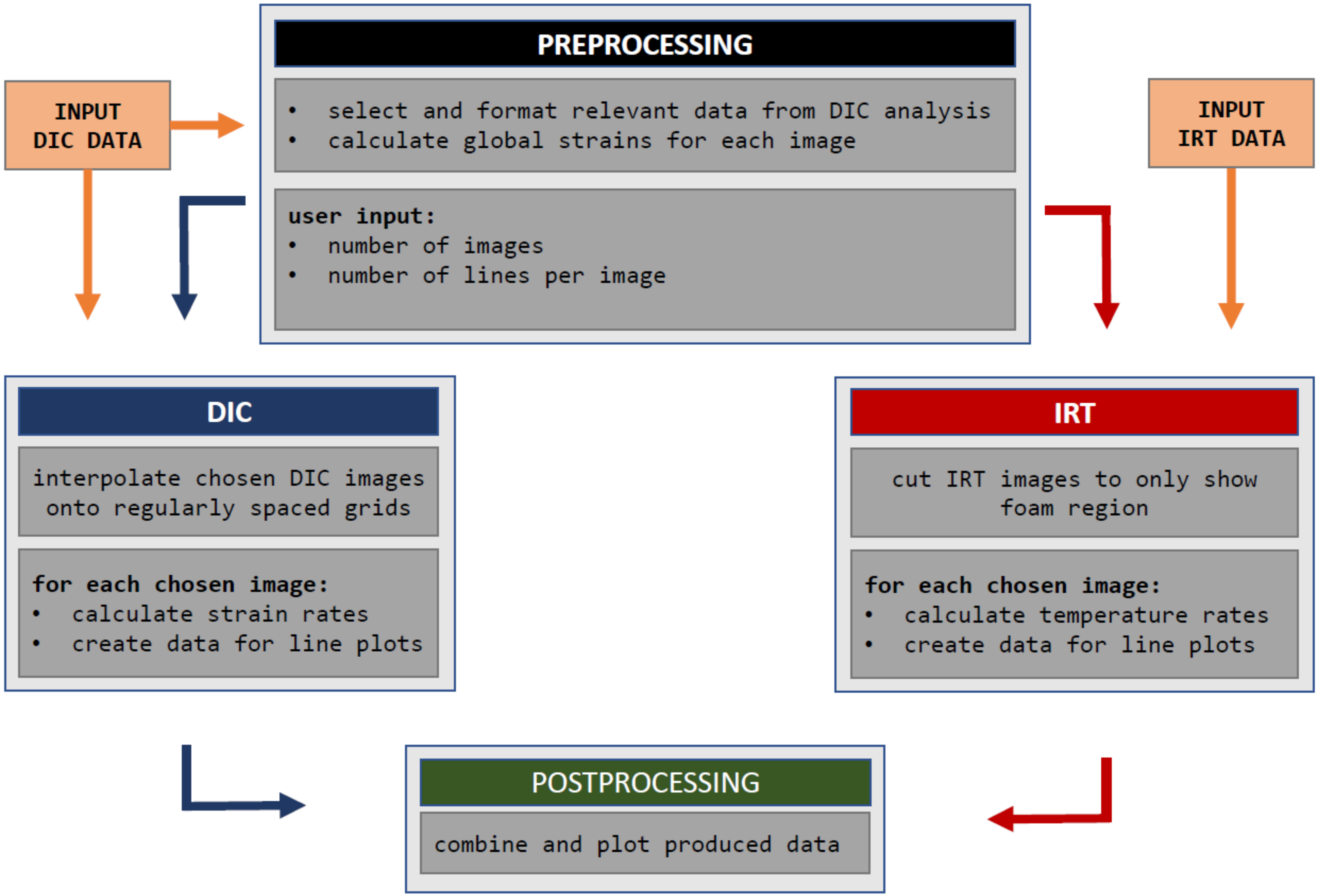

Automated Correlation of Thermography and UV-DIC

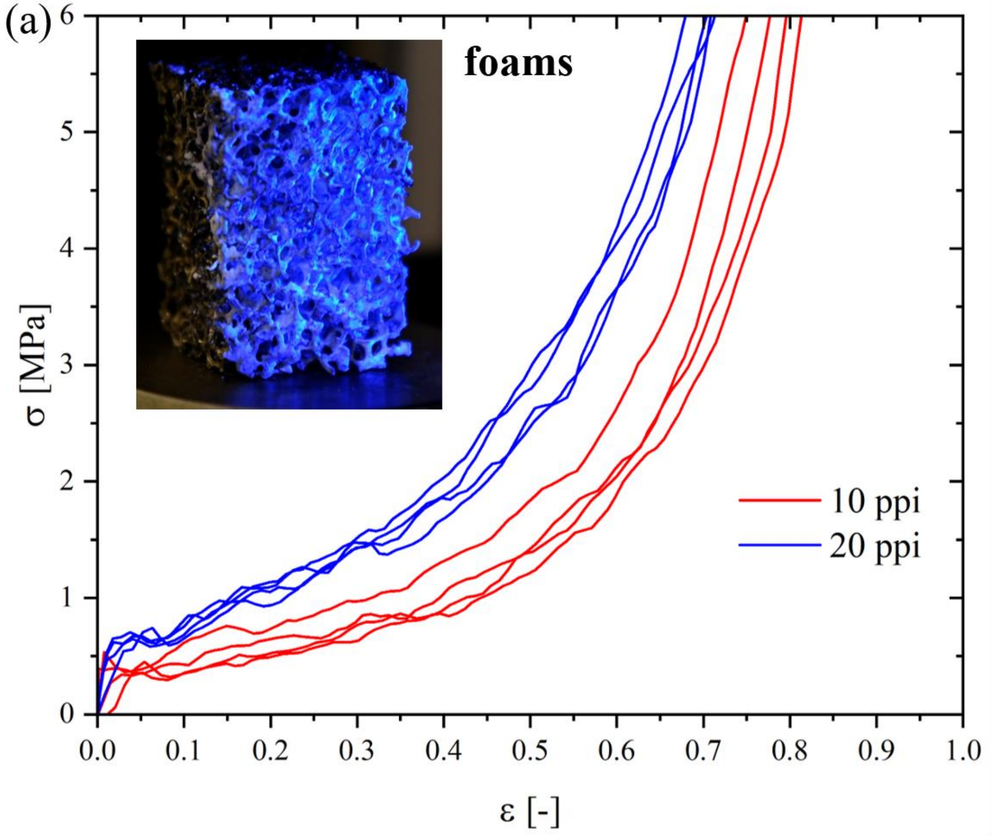

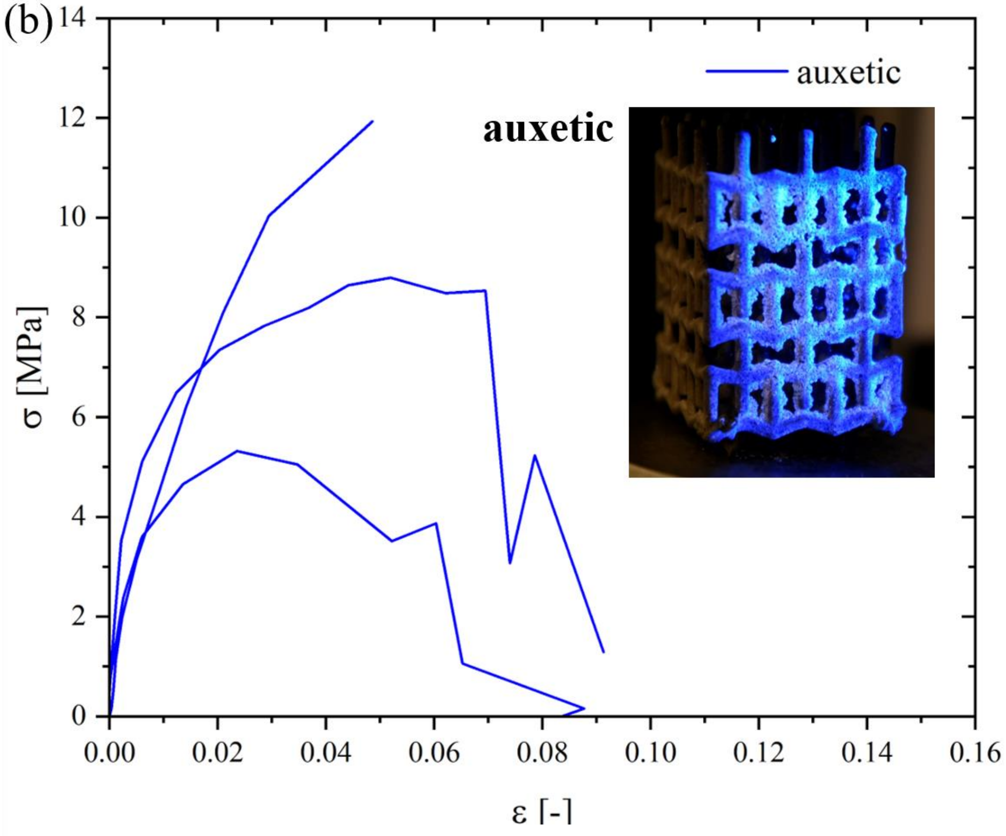

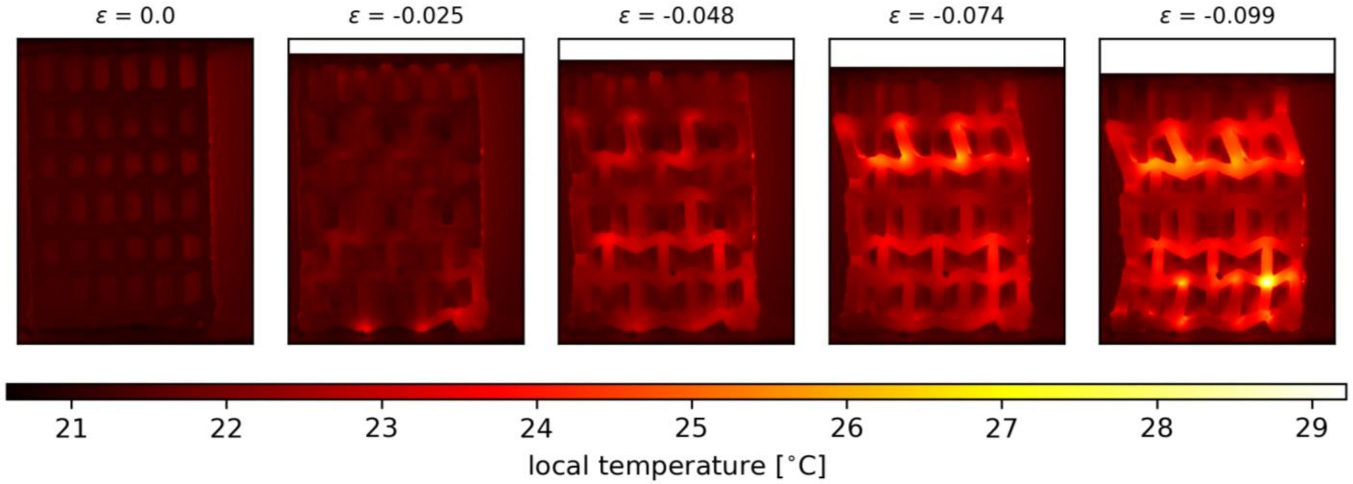

S. Grednev, S. Bronder, F. Kunz, M. Reis, S.-M. Kirsch, F. Welsch, S. Seelecke, S. Diebels, **A. Jung**
GAMM-Mitteilungen 45 (3-4), e202200014 (2022)

Automated Correlation of Thermography and UV-DIC

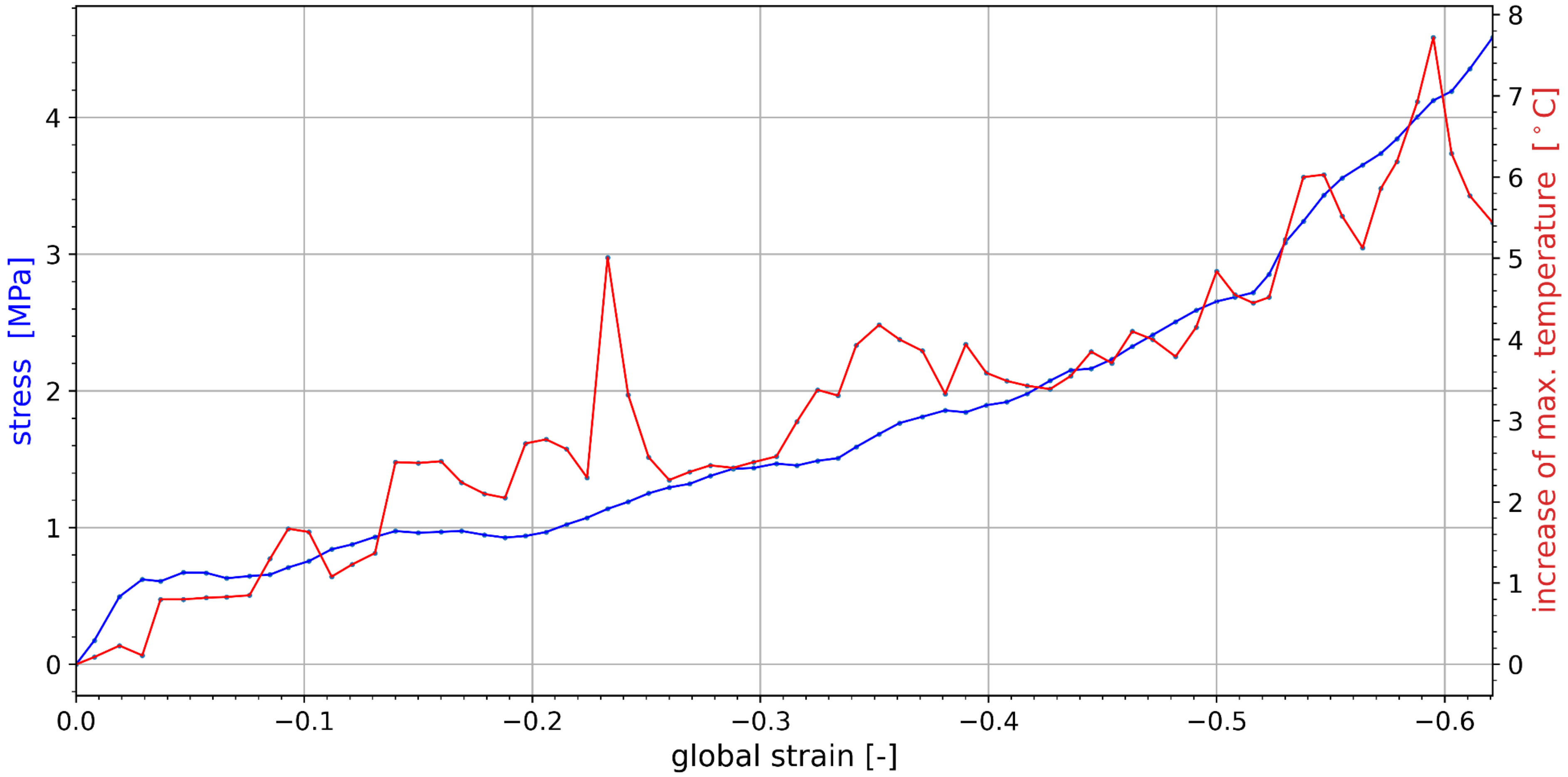

S. Grednev, S. Bronder, F. Kunz, M. Reis, S.-M. Kirsch, F. Welsch, S. Seelecke, S. Diebels, **A. Jung**
GAMM-Mitteilungen 45 (3-4), e202200014 (2022)

Multiaxial Loading – Yield Surfaces

Uniaxial tension/compression

When does failure occur in the specimen?

$$\begin{pmatrix} \sigma_{11} & 0 & 0 \\ 0 & 0 & 0 \\ 0 & 0 & 0 \end{pmatrix}$$

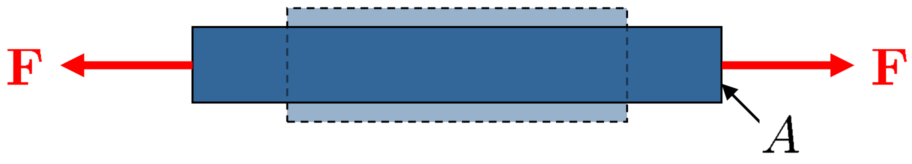

$$\sigma = \frac{F}{A}$$

Failure occurs

- Stress larger than yield stress (yielding)
- Stress larger than ultimate tensile strenght (fracture)

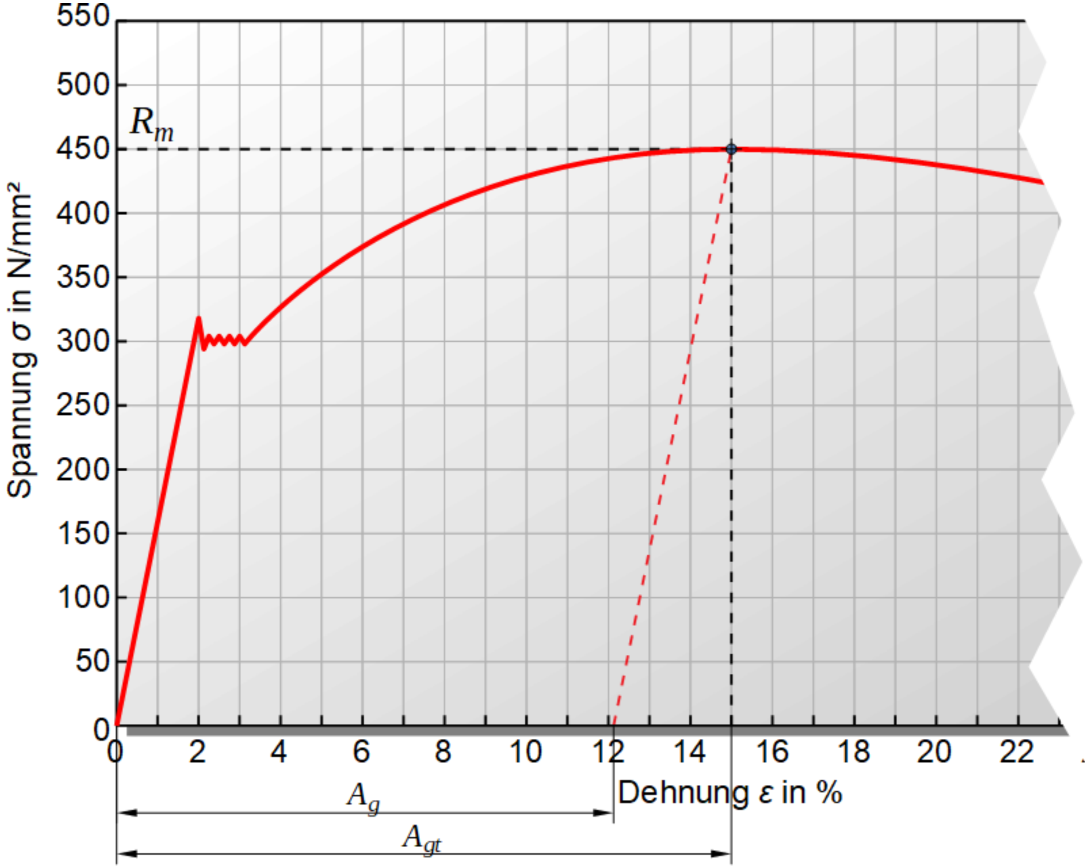

Universität des Saarlandes
Lehrstuhl für Technische Mechanik
AG Foams and Metamaterials
apl. Prof. Dr.-Ing. Dr. rer. nat. Anne Jung

Multiaxial Loading – Yield Surfaces

Multiaxial loading

When does failure occur in the specimen?

$$\begin{pmatrix} \sigma_{11} & \sigma_{12} & \sigma_{13} \\ \sigma_{21} & \sigma_{22} & \sigma_{23} \\ \sigma_{31} & \sigma_{32} & \sigma_{33} \end{pmatrix}$$

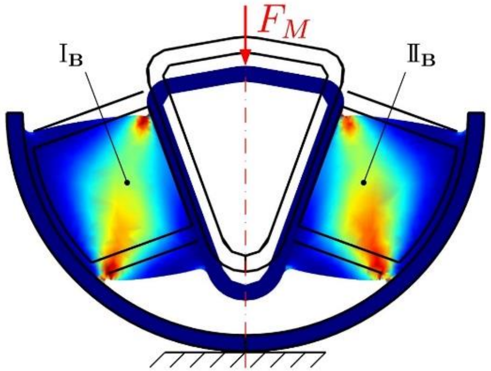

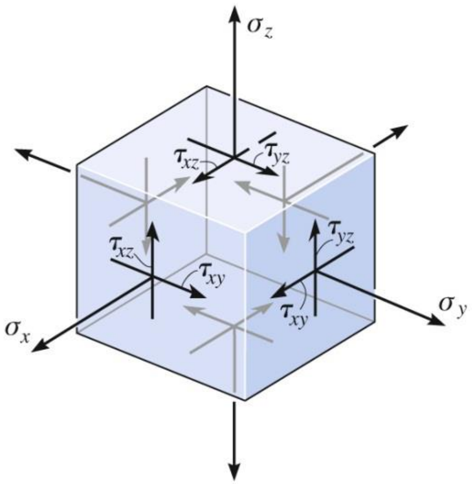

[Seibert2017]

Russell C. Hibbeler – Technische Mechanik 2 – Festigkeitslehre – 8., aktualisierte Auflage © Pearson 2013

Real components

- Usually form a multiaxial stress state under loading
- e.g. superposition of compression with torsion, multiaxial tensile or compressive stresses or bending with superimposed torsion

?

3D yield curve?
3D yield stress?

Multiaxial Loading – Yield Surfaces

- Failure under multiaxial loading ⇒ yield surfaces needed
- Yield surfaces
  - Define elastic and plastic regimes
  - Principal stress space (a) ⇒ $F(\sigma_1, \sigma_2\,\sigma_3)$
  - Deviatoric plane (b) ⇒ $F(I_1, J_2\,J_3)$
  - Hydrostatic plane (c) ⇒ $F(\theta, z\,r)$

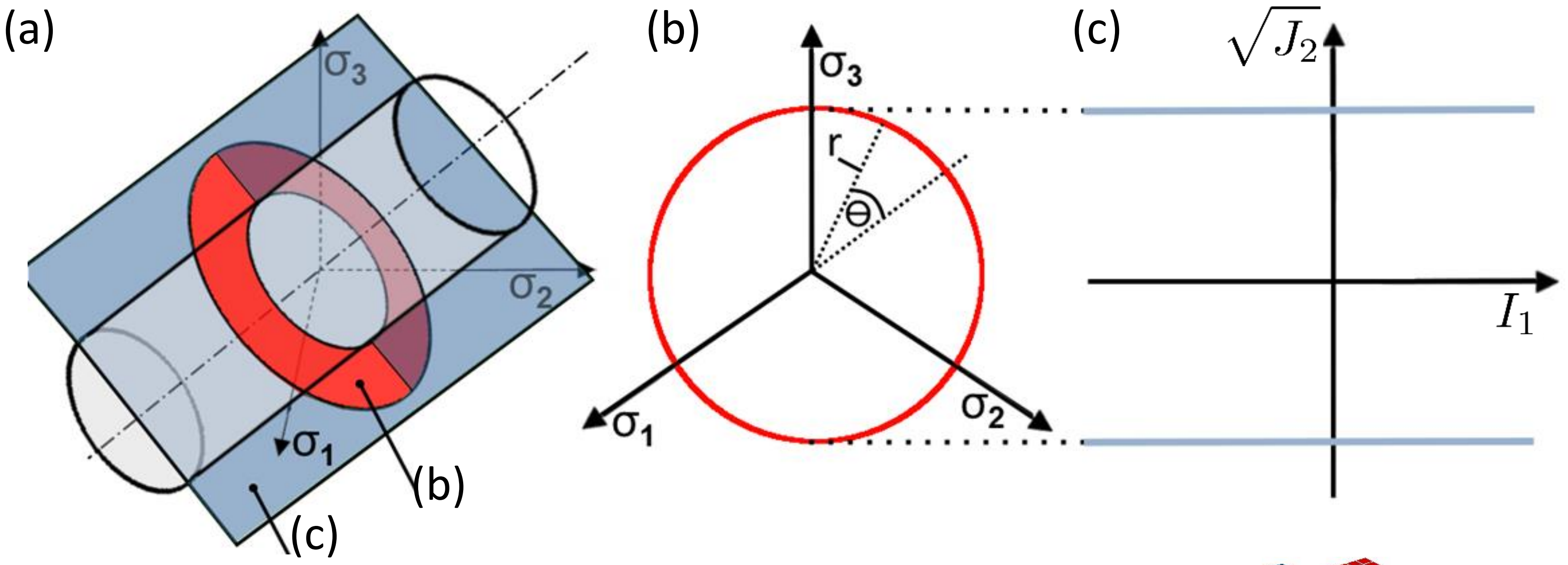

Multiaxial Loading – Yield Surfaces

- **Foams require:**
  - Closed yield surface $\Rightarrow$ compressibility
  - Difference in compression and tensile failure
    $\Rightarrow$ shift or asymmetry
  - Convexity of the yield surface

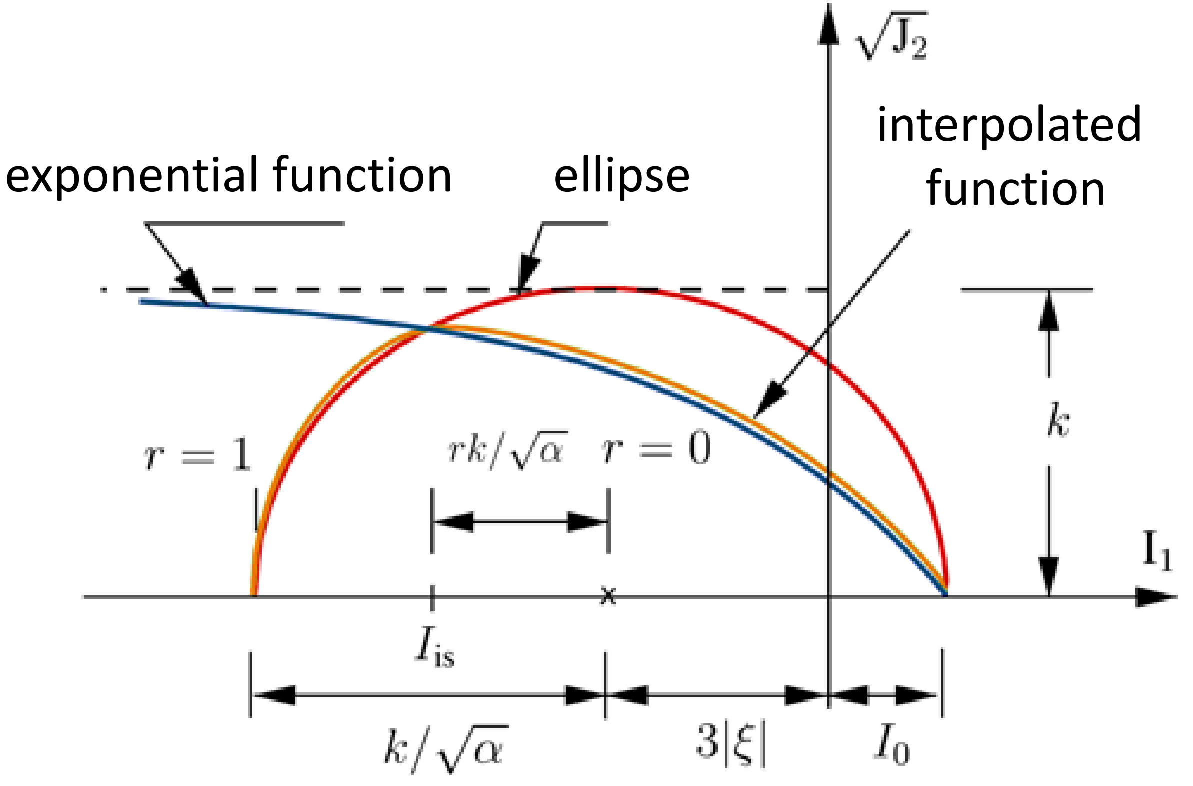

- **Yield surface of Bier et al. [1]**
  - Asymmetric single-surface yield criterion introduced for compacted powder
  - log-log-interpolation
    of ellipse and exponential function

$$F = c \cdot k \ln\left(\frac{e^{(g_1 / c \cdot k)} + e^{(g_2 / c \cdot k)}}{2}\right)$$

$$g_1 = \sqrt{J_2 + \alpha\,(I_1 - 3\,\xi)^2} - k$$

$$g_2 = \sqrt{J_2} - k + A_1\, e^{(A_2\, I_1)}$$

[1] W. Bier, S. Hartmann
Eur. J. Mech. A-Solids 25(6), 1009-1030 (2006)

Multiaxial Loading – Experimental Methodology

Realisation of different shear stress states with different superimposed loads

[0] Specimen preparation of undeformed specimen

[1] **Uniaxial preloading** of specimen up to x % of failure stress

[2] **Torsional loading** of specimen up to failure under **superimposed** constant **uniaxial loading**

[0] undeformed

[1] preloading (% PCS)

[2] superimposed uniaxial load + 90° torsion

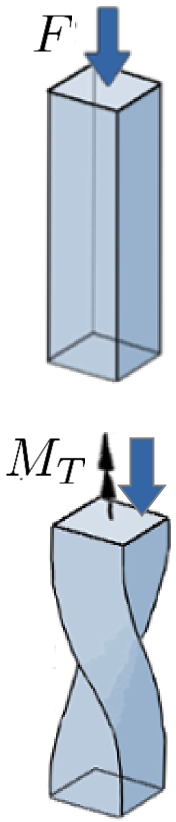

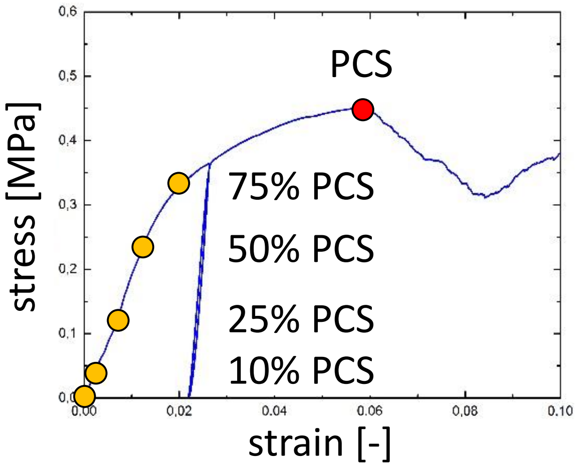

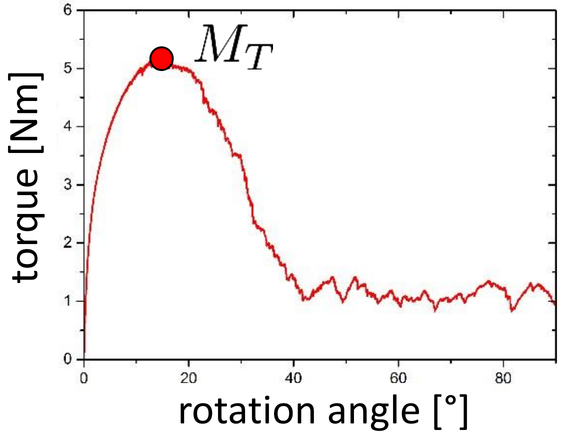

Multiaxial Loading – Experimental Setup

- Cuboid specimens of 10 ppi/20 ppi Al foams and 20 ppi Ni/PU hybrid foams cut from in-plane direction
- Infiltration of open porous foam structure by polymeric resin to guarantee for clamping
  ⇒ remaining height : width = 2:1
- Cuboid specimens
  ⇒ problem of **warping torsion**
  ⇒ Saint Venant torsion with correction factor

$$\tau = \frac{3 + 1.8\,(depth/widh)}{width \cdot depth^2} M \qquad \text{and}$$

$$\gamma = \frac{depth\,\theta}{height} \left(1 - 0.378 \frac{depth^2}{width^2}\right)$$

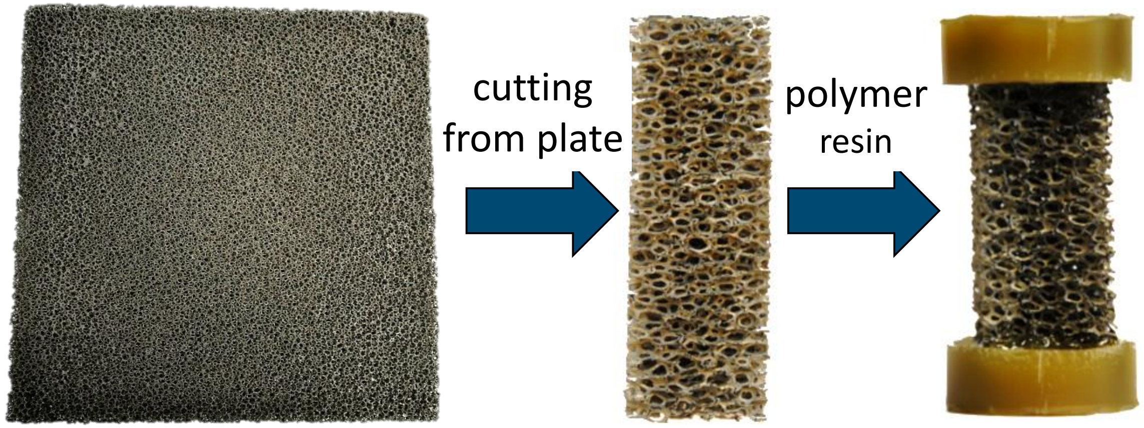

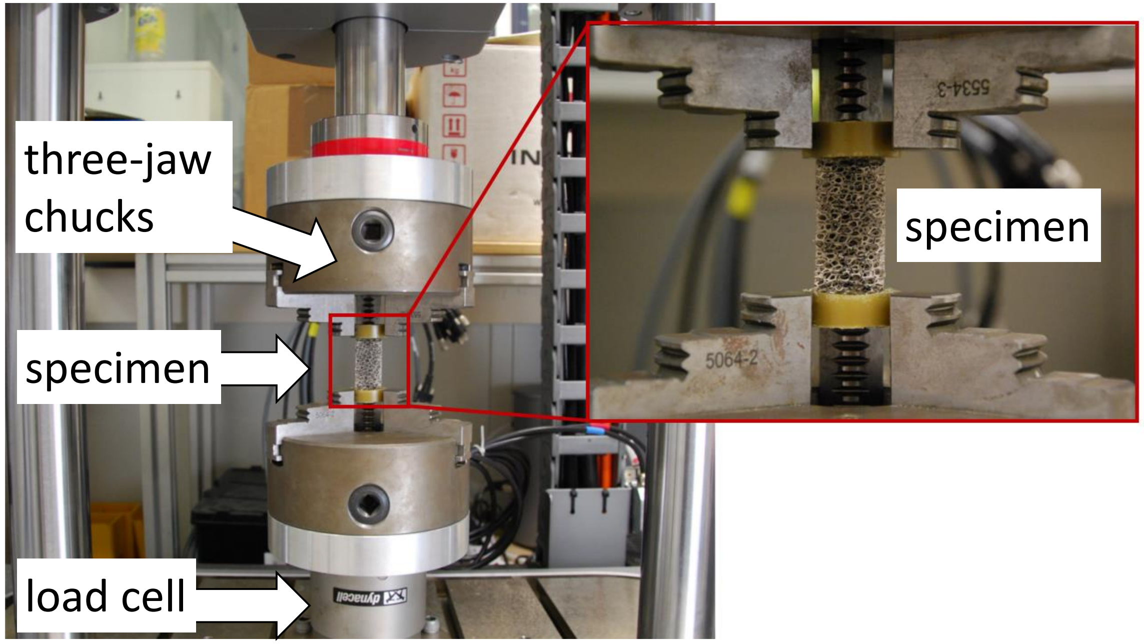

M. Felten, S. Diebels, **A. Jung**
Mater. Sci. Eng. A 791, 139762 (2020)
AG Foams and Metamaterials
apl. Prof. Dr.-Ing. Dr. rer. nat. Anne Jung

Multiaxial Loading – Al Foams

- Elliptic, symmetric yield surface for 10 ppi foams
- Equal failure stress for tensile and compression loading
- Highest failure stresses for torsion loading

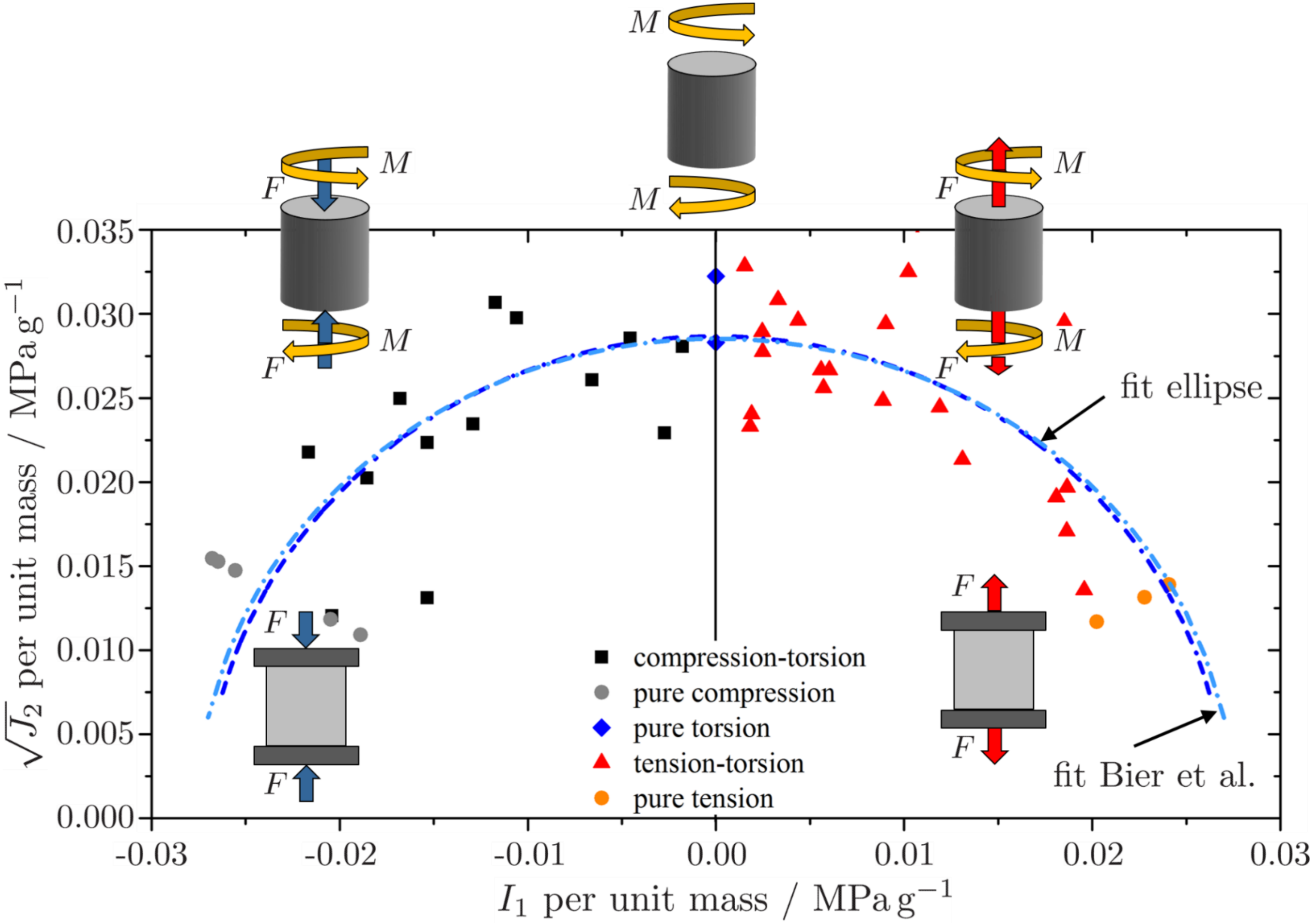

A. Jung, S. Diebels
Mater. Des. 131, 252-264 (2017)

Multiaxial Loading – Al Foams

- Yield surface depends on strut geometry
- 10 ppi: elliptic yield surface
- 20 ppi: asymmetric yield surface

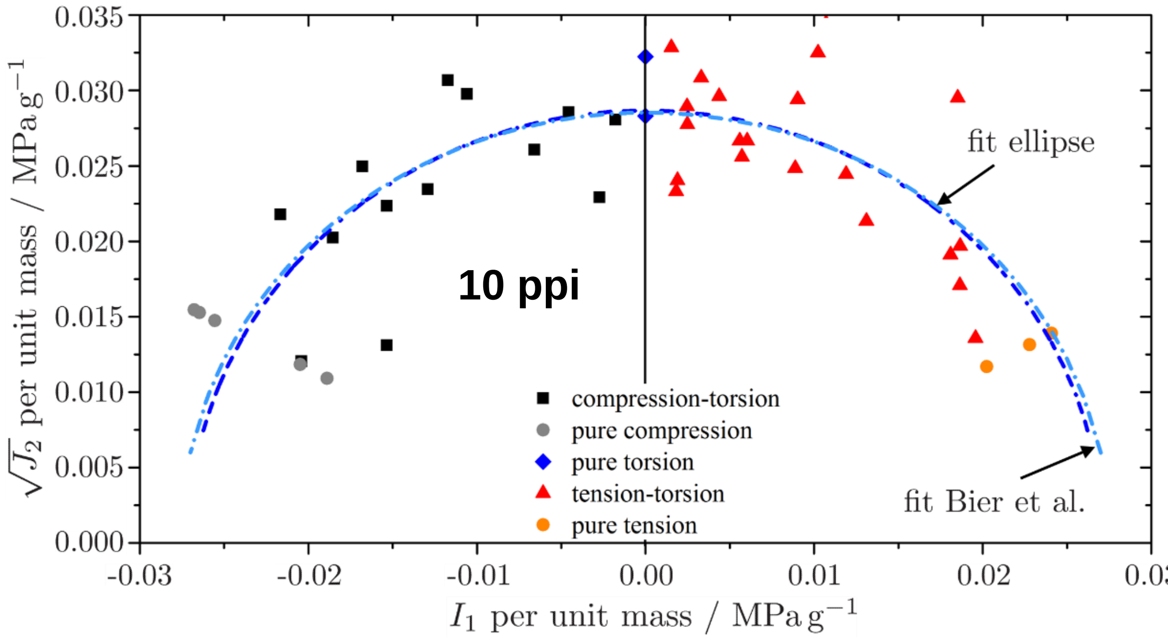

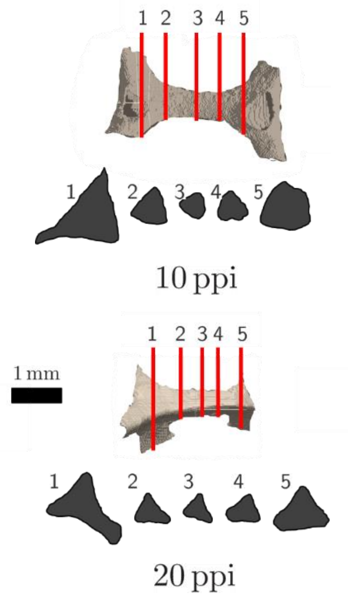

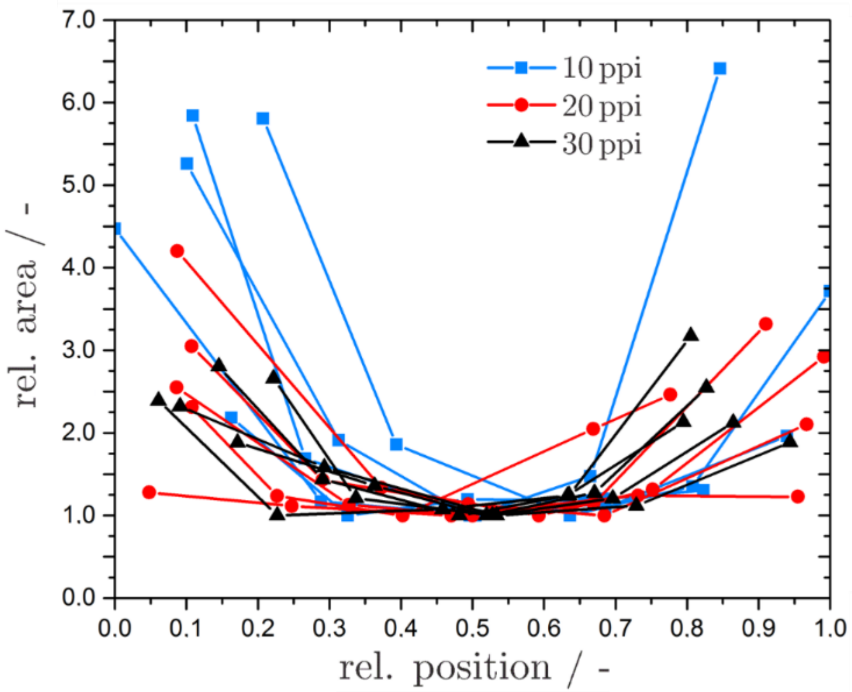

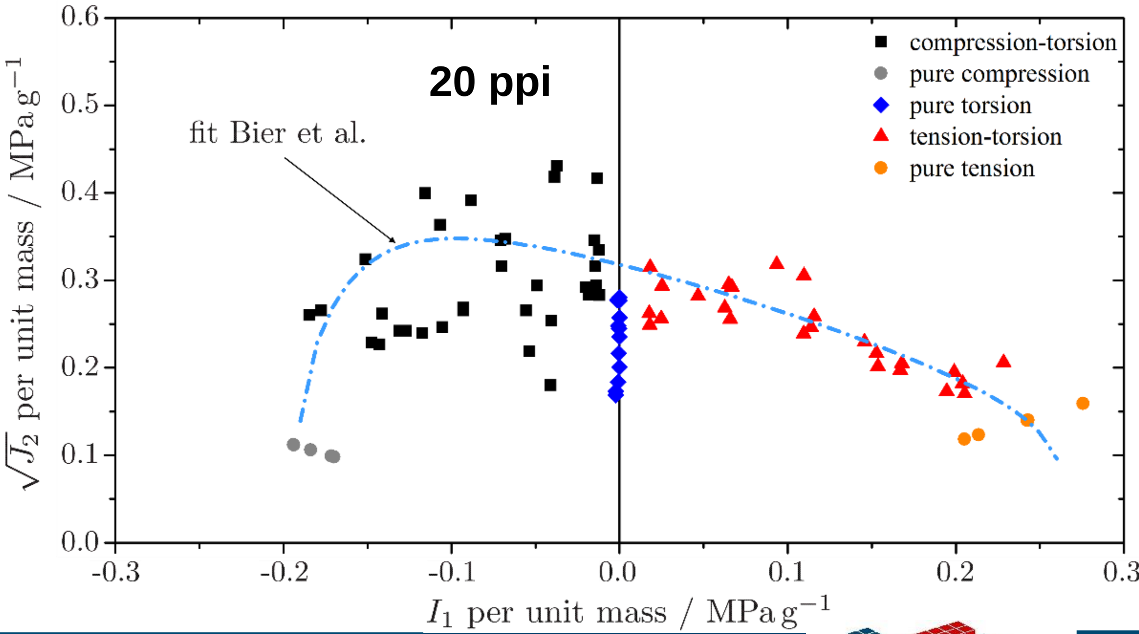

Universität des Saarlandes
Lehrstuhl für Technische Mechanik
A. Jung, S. Diebels
Mater. Des. 131, 252-264 (2017)
AG Foams and Metamaterials
apl. Prof. Dr.-Ing. Dr. rer. nat. Anne Jung

Multiaxial Loading – Ni/PU Hybrid Foams: Initial Yield Surface

coating thickness: 100 µm

- **Elliptic** yield surface
- ↑ hydrostatic stress component
  ⇒ ↓ deviatoric stress component
- Yield surface **symmetrical to origin** of the coordinate system
- Use of **Green's yield surface** [2]

$$F = \left(\frac{I_1}{a}\right)^2 + \left(\frac{\sqrt{J_2}}{b}\right)^2 - 1 = 0$$

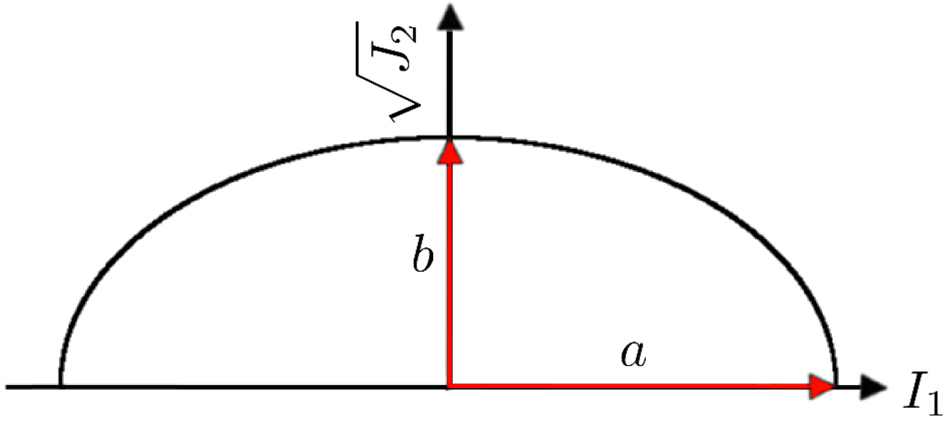

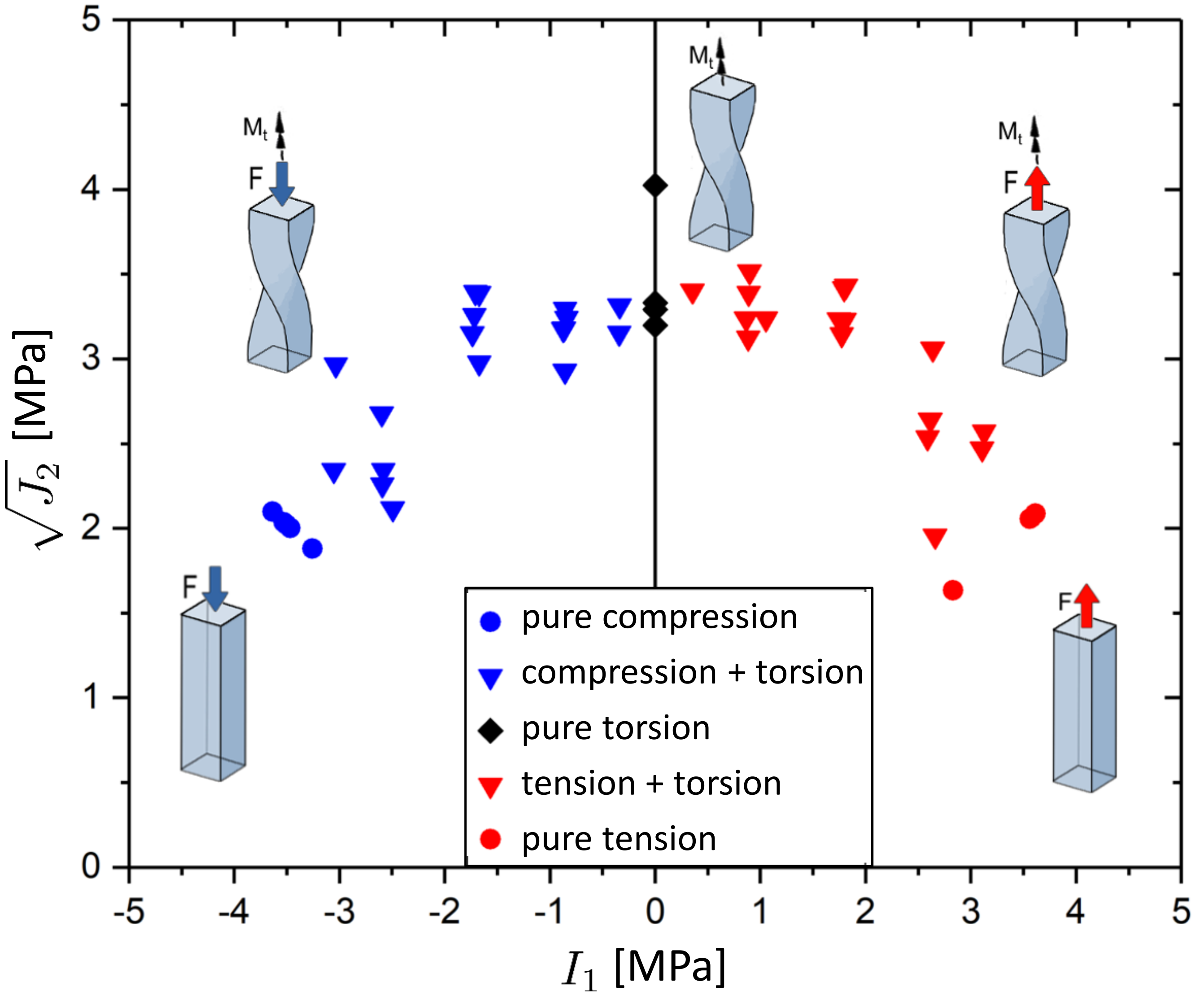

Universität des Saarlandes
Lehrstuhl für Technische Mechanik
AG Foams and Metamaterials
apl. Prof. Dr.-Ing. Dr. rer. nat. Anne Jung
[2] R. Green Int. J. Mech. Sci. 14(4), 215-224 (1972)

Multiaxial Loading – Ni/PU Hybrid Foams: Initial Yield Surface

[2] R. Green
Int. J. Mech. Sci. 14(4), 215-224 (1972)

- Yield surfaces fitted according to Green [2]
- ↑ density ⇒ ↑↑a and ↑b
- Larger influence of coating thickness and density on hydrostatic stress component

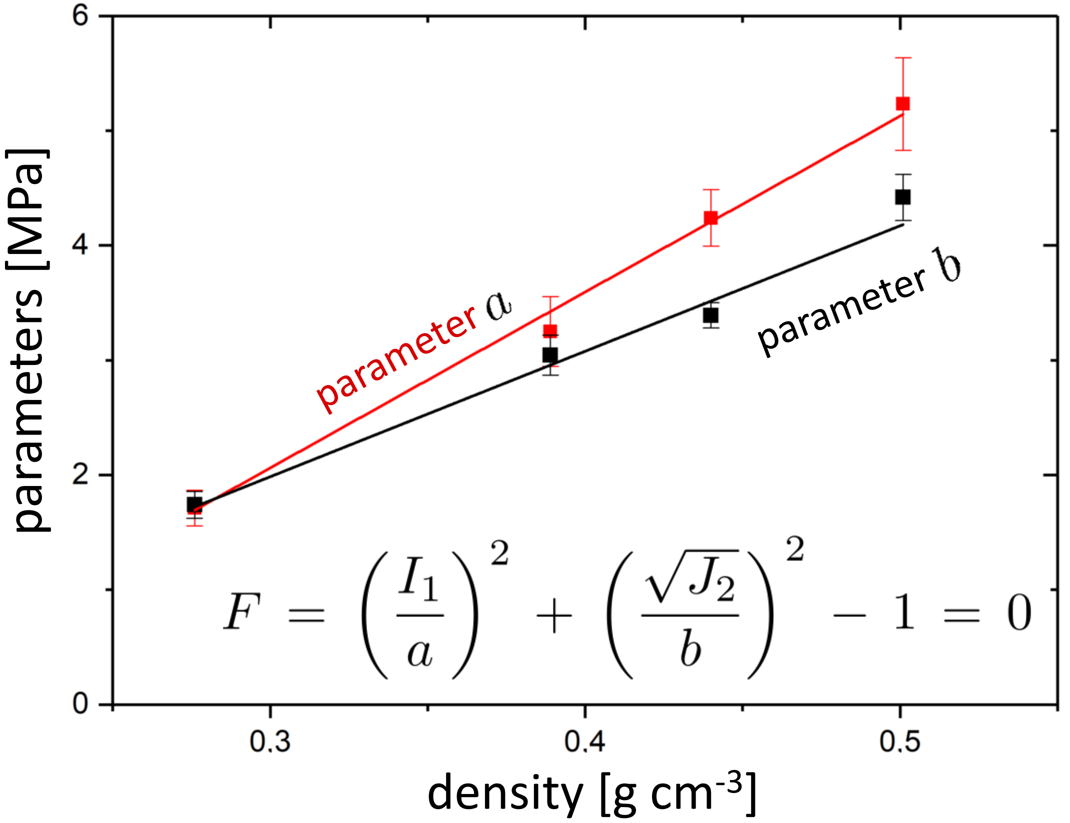

$$F = \left(\frac{I_1}{a}\right)^2 + \left(\frac{\sqrt{J_2}}{b}\right)^2 - 1 = 0$$

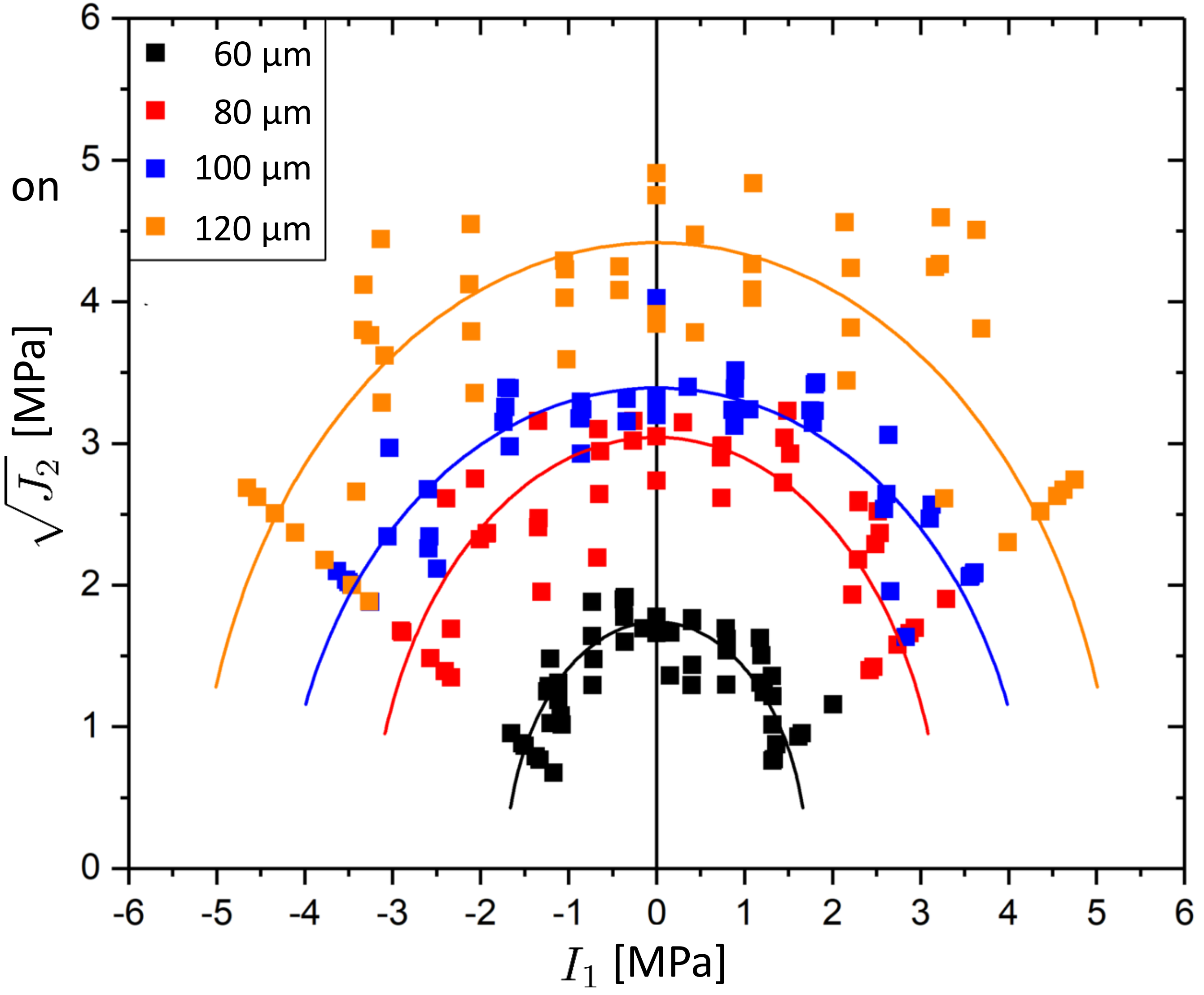

M. Felten, S. Diebels, **A. Jung**
Mater. Sci. Eng. A 791, 139762 (2020)

AG Foams and Metamaterials
apl. Prof. Dr.-Ing. Dr. rer. nat. Anne Jung

Microscale

single struts

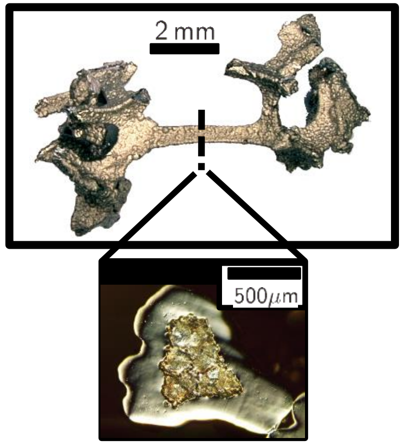

Mesoscale

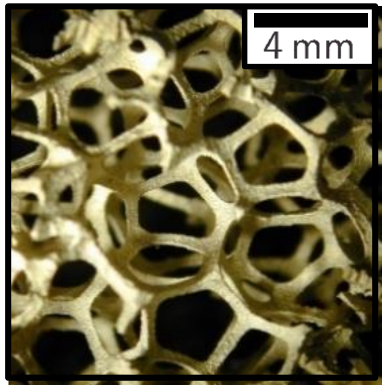

single pores

Micromaterial Properties

- Global properties depend on strut material and microstructure
- bulk properties significantly differ from those measured at single struts due to
  - different cooling rates
  - surface-to-volume ratio
  - imperfections
  - …

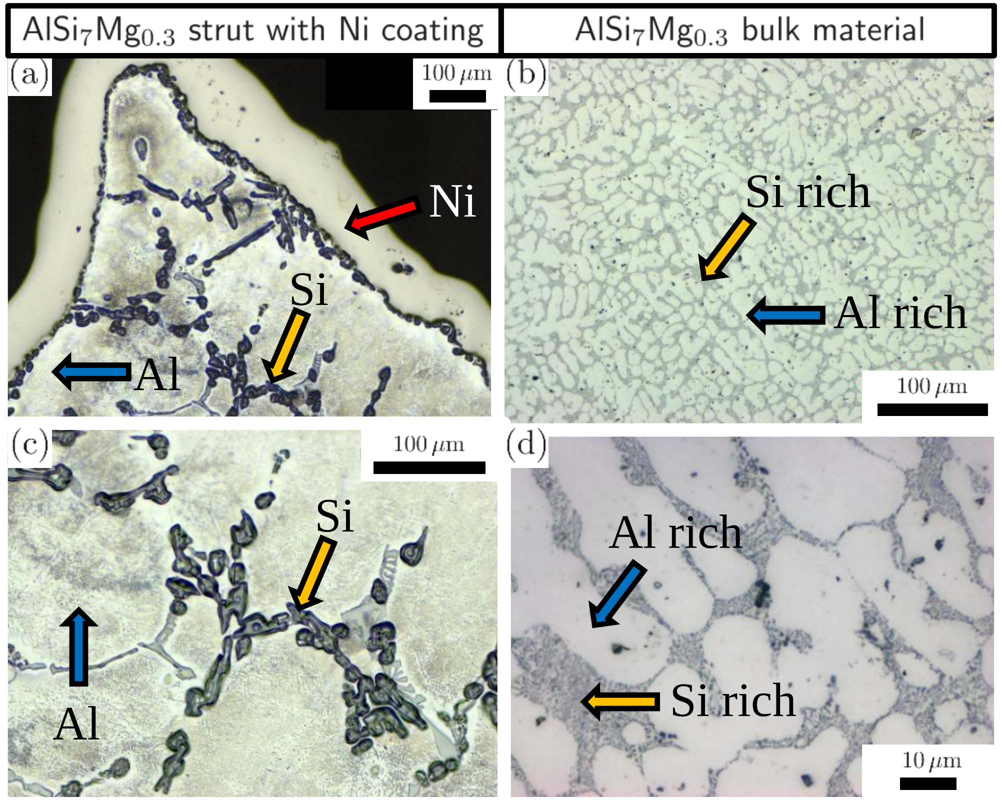

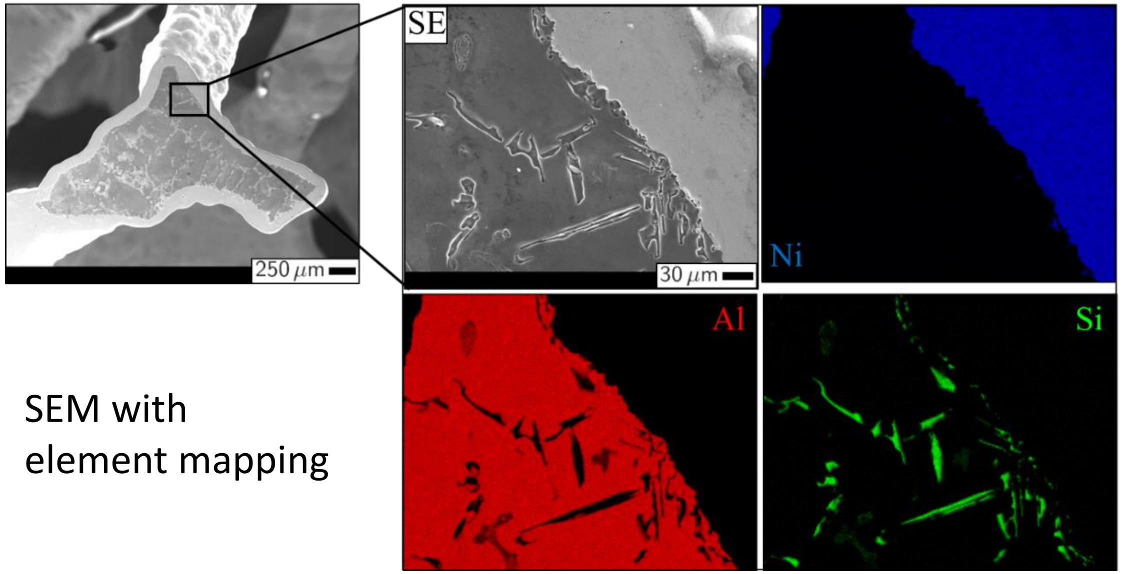

SEM with element mapping

- **Micromechanical testing** very challenging
  ⇒ Pioneering work in this field

A. Jung, Z. Chen, J. Schmauch, Ch. Motz, S. Diebels
Acta Mater. 102, 38-48 (2016)

Universal Microtesting Device

- Microtesting device
- Max. force 6 kN
- Spatial resolution from
  - 0.2 µm up to 1.5 kN to
  - 3 µm at 6 kN
- Max. speed 5 mm/s
- **Tensile and Compression**

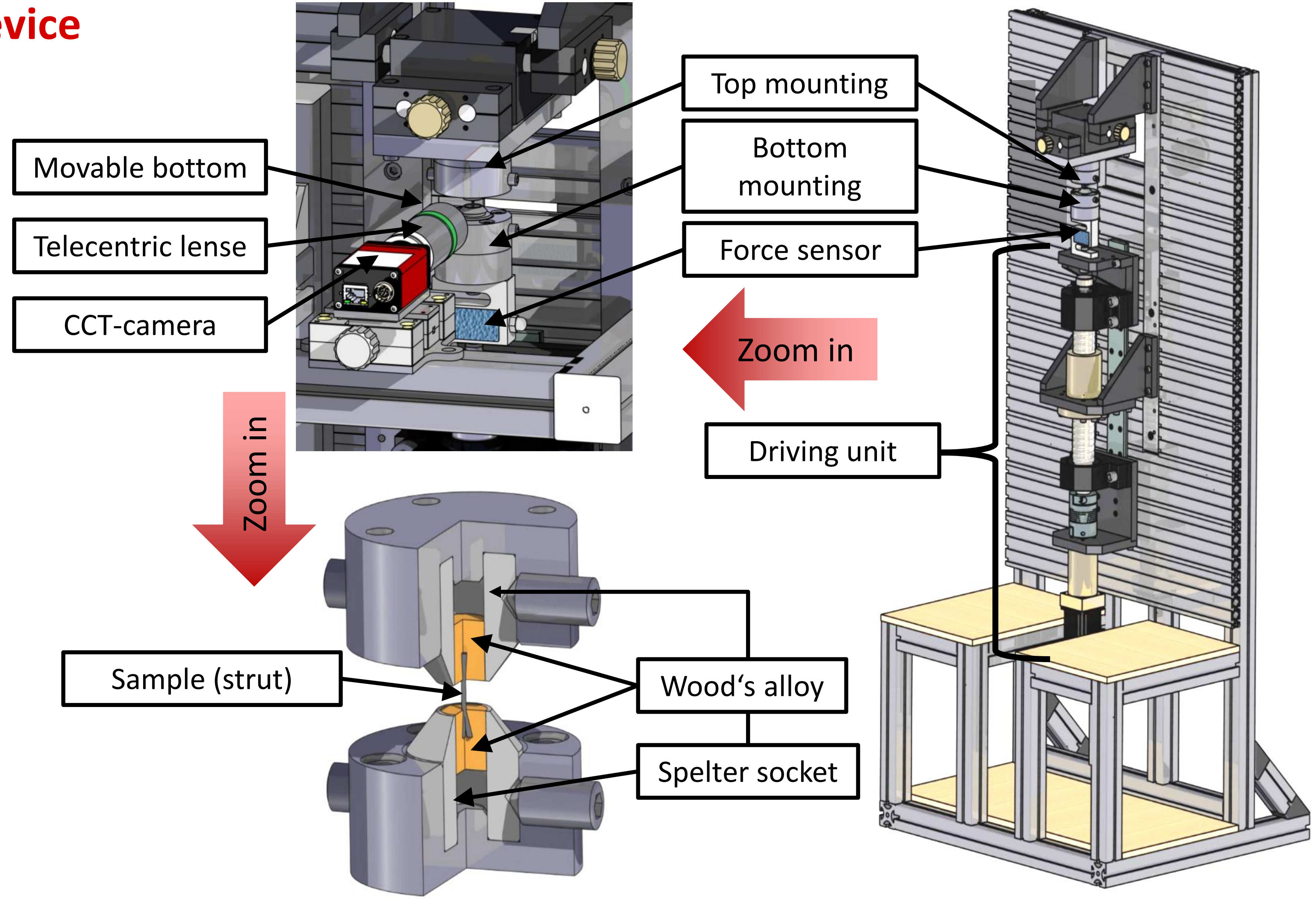

M. Reis, K. König, S. Diebels, **A. Jung**
Materials 13 (17), 3746 (2020)

AG Foams and Metamaterials
apl. Prof. Dr.-Ing. Dr. rer. nat. Anne Jung

Universal Microtesting Device

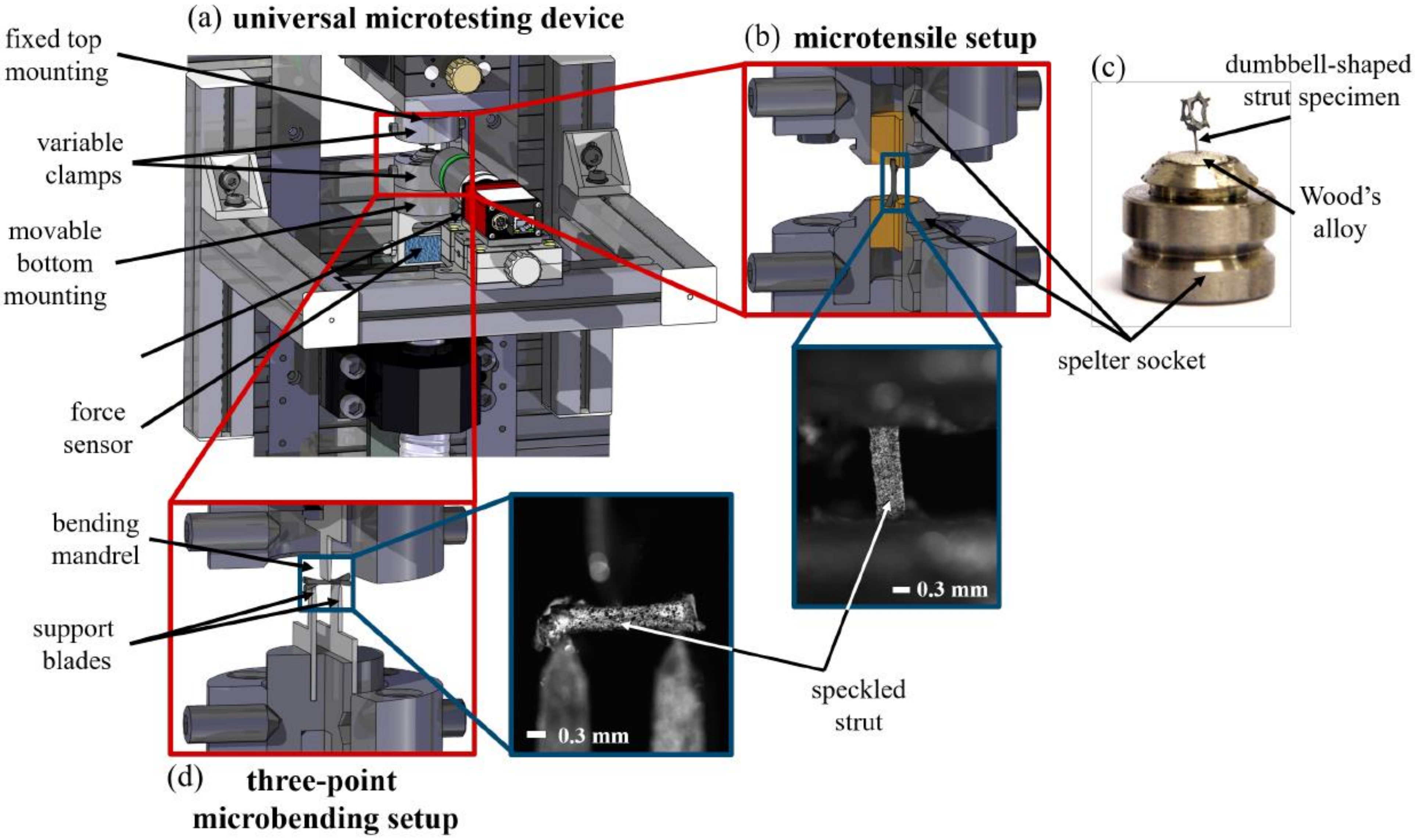

M. Reis, K. König, S. Diebels, **A. Jung**
Materials 13 (17), 3746 (2020)

Universal Microtesting Device

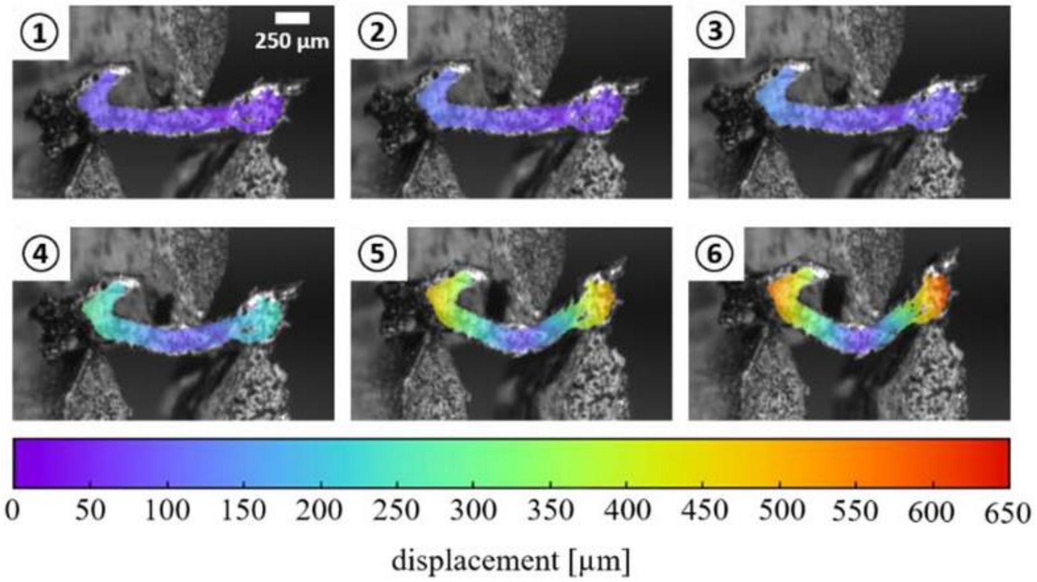

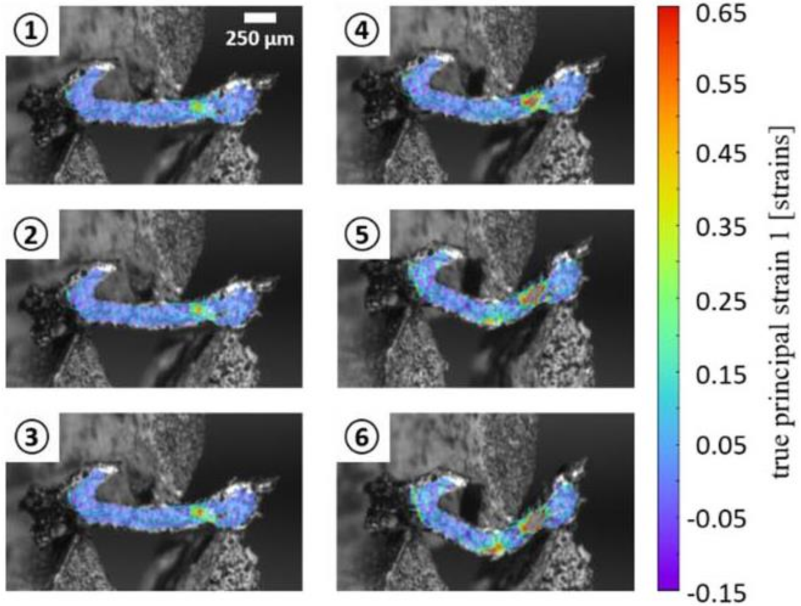

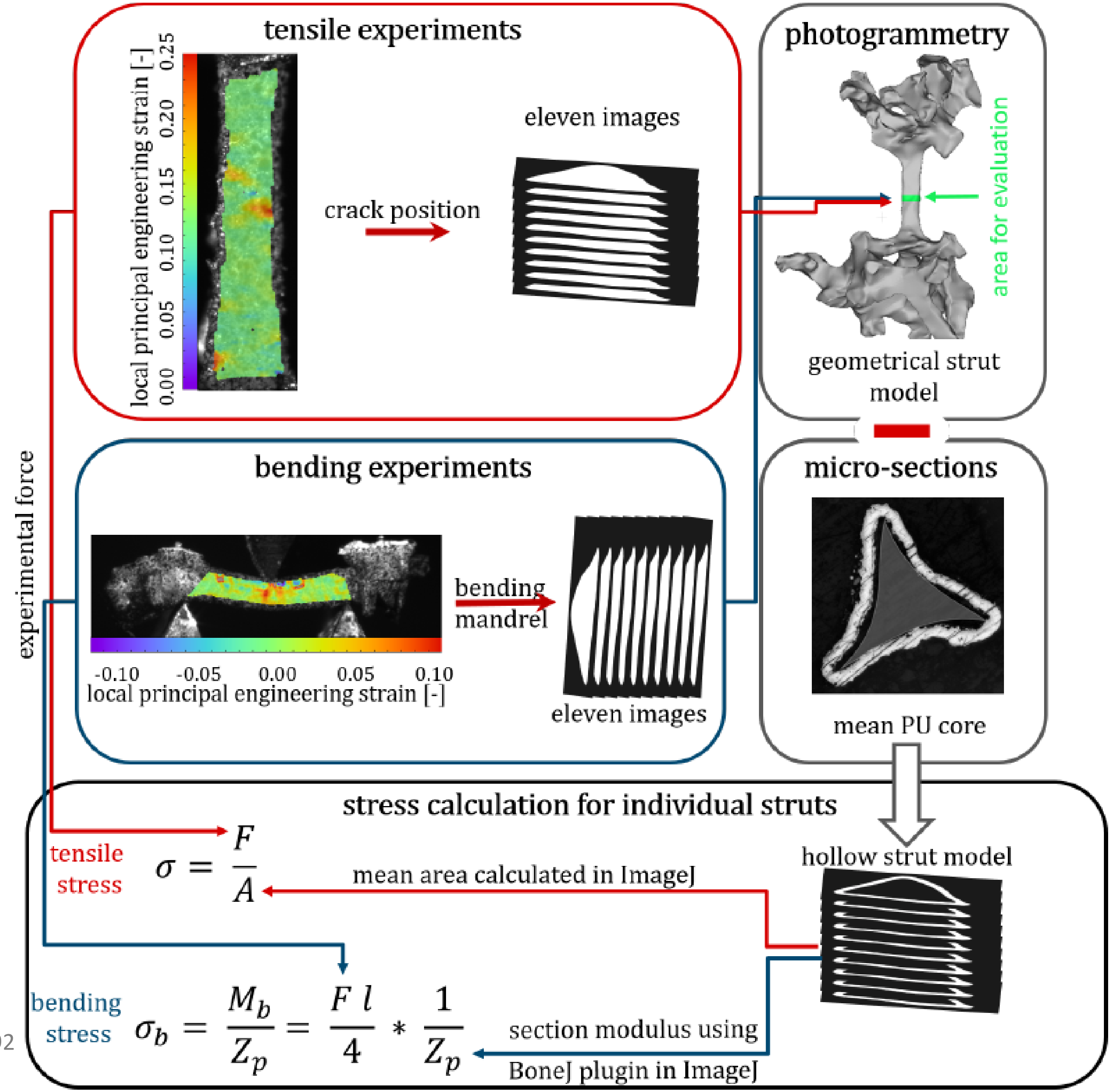

M. Reis, M. Adorna, O. Jiroušek, **A. Jung,** Adv. Eng. Mater. 21 (7), 1900092
M. Reis, K. König, S. Diebels, **A. Jung,** Materials 13 (17), 3746 (2020)

Photogrammetry for 3D Model Generation

- Alternative method to create 3D models
- **Procedure:**
  - Print calibration target (1.5 x specimen size)
  - Place specimen in the center
  - Pictures 360° around the specimen
  - Under two different angles to the horizontal
- Custom made chamber
  - Guarantee reproducibility
  - Fix mounting points
  - Automated rotation

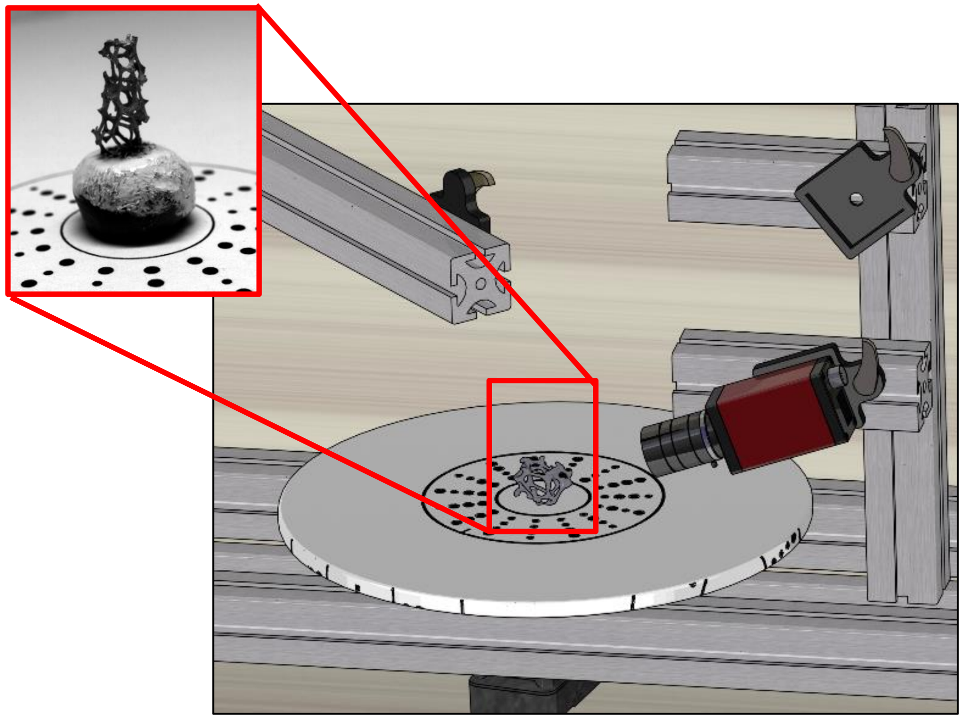

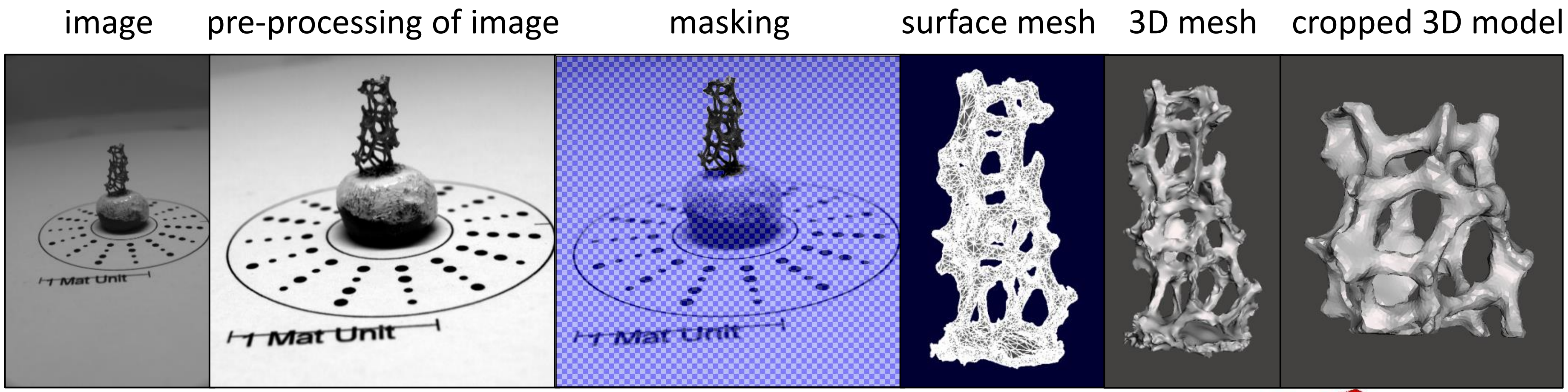

Universität des Saarlandes
Lehrstuhl für Technische Mechanik
AG Foams and Metamaterials
apl. Prof. Dr.-Ing. Dr. rer. nat. Anne Jung

Photogrammetry for 3D Model Generation

Custom-build device

Images from all sides

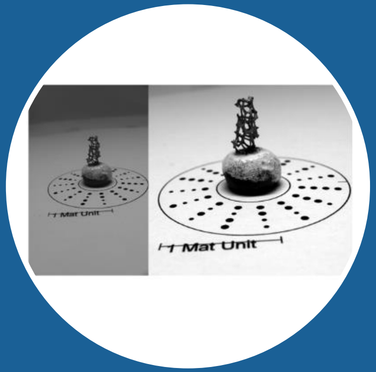

Image processing software

Crop & enhance contrast

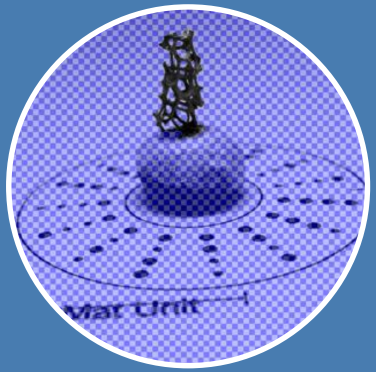

Create mask to separate background

Commercial software 3DSOM™

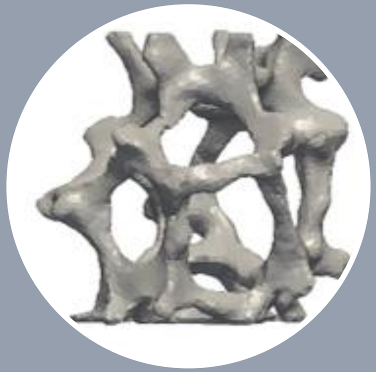

Creation of a 3D surface model (3DSOM™)

Transformation in volume mesh (e.g. LSPrepost™)

FE simulation

Inverse calculation

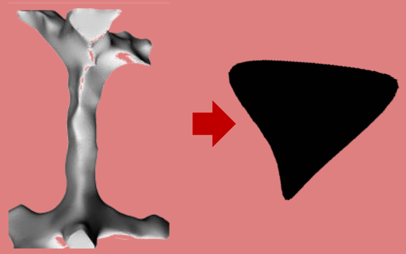

Geometry information (e.g. cross-section)

Stochastic Analysis

- CT model of a 10 ppi metal foam
- Strut length for entire foam (grey)
- Strut length for microsphere categories (corresponding to microsphere colors)
- Struts length increases with category

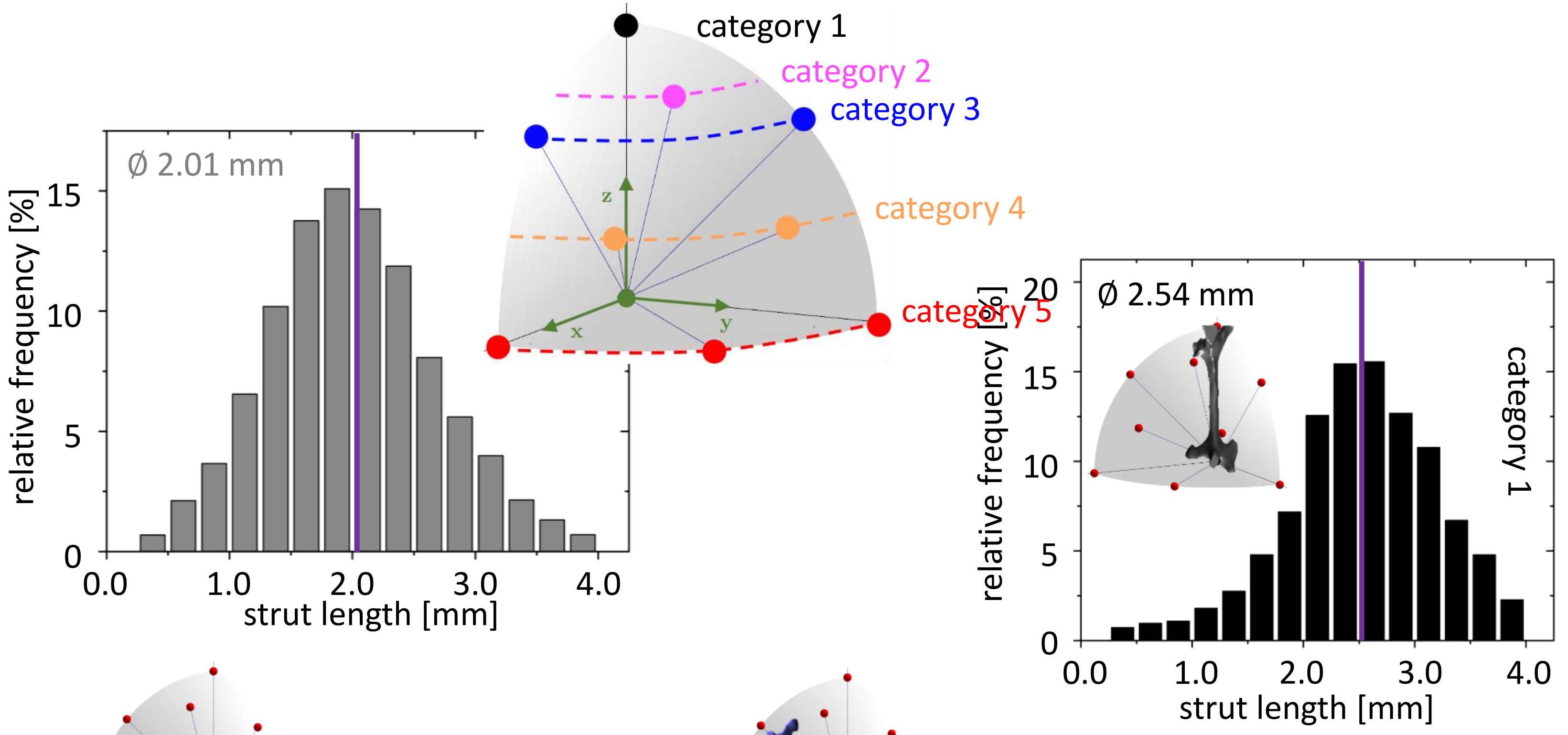

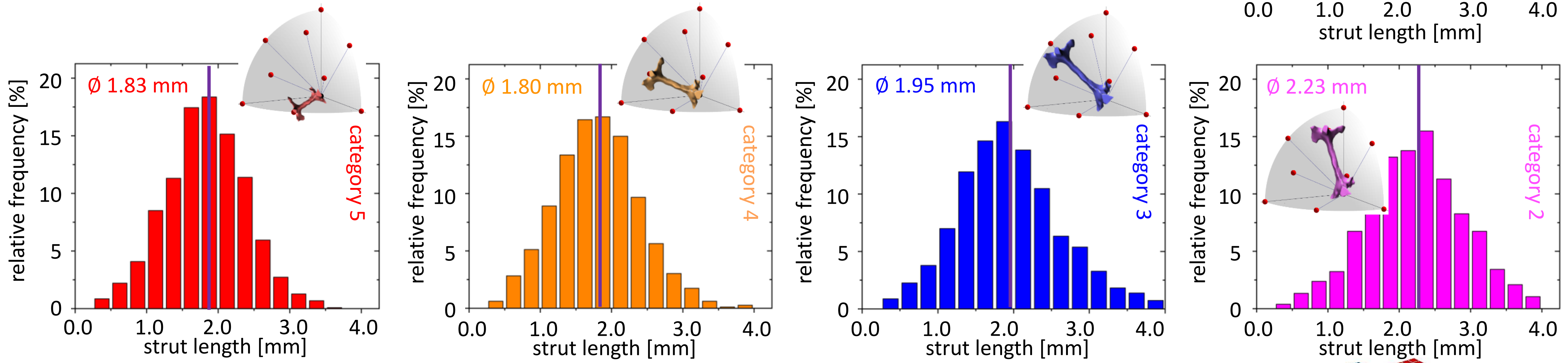

T. Bleistein, M. Reis, X. Cheng, C. Redenbach, S. Diebels, **A. Jung**
Mech. Mater. 142, 103295 (2020)

Material Parameters From Struts

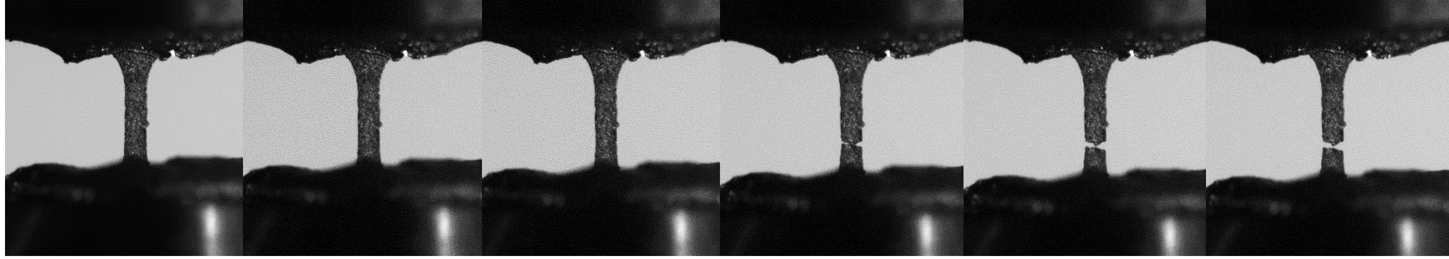

Tensile experiment

- Strain using DIC (**D**igital **I**mage **C**orrelation)
- Stress using slices through 3D geometry model

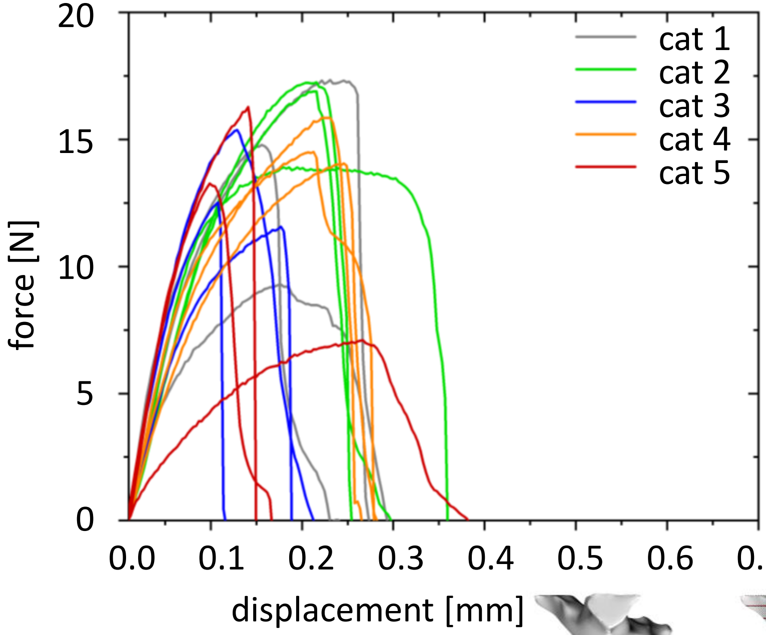

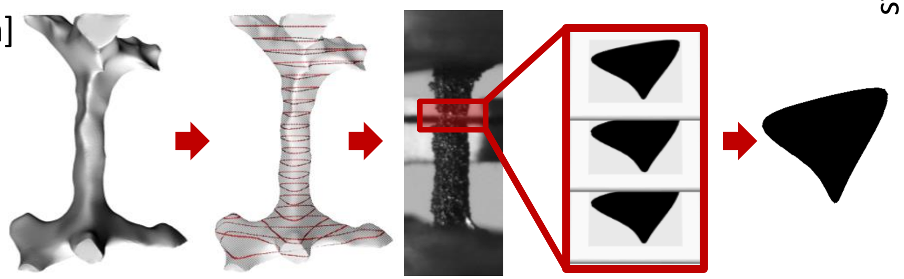

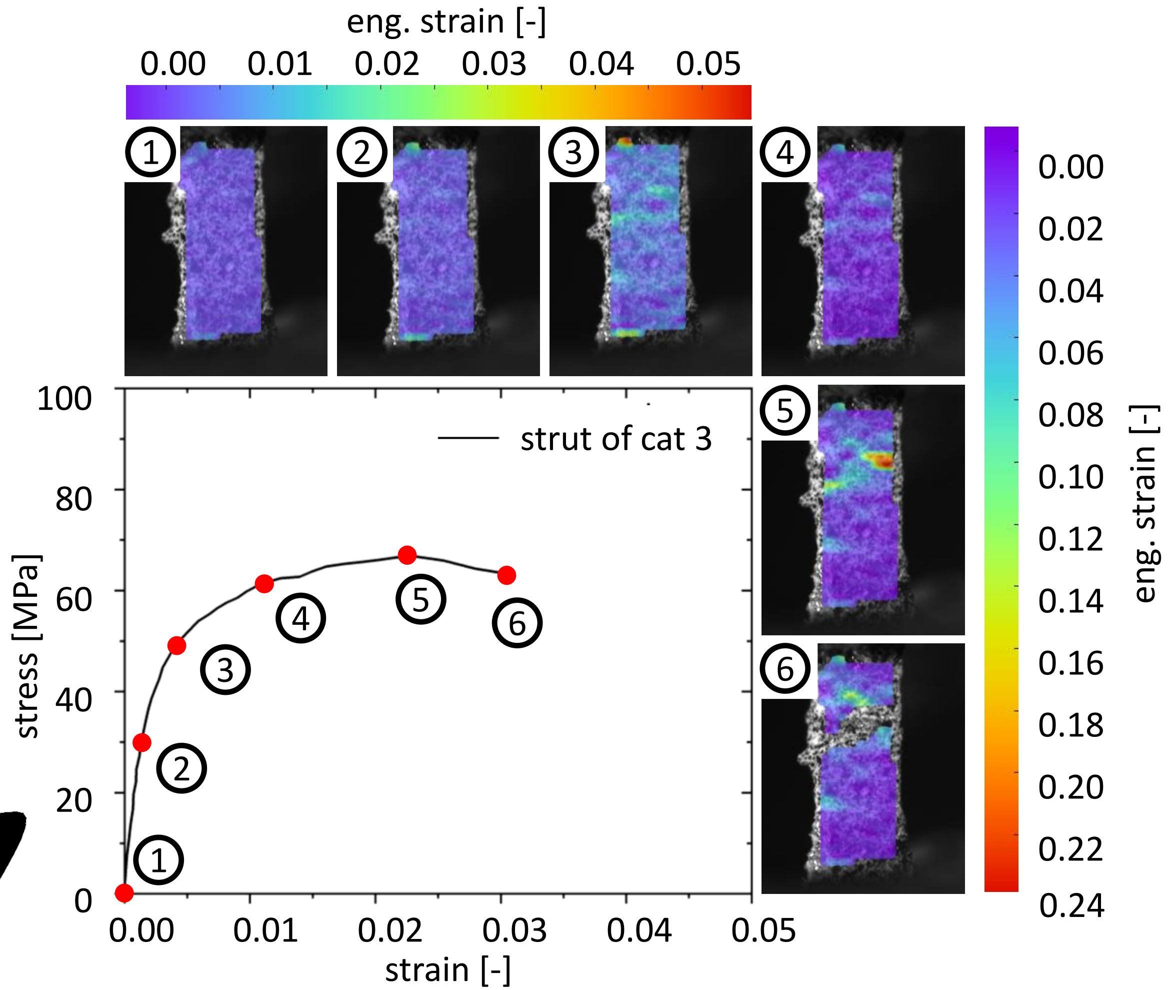

T. Bleistein, M. Reis, X. Cheng, C. Redenbach, S. Diebels, **A. Jung**
Mech. Mater. 142, 103295 (2020)

AG Foams and Metamaterials
apl. Prof. Dr.-Ing. Dr. rer. nat. Anne Jung

Material Parameters From Struts

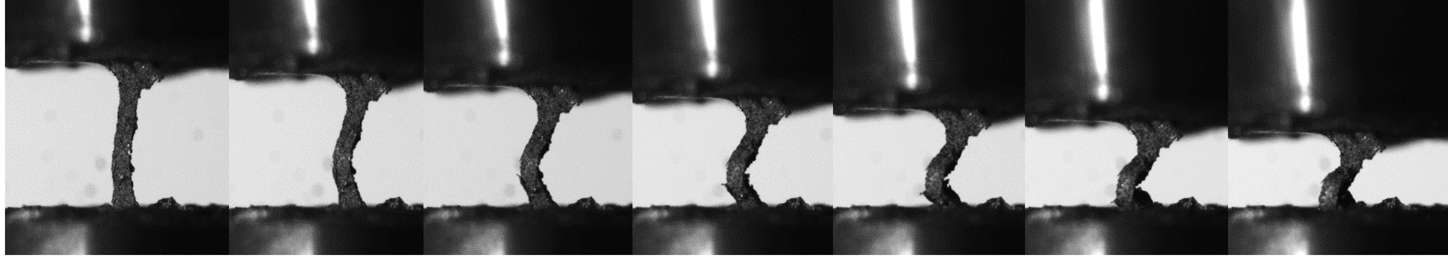

Compression experiment

- Strain using DIC (**D**igital **I**mage **C**orrelation)
- Stress using slices through 3D geometry model

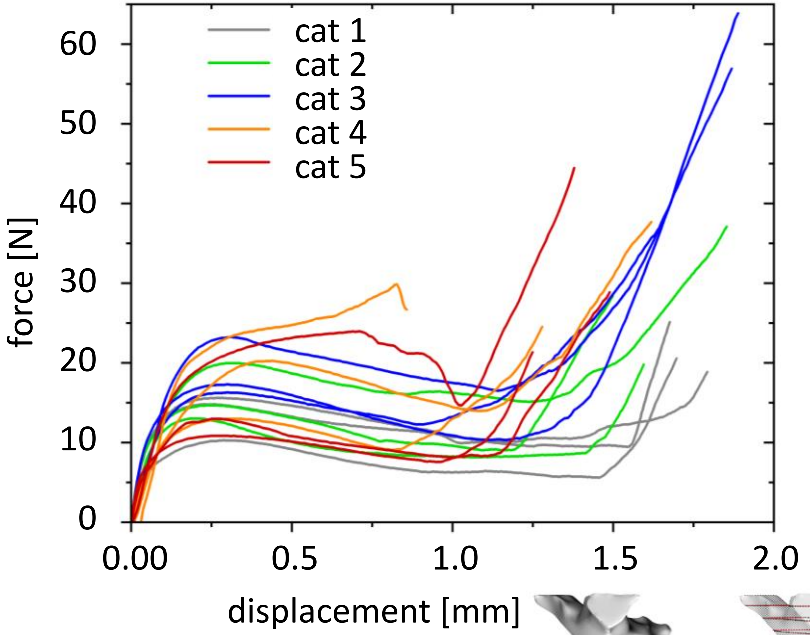

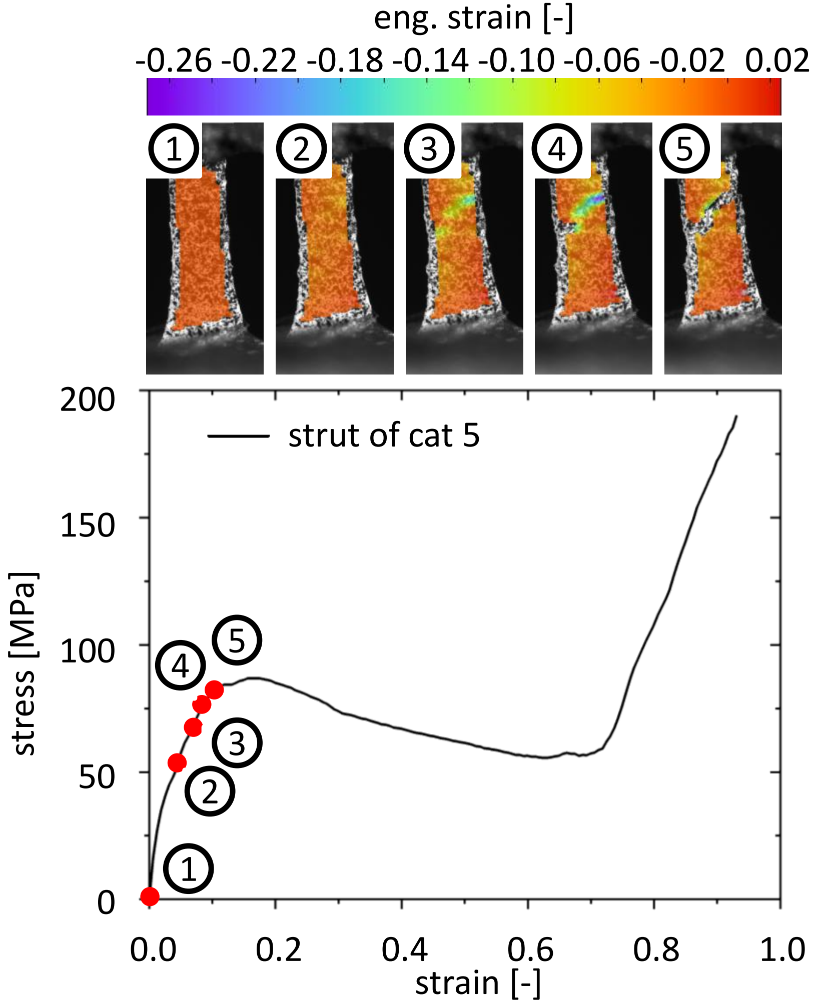

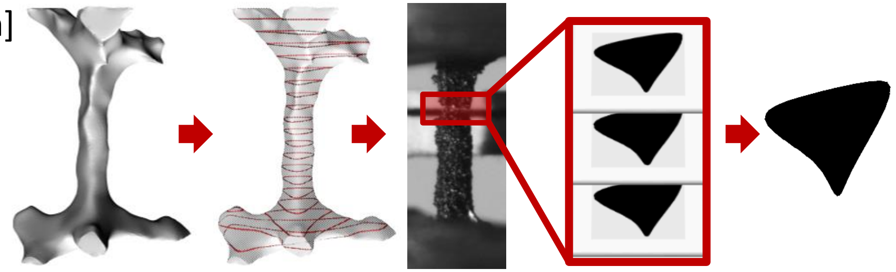

T. Bleistein, M. Reis, X. Cheng, C. Redenbach, S. Diebels, **A. Jung**
Mech. Mater. 142, 103295 (2020)

AG Foams and Metamaterials
apl. Prof. Dr.-Ing. Dr. rer. nat. Anne Jung

Material Parameters From Individual Pores

- Bulk material properties differ significantly from strut properties
  bulk $\neq$ strut
- Development of **universal microtesting device** for individual pores and struts

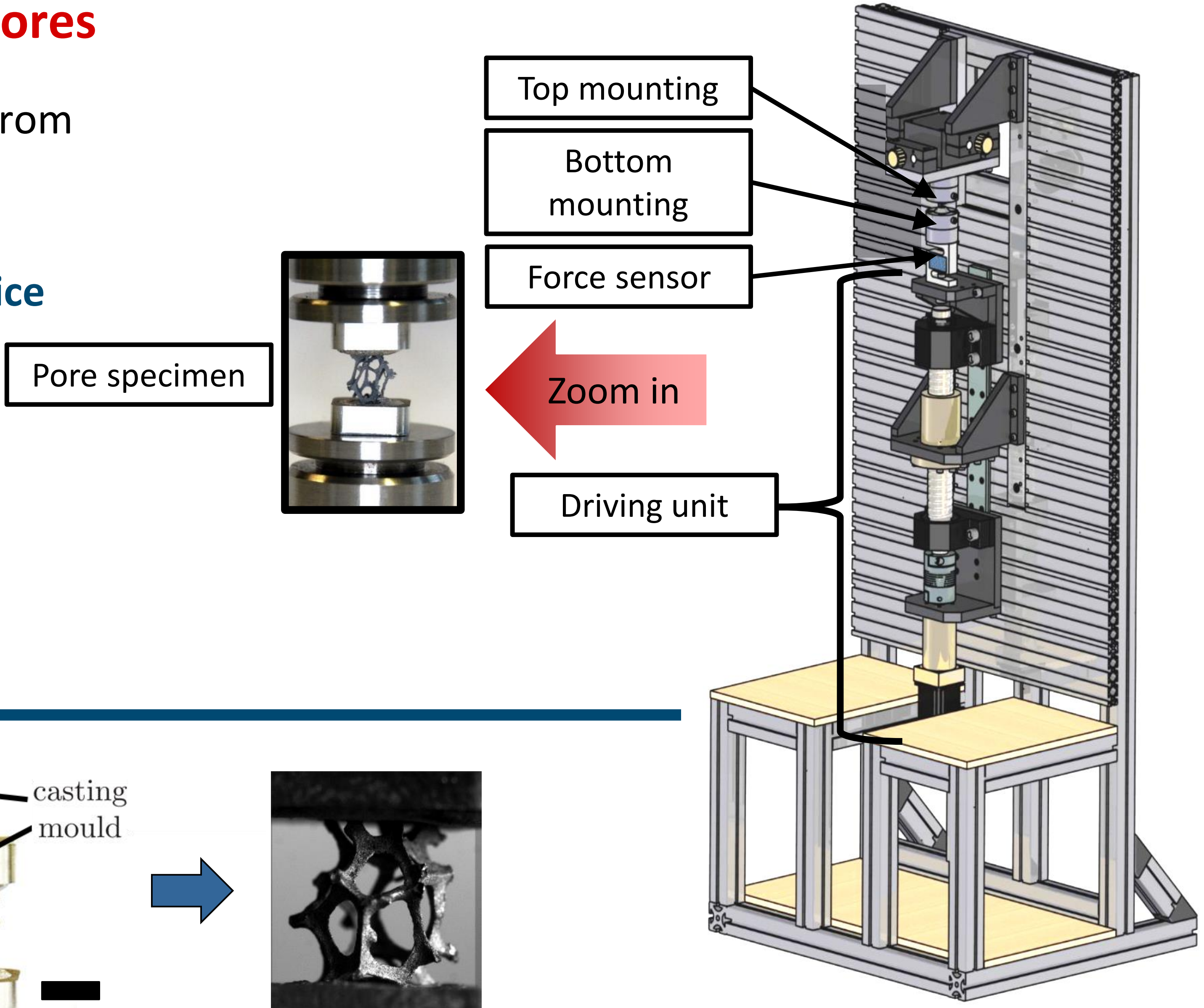

Pore preparation

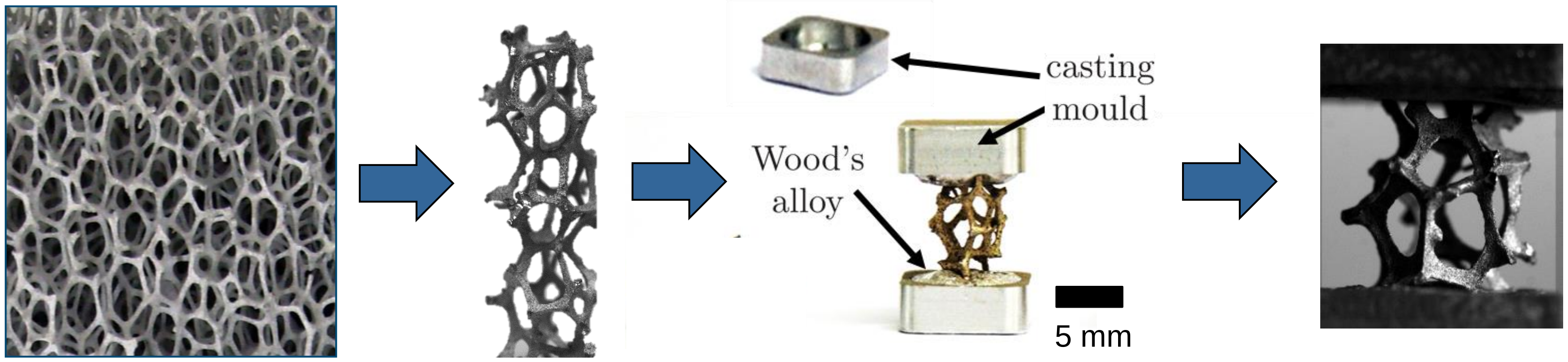

A. Jung, M. Wocker, Z. Chen, H. Seibert
Mater. Des. 88, 1021-1030 (2015)

Material Parameters From Individual Pores

compression tests on individual geometry

↓

individual force-displacement curves dependent on pore geometry

↓

material parameters by inverse calculation

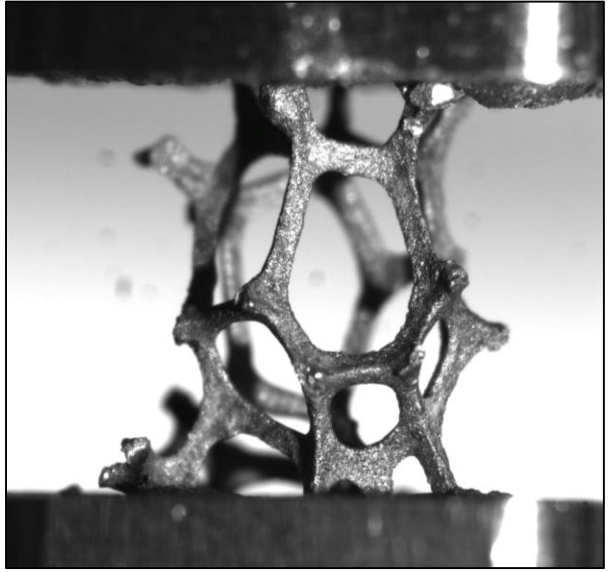

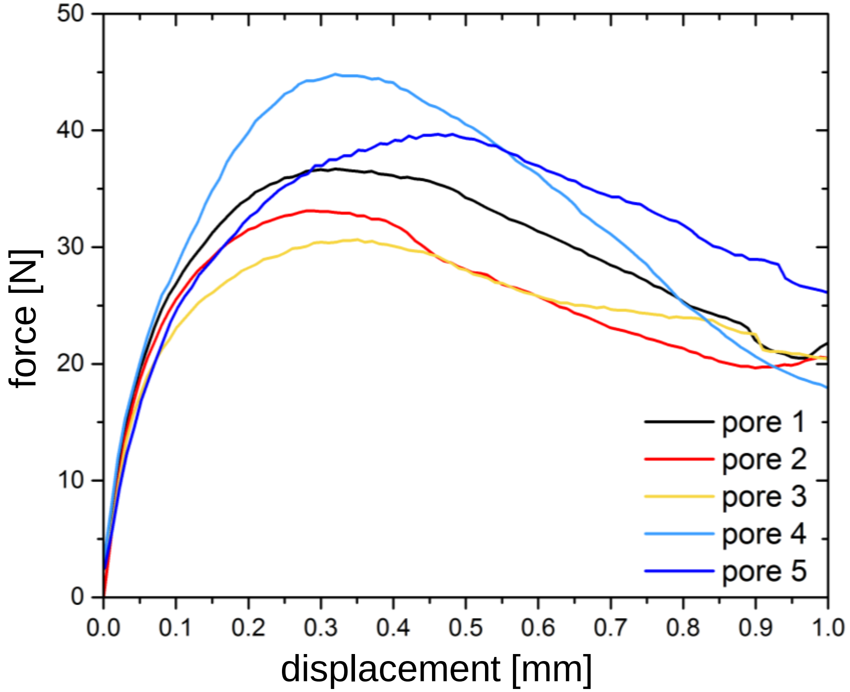

S. Heinze, T. Bleistein, A. Düster, S. Diebels, **A. Jung**
Z. Angew. Math. Mech. 98, 682-695 (2018)

Material Parameters From Individual Pores

- Digitalisation of 6 pores

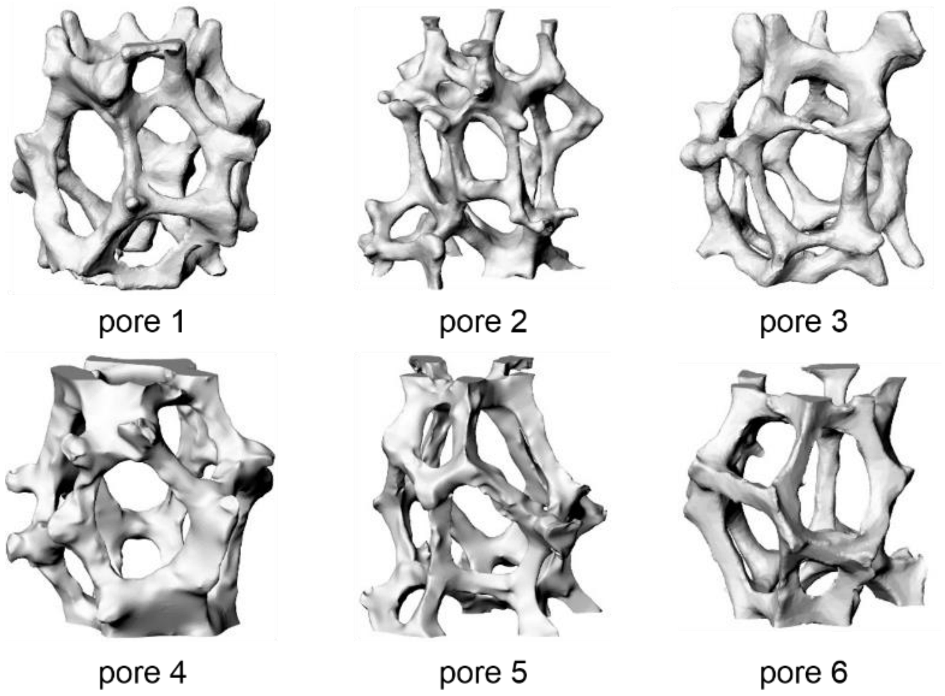

- FE simulation of compression tests
- Parameter identification by inverse calculation

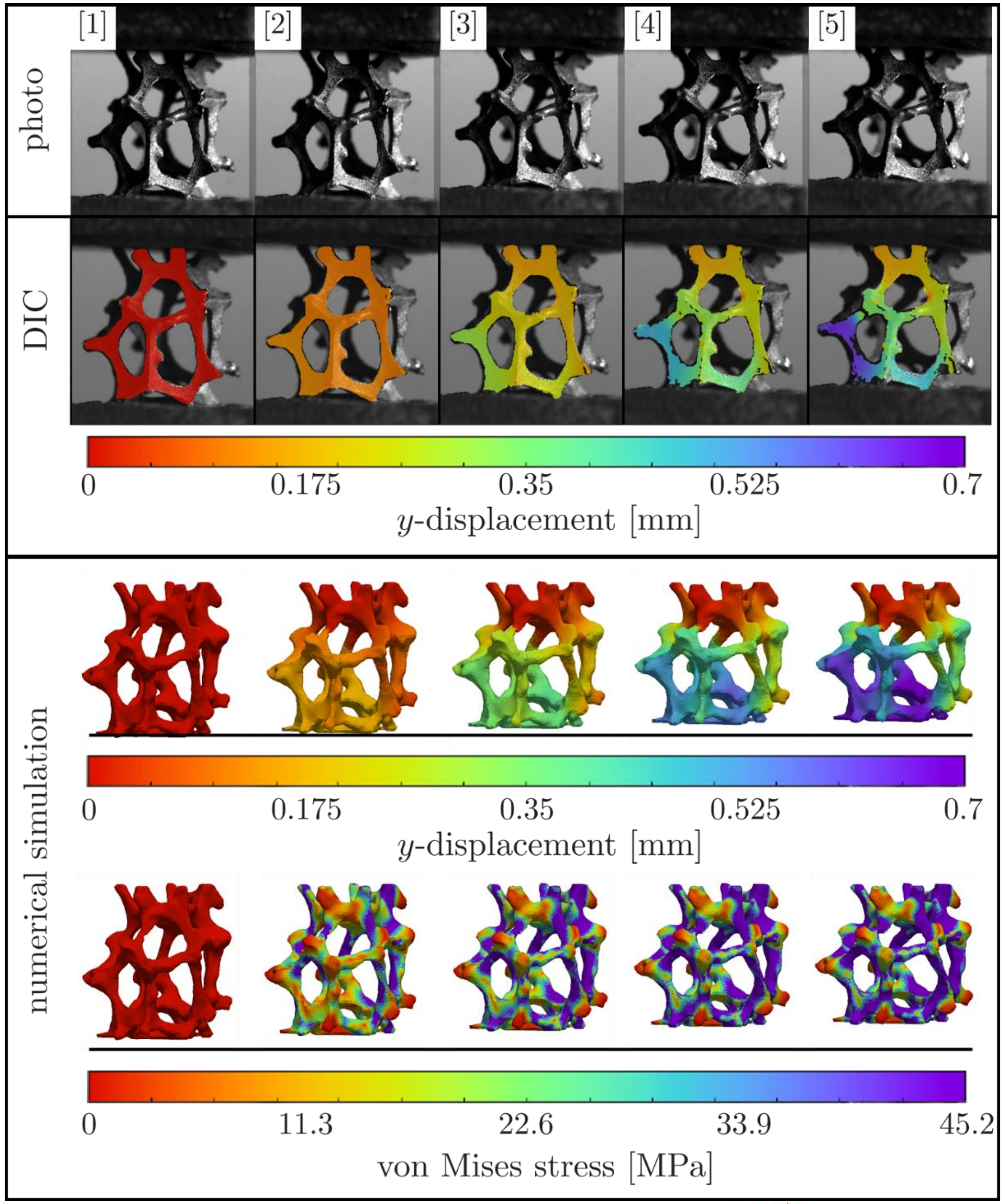

S. Heinze, T. Bleistein, A. Düster, S. Diebels, **A. Jung**
Z. Angew. Math. Mech. 98, 682-695 (2018)

Parameter idenification by inverse calculation

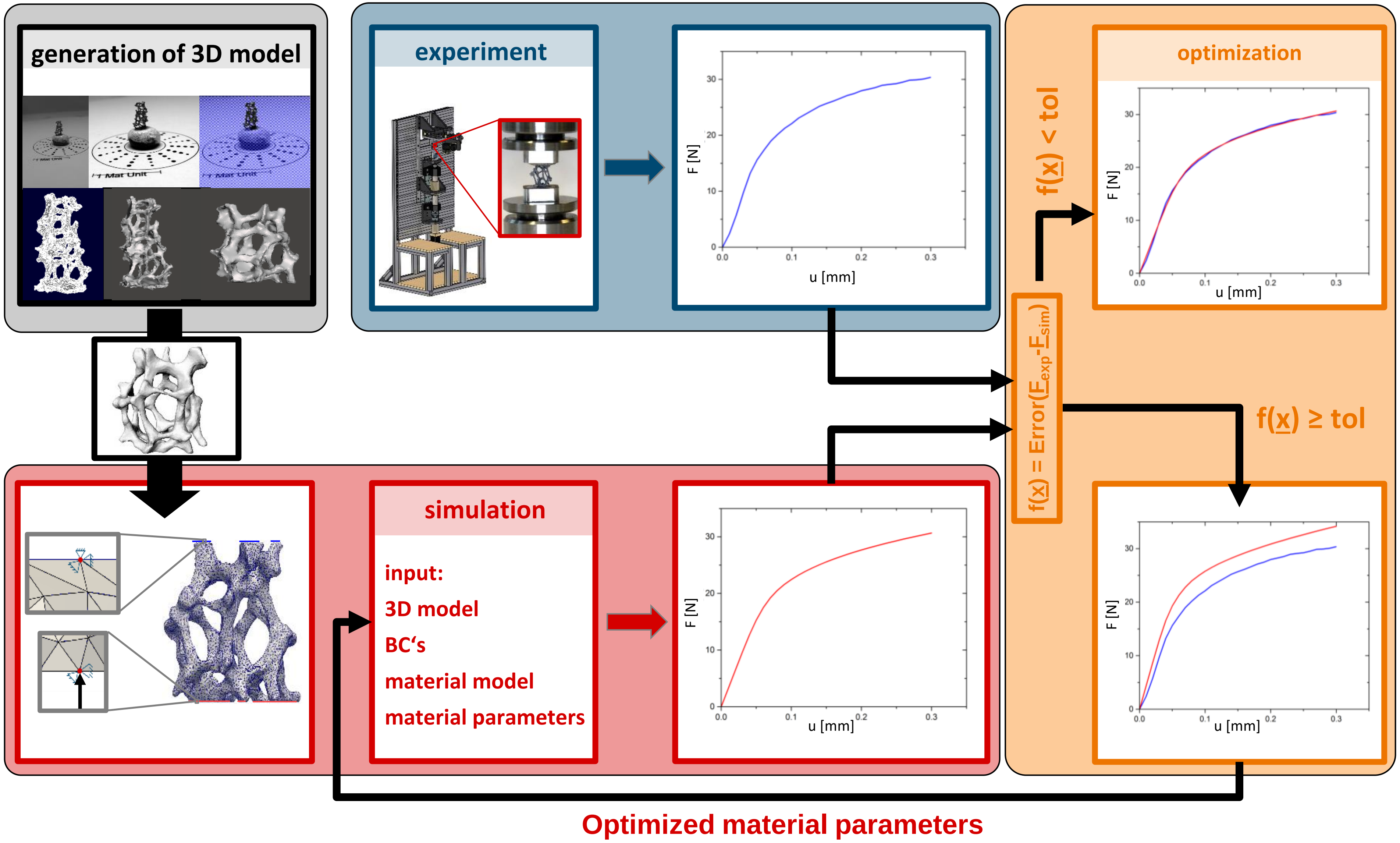

S. Heinze, T. Bleistein, A. Düster, S. Diebels, **A. Jung**
Z. Angew. Math. Mech. 98, 682-695 (2018)

AG Foams and Metamaterials
apl. Prof. Dr.-Ing. Dr. rer. nat. Anne Jung

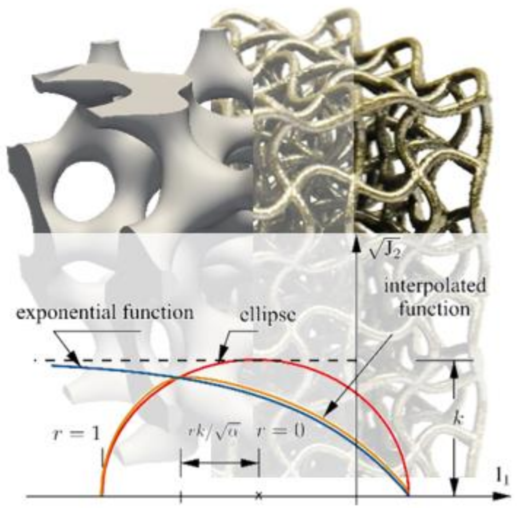

Simulation and Topology Optimisation

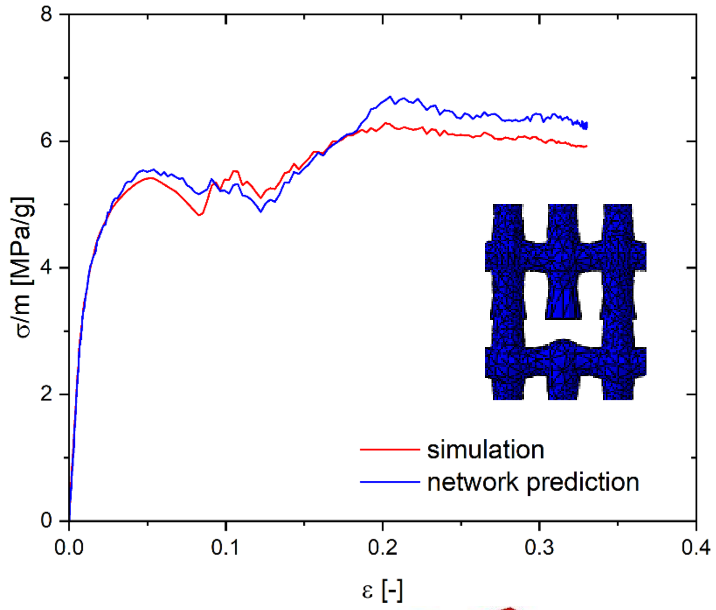

Universität des Saarlandes
Lehrstuhl für Technische Mechanik
AG Foams and Metamaterials
apl. Prof. Dr.-Ing. Dr. rer. nat. Anne Jung

How does the Yield Surface of Chiral Auxetic Materials look like?

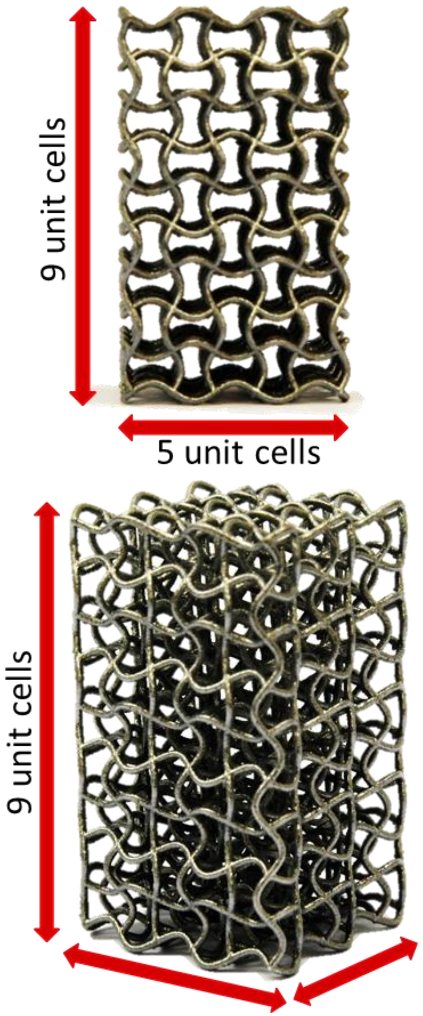

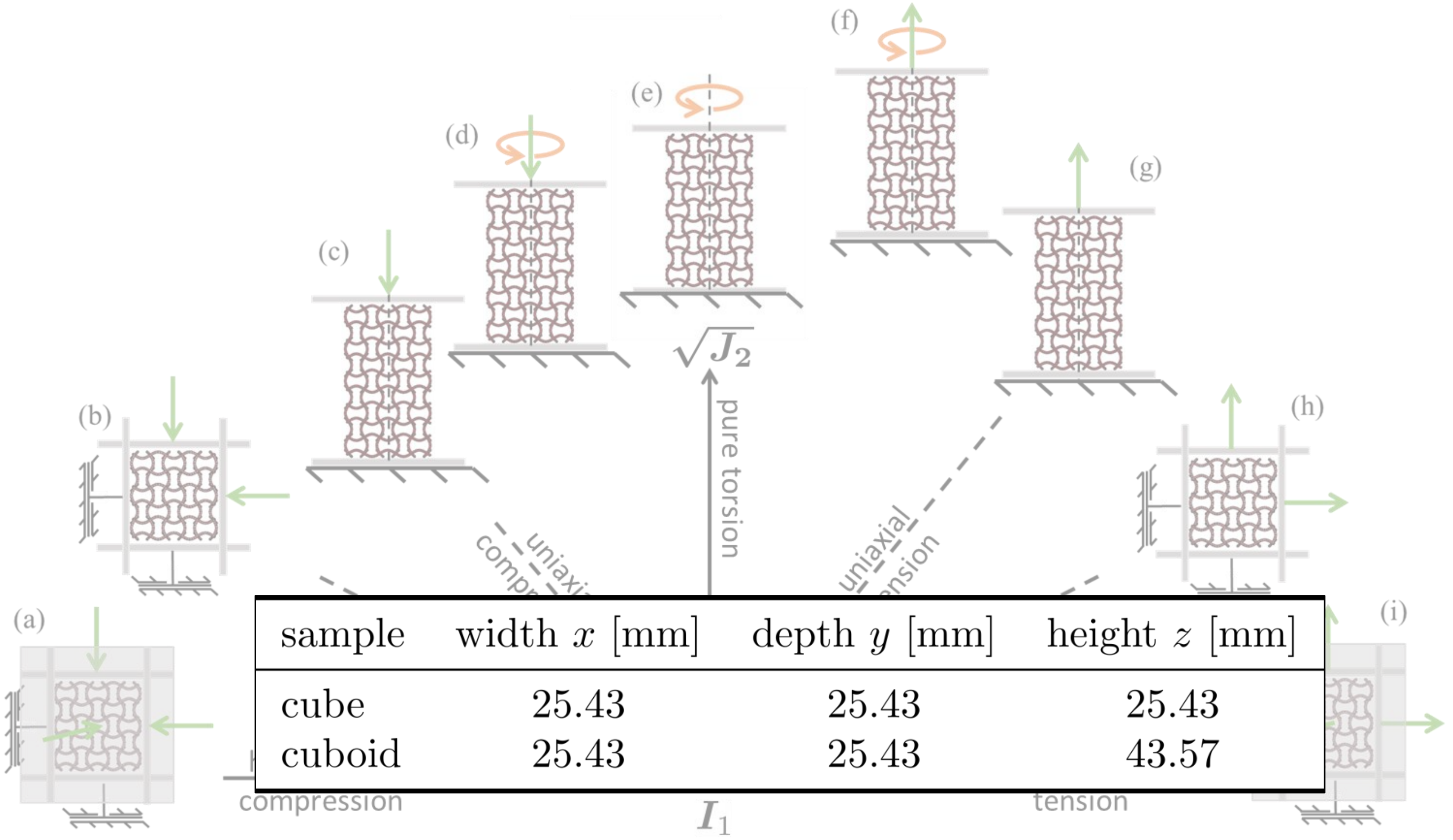

sample	width x [mm]	depth y [mm]	height z [mm]
cube	25.43	25.43	25.43
cuboid	25.43	25.43	43.57

Chiral Auxetic Structures – Multiaxial Loading (Simulation)

- Explicit solver in LS-DYNA®
- Elasto-plastic with hardening
- Material parameters calibrated from previous uniaxial tests
- BC similar to experiments
- Load application to top, bottom and side plates
  - Velocity-controlled (150 mm/s)
  - Force-controlled
    (torsion with superimposed uniaxial loading,
    hydrostatic, -250 N/s, 100 N/s)

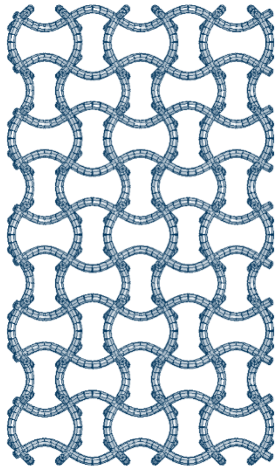

view in x-direction

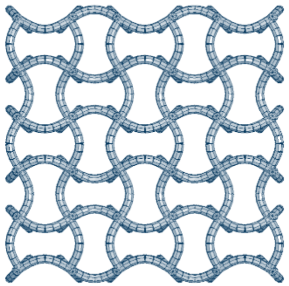

Material	Density	Young's modulus	Poisson's ratio	fail	MAT-Model	Hardening curve (ε_{pl} against σ_{yield})	
	[t/mm^3]	[N/mm^2]	[-]			[-]	[N/mm^2]
Steel	7.850e-09	2.100e+05	0.3	-	MAT_001	-	
Structure	2.670e-09	7.000e+04	0.3	0.04	MAT_024	0	210
						0.05	520
						0.95	10

Chiral Auxetic Structures – Uniaxial Loading

- Brittle failure under tensile and compression loading

$$\varepsilon_{ten.} \approx 0.06 < \varepsilon_{comp.} \approx 0.10$$

$\Rightarrow$ earlier failure under tensile loading

- Yield point = Plastic collapse stress (PCS)

$$\sigma_{y,ten.} \approx 2.55\,\mathrm{MPa} < \sigma_{y,comp.} \approx 2.05\,\mathrm{MPa}$$

- Higher stiffness and higher yield point for tensile loading

- 9 oscillations in compression curve $\rightarrow$ 9 unit cells

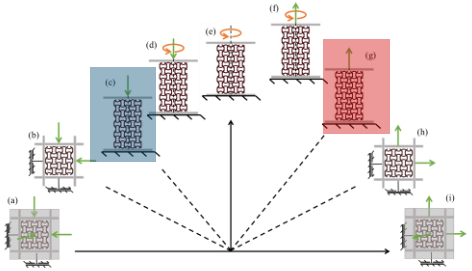

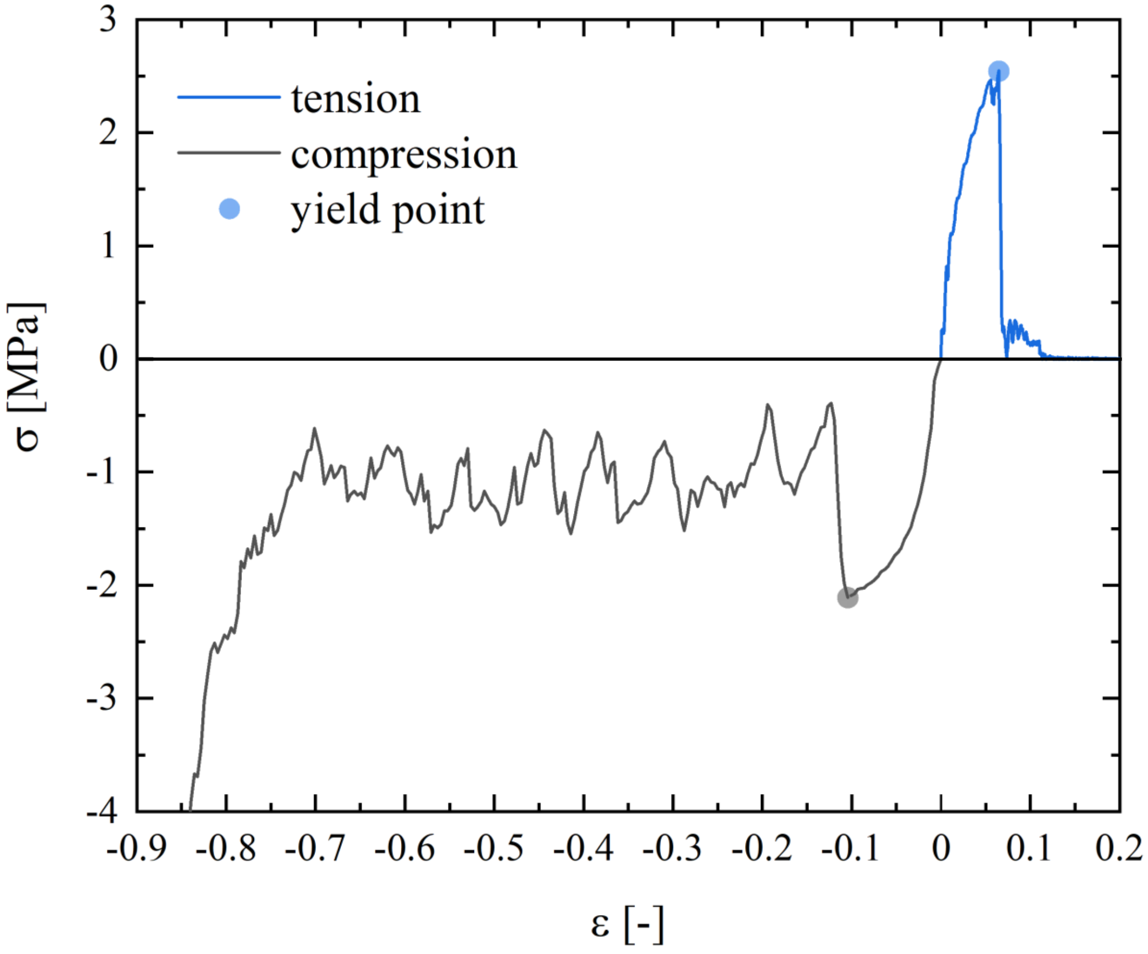

Universität des Saarlandes
Lehrstuhl für Technische Mechanik
AG Foams and Metamaterials
apl. Prof. Dr.-Ing. Dr. rer. nat. Anne Jung

Chiral Auxetic Structures – Torsion with Superimposed Uniaxial Loading

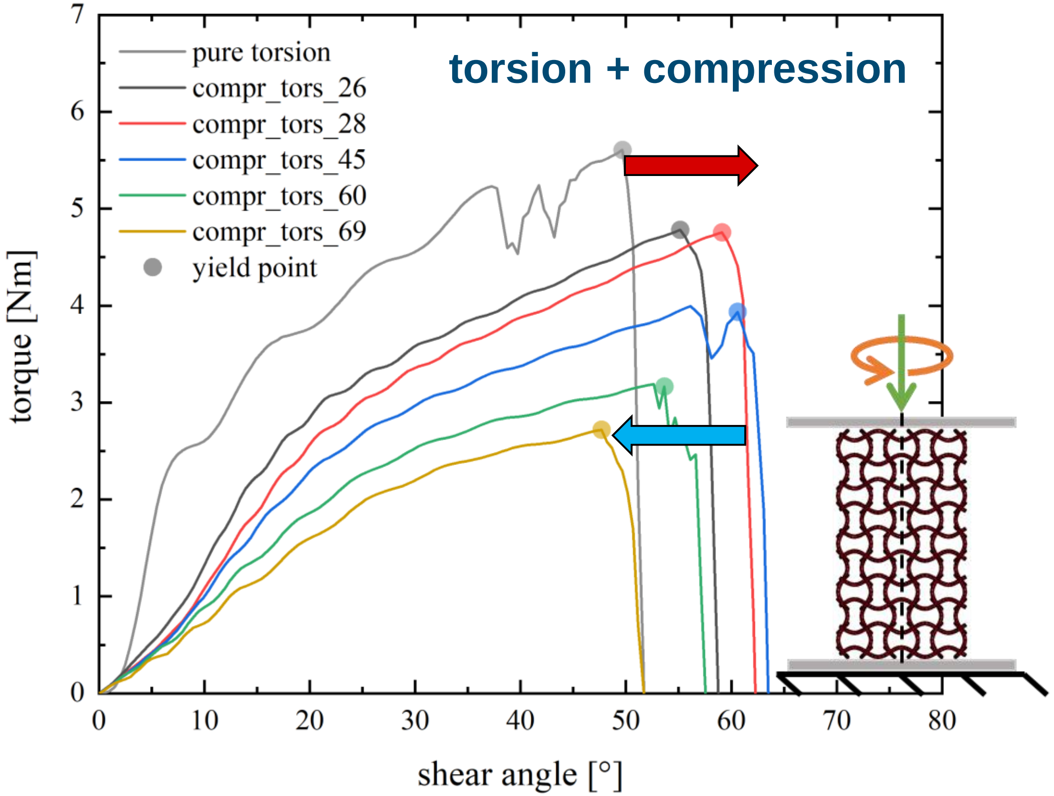

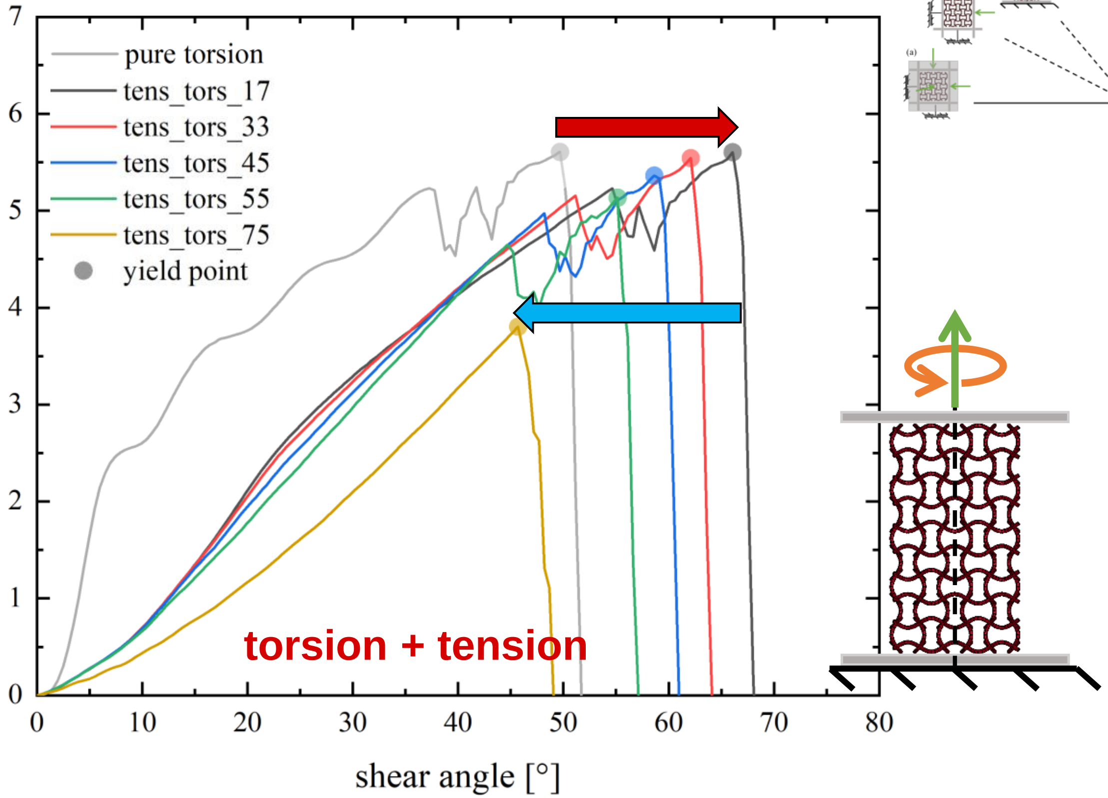

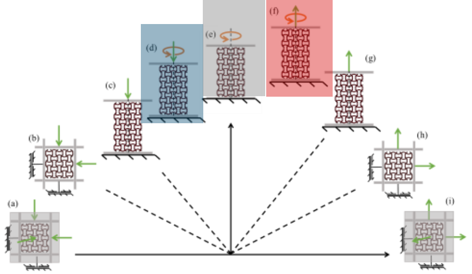

- Max. shear angle and max. torque: torsion + tension > torsion + compression
- ↑superimposed uniaxial load (tens./comp.) ⇒ ↓ max. torque (much lower effect for tension)

⇒ Structure more stable under tensile loading

Universität des Saarlandes
Lehrstuhl für Technische Mechanik
AG Foams and Metamaterials
apl. Prof. Dr.-Ing. Dr. rer. nat. Anne Jung

Chiral Auxetic Structures – Determination of Yield Surface

- Non-convex yield surface
- Shift along hydrostatic axis to tensile side for combinded torsion + uniaxial loading
  BUT: nearly symmetric for biaxial and triaxial loading to shear axis
- Torsion + tension provides better shear stability than torsion + comp.
- Splitting of yield points for biaxial and triaxial loading
- Larger stability under tensile loads and combined tensile loads

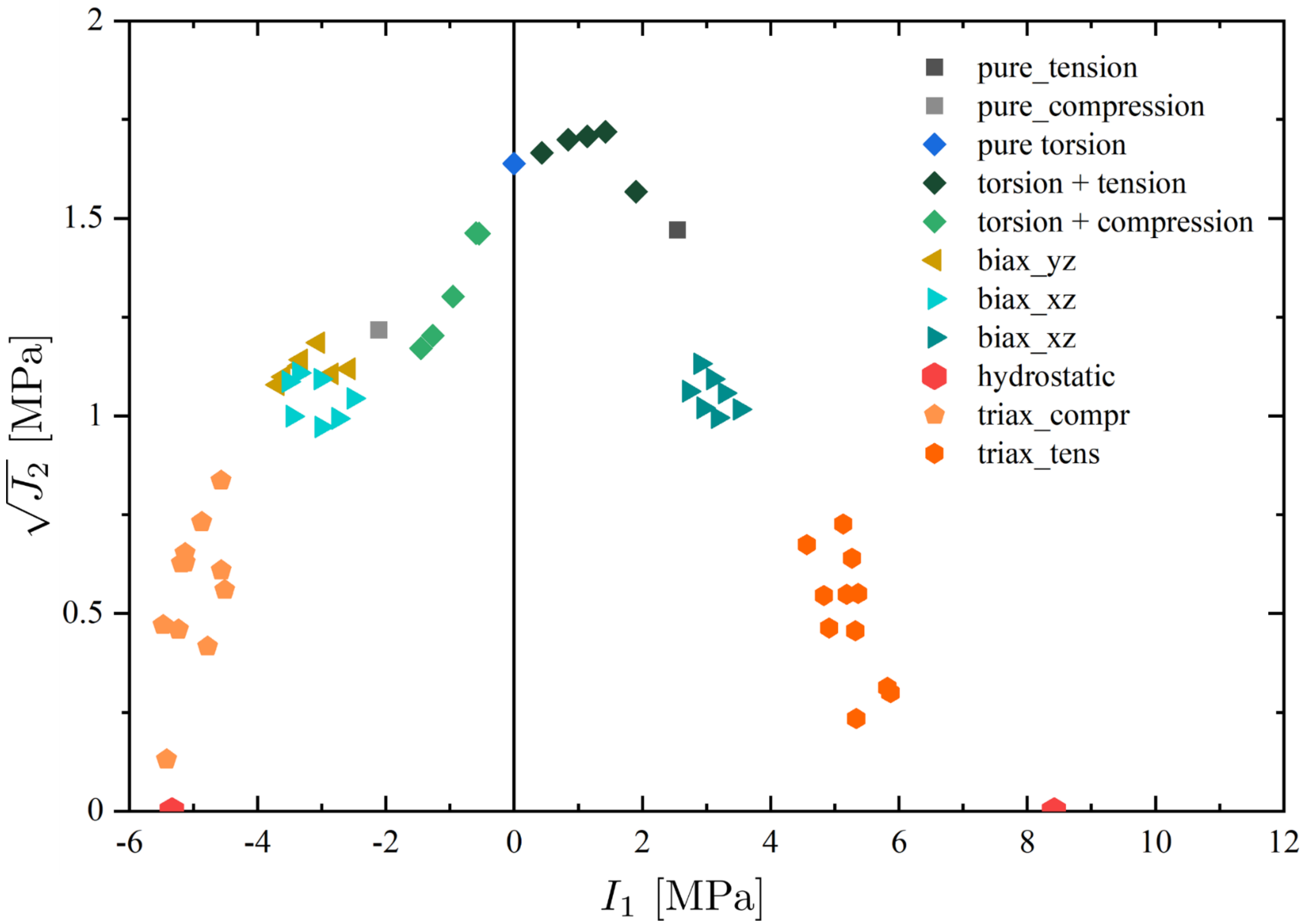

Chiral Auxetic Structures – Determination of Yield Surface

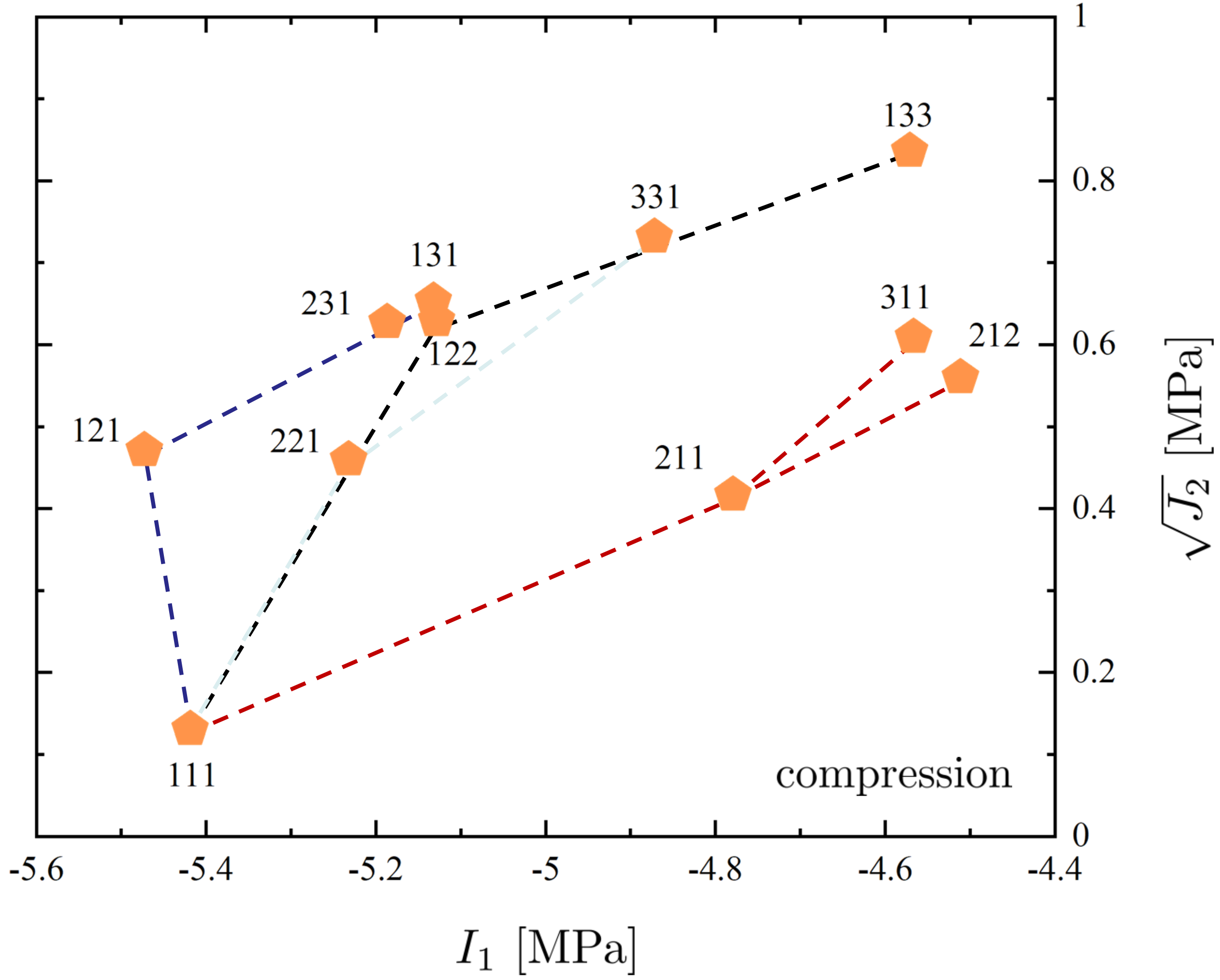

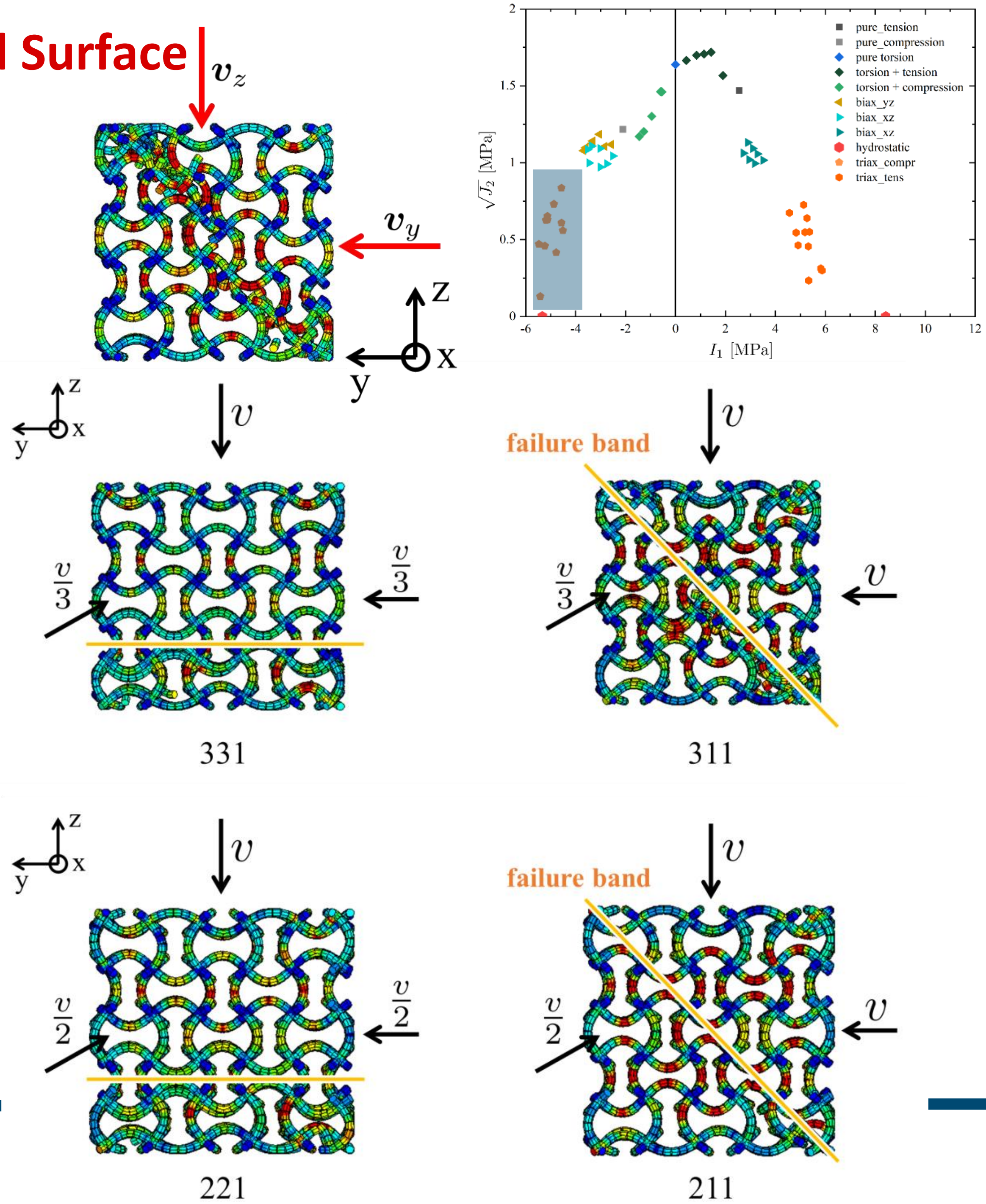

- Change in failure mode by loading ratio
- Strong influence of anisotropic structure

Chiral Auxetic Structures – Energy Absorption Capacity (EAC)

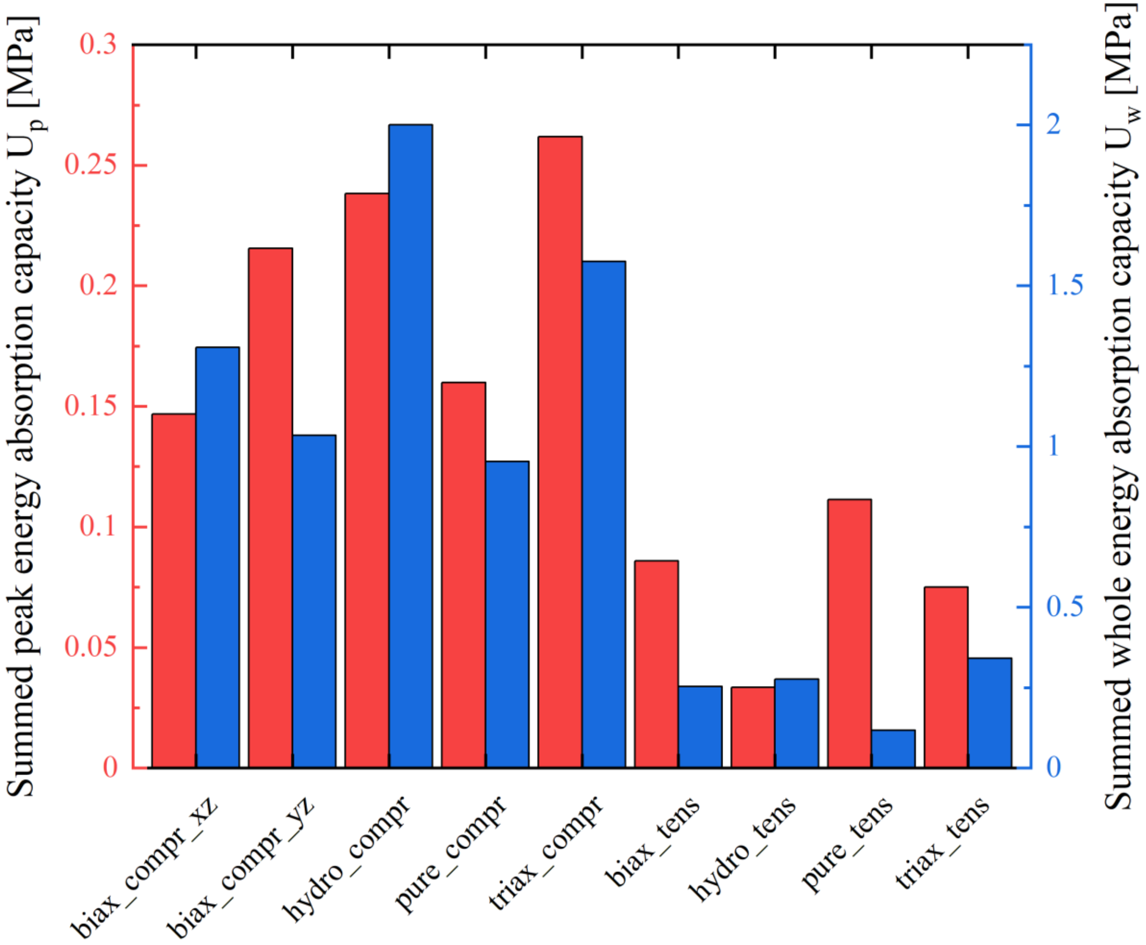

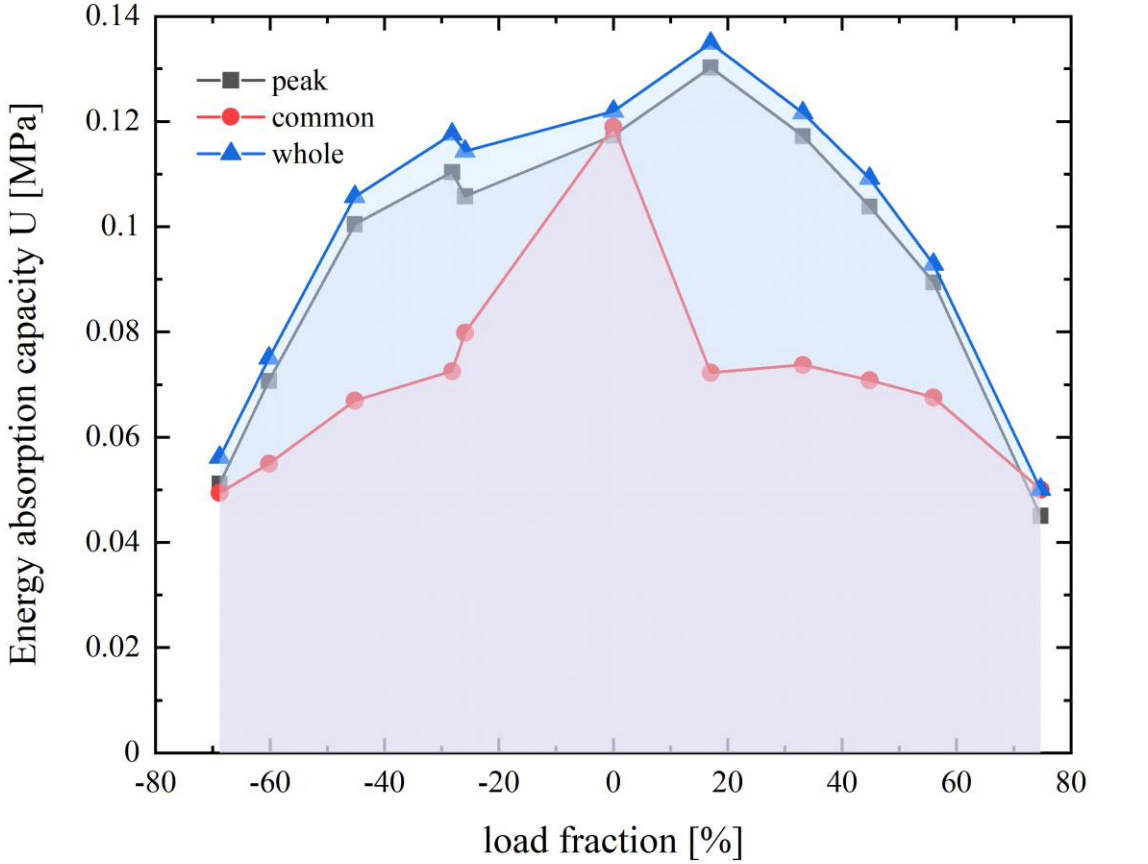

- ↑ Auflast ⇒ ↓ EAC
- Max. EAC for slight superimposed tension

- $EAC_{comp.} > EAC_{tens.}$
- $EAC_{hydro.} > EAC_{triax.} > EAC_{biax._{x}z} > EAC_{biax._{y}z} > EAC_{uniax.}$

Chiral Auxetic Structures – Poisson's Ratio

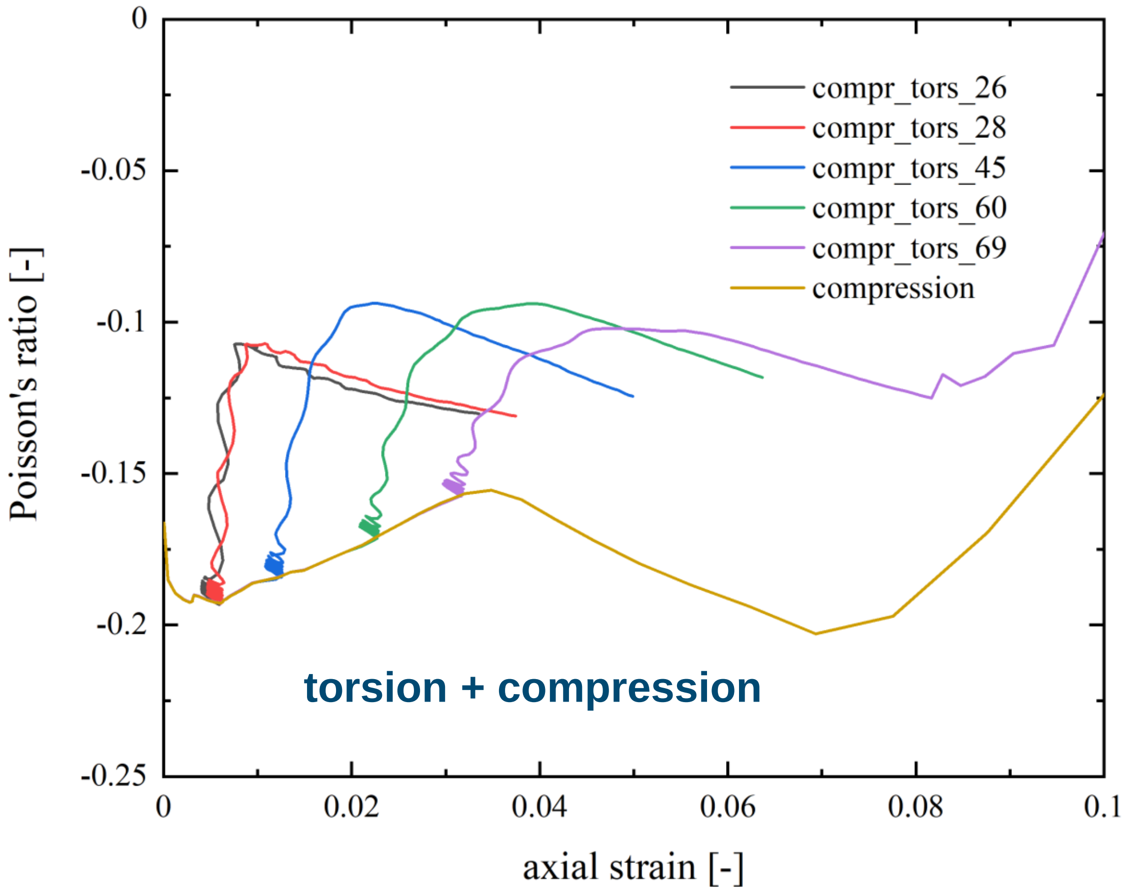

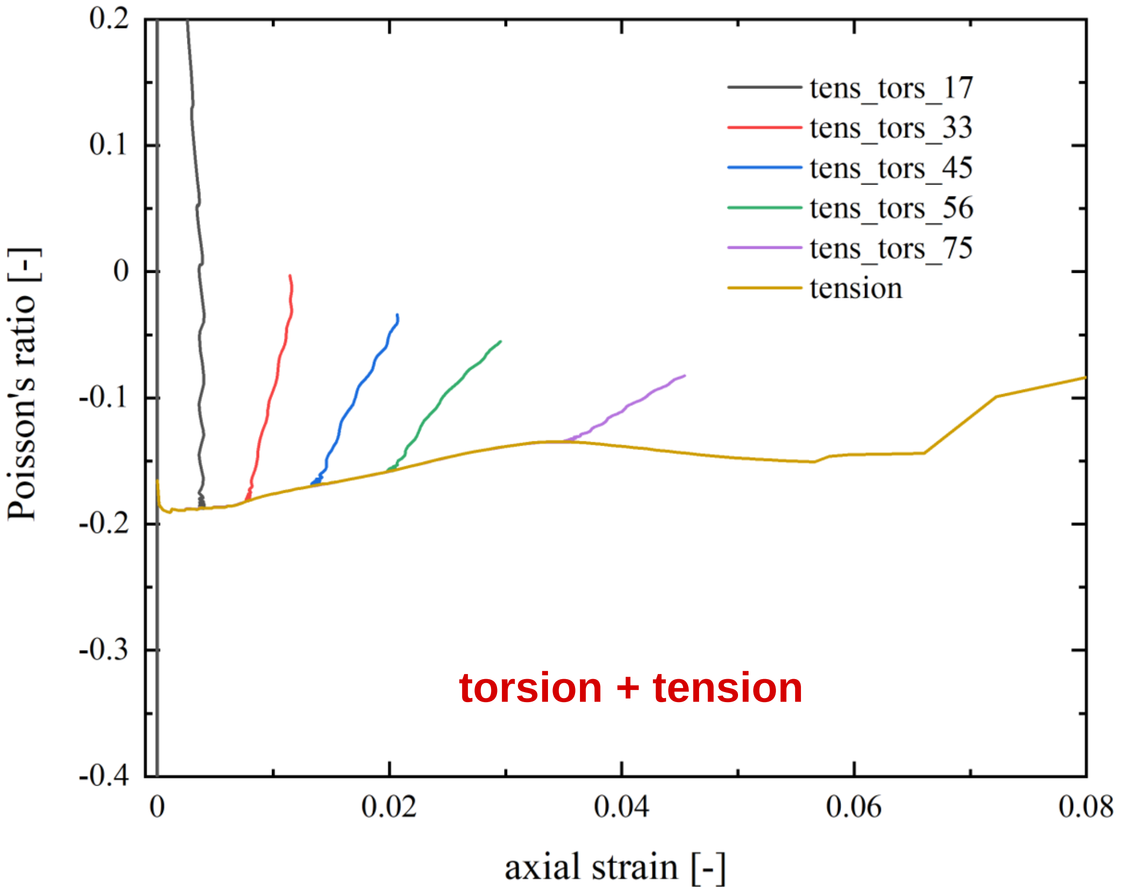

- Poisson‘s ratio for torsion + compression and torsion + tension ≈ -0.2
- Strong increase in Poisson‘s ratio from start of torsional loading

Auxetics - Optimisation with Neural Networks

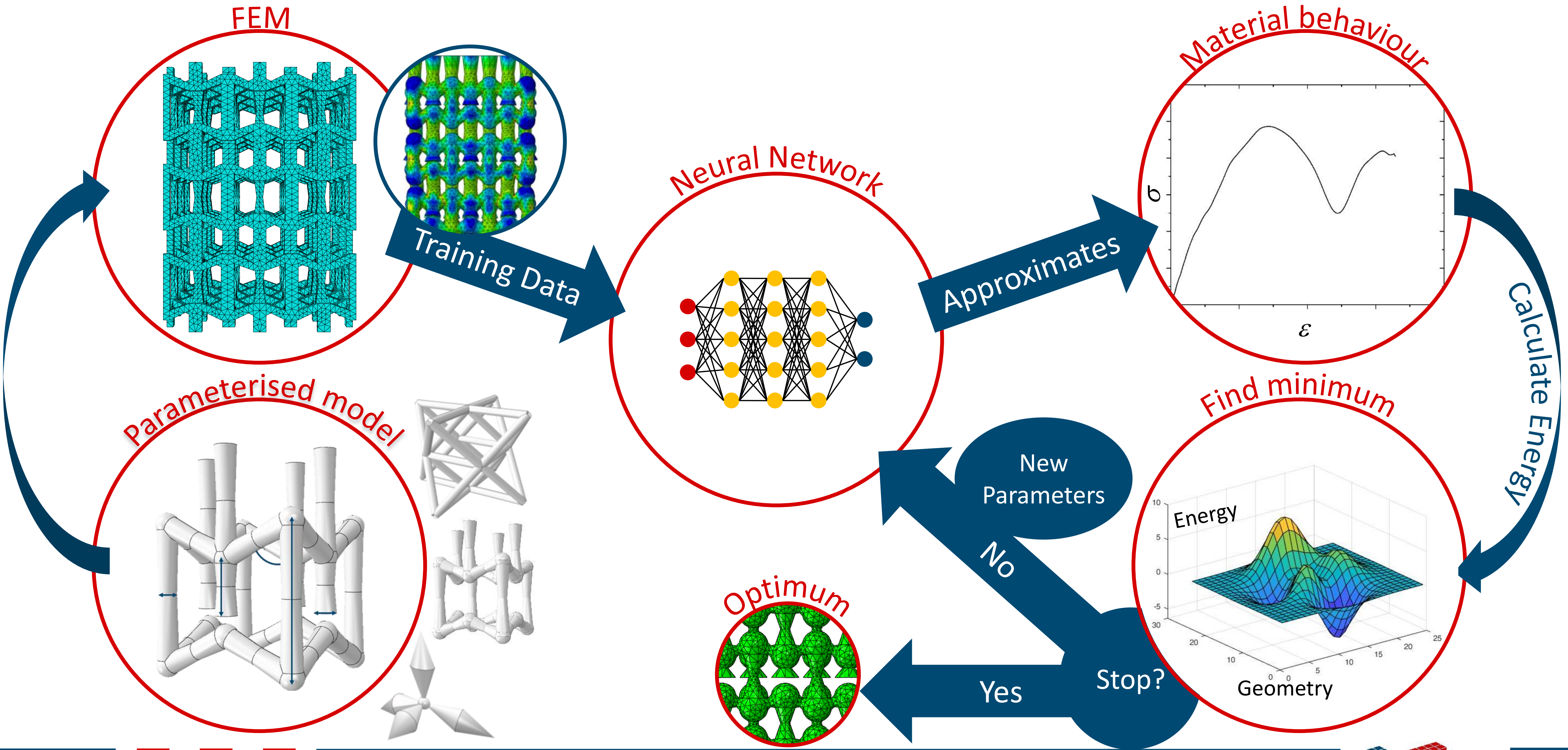

Universität des Saarlandes
Lehrstuhl für Technische Mechanik
AG Foams and Metamaterials
apl. Prof. Dr.-Ing. Dr. rer. nat. Anne Jung

Neural Networks

- Supervised machine learning algorithm
- Consisting of layers of artificial neurons
- Artificial Neurons:
  - Take multiple input values
  - Calculate weighted sum plus bias
  - Apply activation function
  - Output single value
- For any function f(x), there exists a neural network that approximates it closely

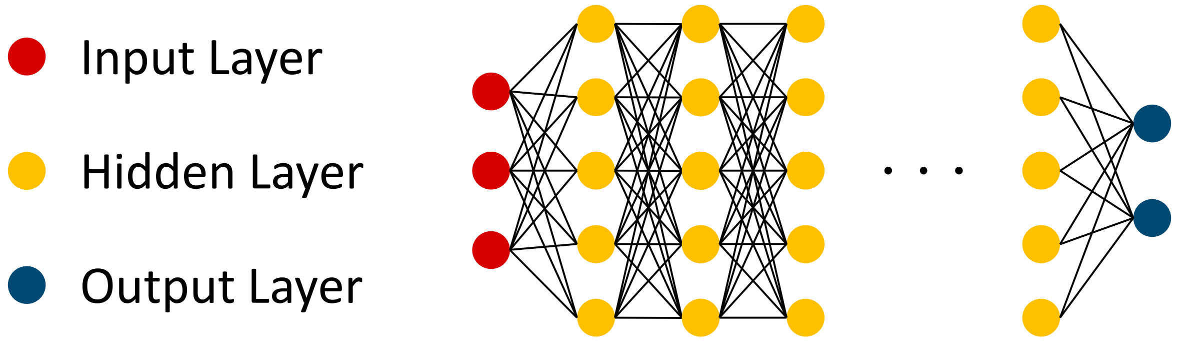

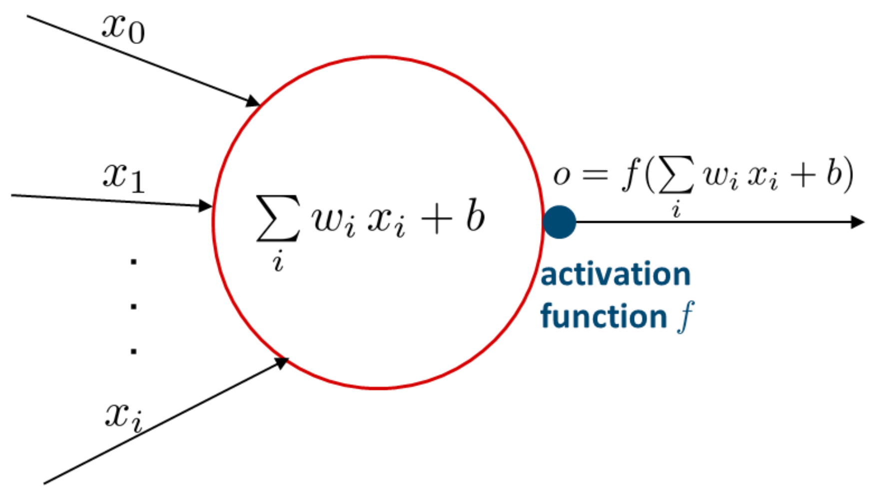

Modified Auxetic - Parameterised Model

- Re-entrant honeycomb based
- 5 geometry parameters:
  - pore size
  - Strut thickness
  - Strut waist
  - Re-entrant angle
  - Length of halfstrut

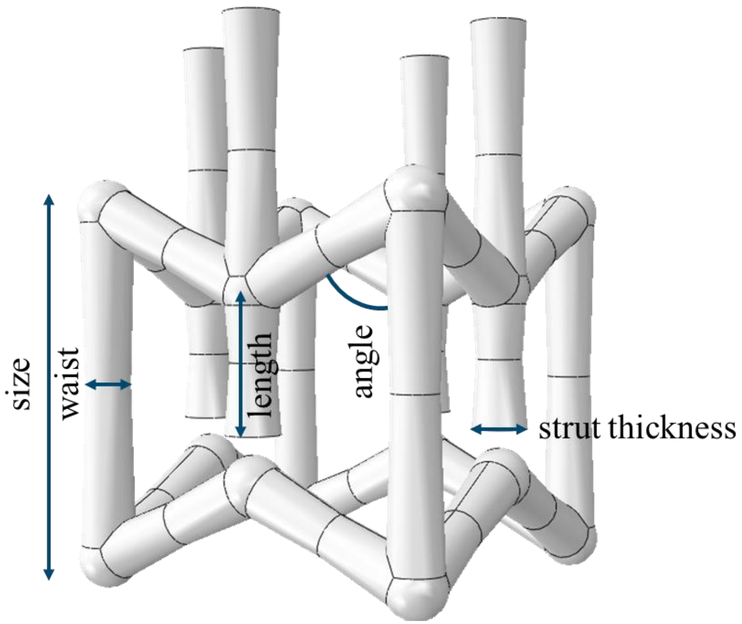

- Half strut provides additional stability after reaching contact

	waist [mm]	strut thickness [mm]	pore size [mm]
min (-1)	0.5	0.5	7
max (1)	1.5	1.5	20

- Varies 3 out of 5 geometry parameters
- Establishes:
  - Impact on energy absorption capacity + Poisson's ratio
  - Interaction between parameters

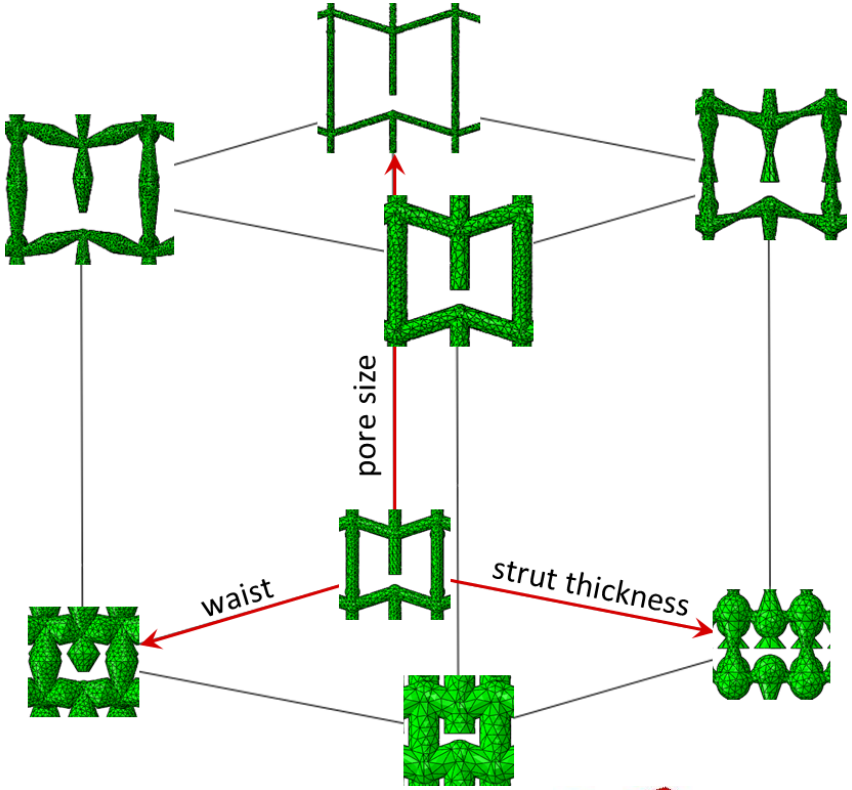

S. Bronder, F. Herter, A. Röhrig, D. Bähre, **A. Jung**
Adv. Eng. Mater. 24 (1), 2100816(2022)

AG Foams and Metamaterials
apl. Prof. Dr.-Ing. Dr. rer. nat. Anne Jung

Factorial Testing Plan

- Small structure + thick struts
  $\Rightarrow$ E + $\nu\uparrow$
- Big structure
  + small struts
  $\Rightarrow$ E + $\nu\downarrow$
- Wide stress-strain range

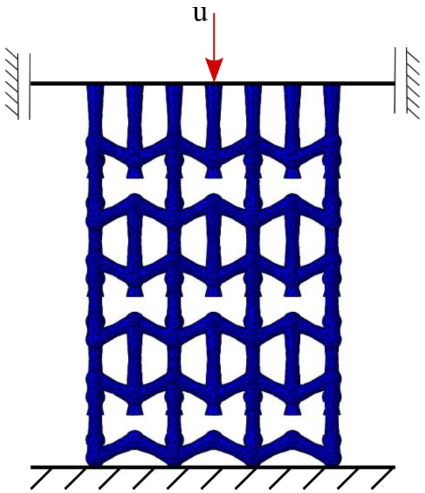

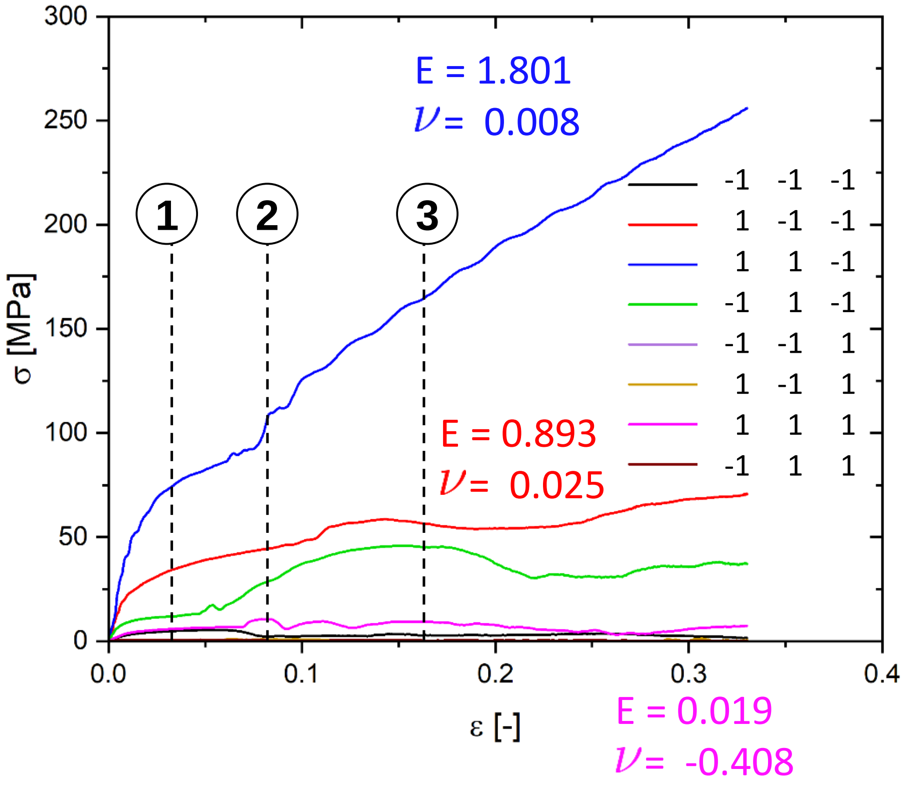

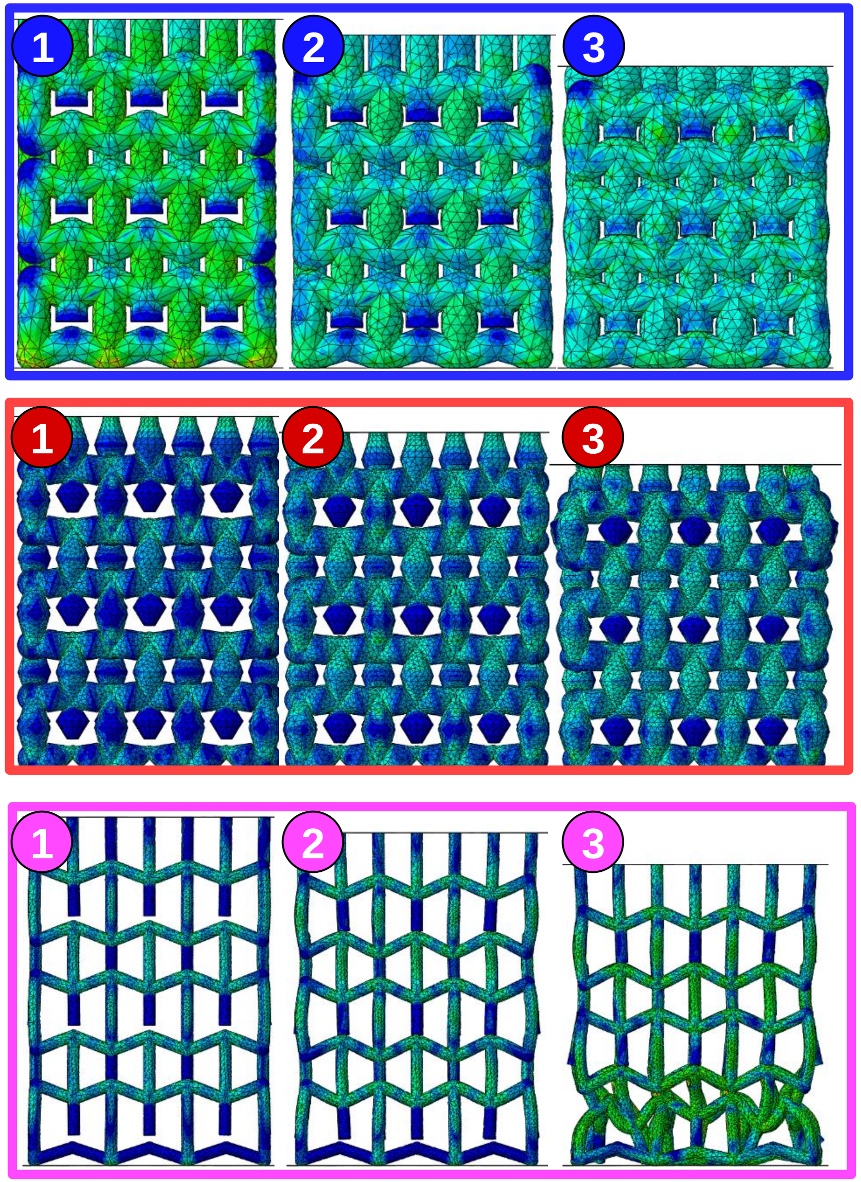

S. Bronder, F. Herter, A. Röhrig, D. Bähre, **A. Jung**
Adv. Eng. Mater. 24 (1), 2100816(2022)

AG Foams and Metamaterials
apl. Prof. Dr.-Ing. Dr. rer. nat. Anne Jung

Factorial Testing Plan - Experimental Results

- Simulation overestimates results
- Overall tendencies intact
- small waisted structure best compromise

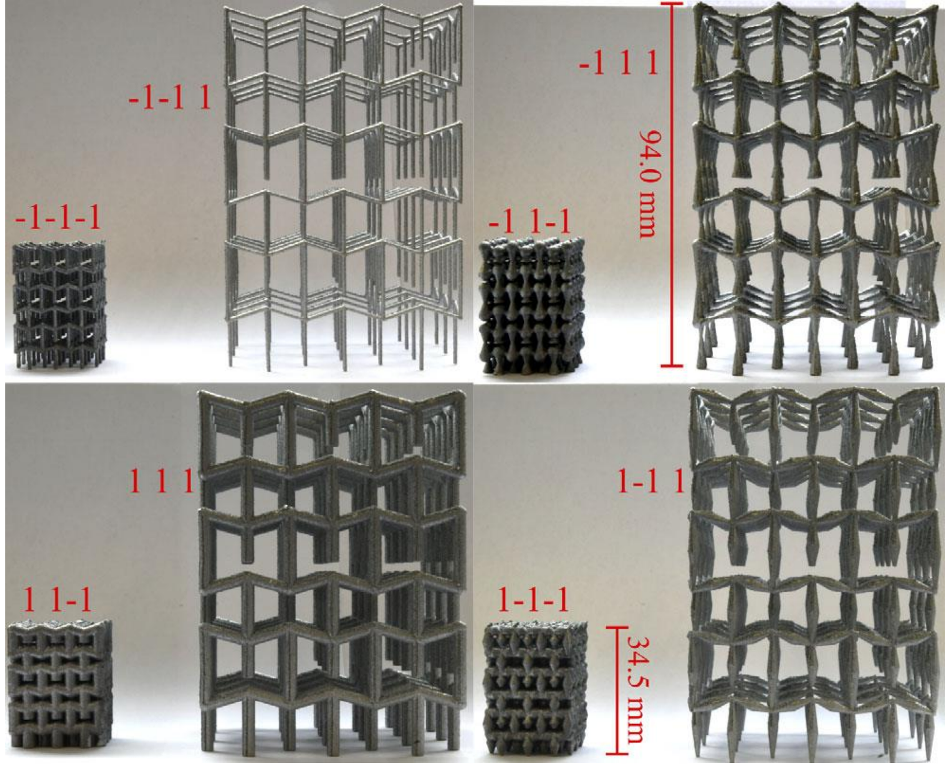

	parameter level	ν_{exp} [-]	ν_{sim} [-]	A_{exp} [mJ mm^{-3}]	A_{sim} [mJ mm^{-3}]
small	-1-1-1	-0.4	-0.33	0.137	0.201
	1-1-1	0.13	0.03	1.564	1.456
	1 1-1	0.16	0.01	3.443	3.246
	-1 1-1	-0.22	-0.45	0.313	0.529
large	-1-1 1	-0.51	-0.64	0.002	0.007
	1-1 1	-0.4	-0.67	0.009	0.022
	1 1 1	-0.36	-0.44	0.141	0.249
	-1 1 1	-0.34	-0.41	0.013	0.029

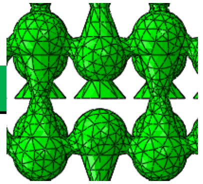

S. Bronder, F. Herter, A. Röhrig, D. Bähre, **A. Jung**
Adv. Eng. Mater. 24 (1), 2100816(2022)

AG Foams and Metamaterials
apl. Prof. Dr.-Ing. Dr. rer. nat. Anne Jung

Specimen manufacturing

- Manufacturing with SLM
- Aluminium as base material
- Production process optimised
  - ⇒ Material parameter differ
  - ⇒ Material model needs recalibrating

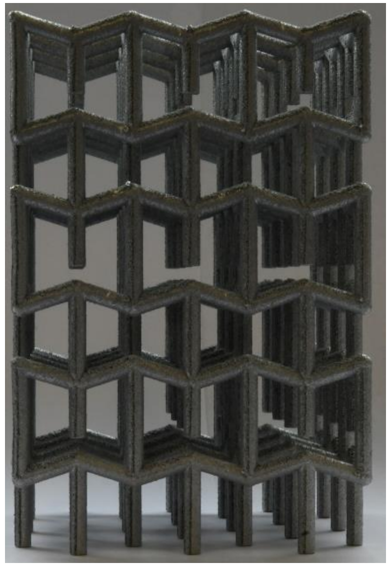

SLM parameter [unit]	value
laser wave length [nm]	1064
laser Power [W]	250
scan speed [mm s^{-1}]	2000
layer thickness [µm]	30
laser hatch distance [mm]	0.114
scanning strategy	„total fill“

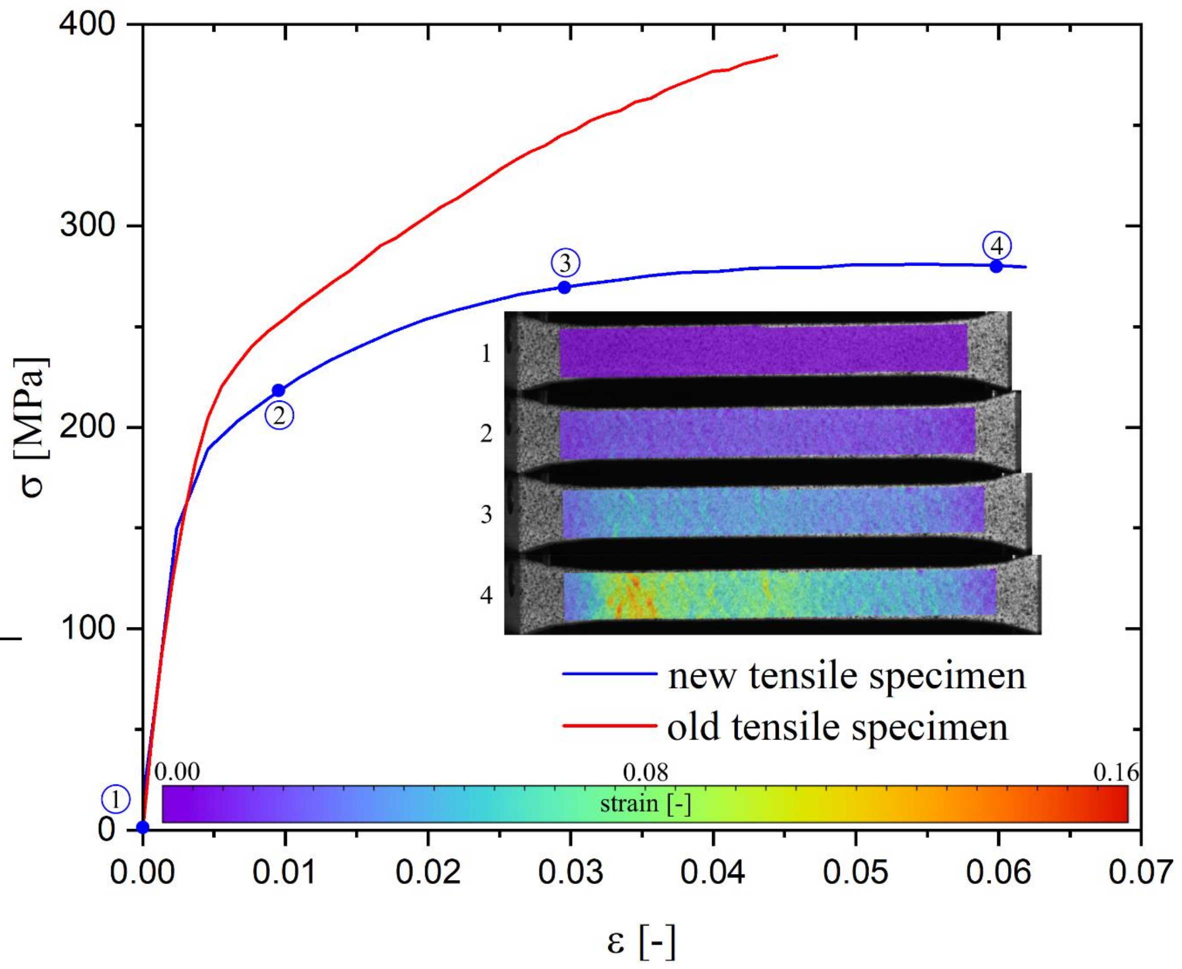

S. Bronder, F. Herter, D. Bähre, **A. Jung**
Materials Today Communications 32, 103931 (2022)

Prediction and Optimisation by Neural Network

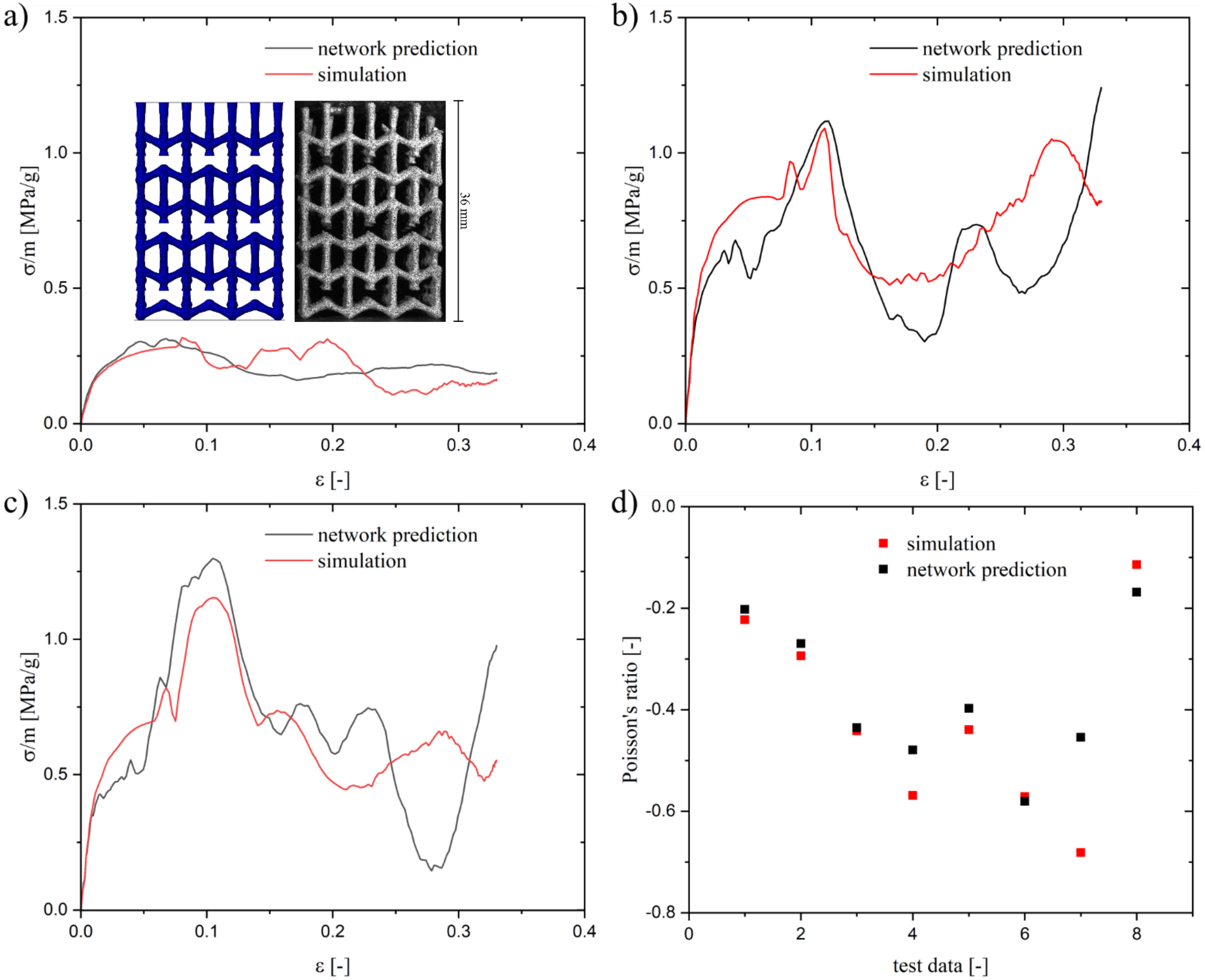

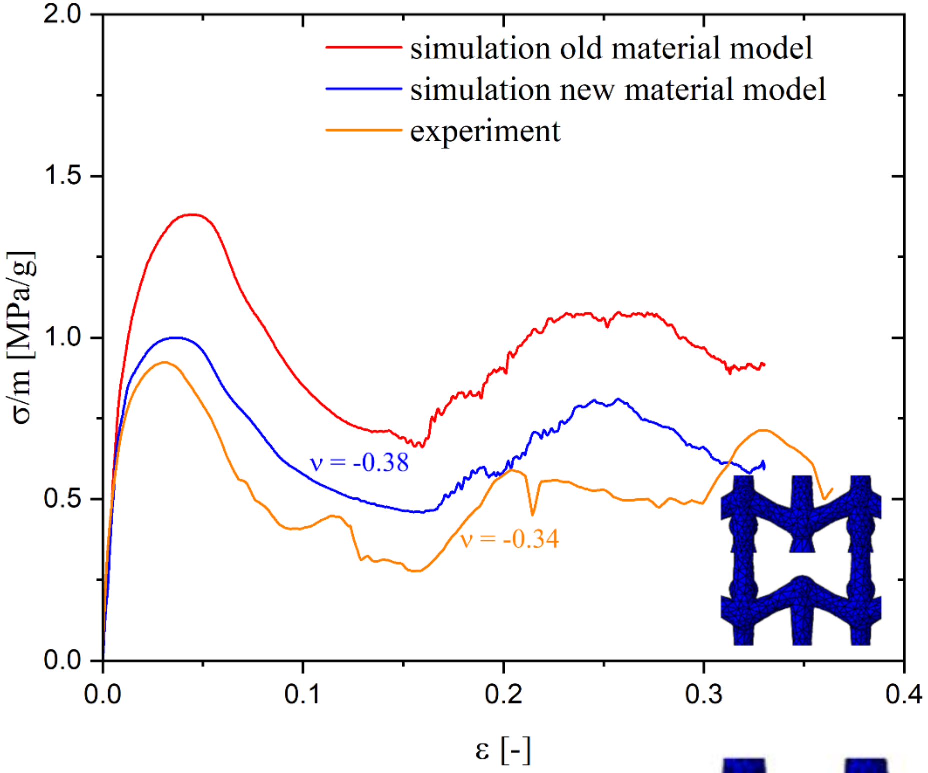

parameter	value
waist	0.56 mm
strut thickness	0.78 mm
re-entrant angle	65.61 °
cell size	7.29 mm
half strut length	1.66 mm

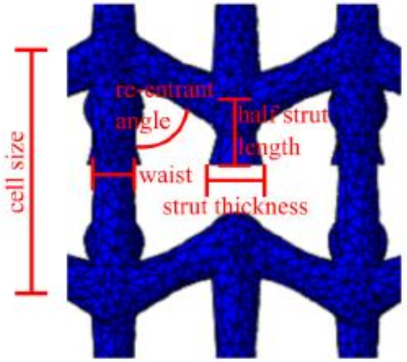

S. Bronder, F. Herter, D. Bähre, **A. Jung**
Materials Today Communications 32, 103931 (2022)

AG Foams and Metamaterials
apl. Prof. Dr.-Ing. Dr. rer. nat. Anne Jung

Thanks to my Group

AG Foams und Metamaterials

Michael Fries, M.Sc.
Optimierung einer additiv gefertigten porösen NiTi-Struktur für den Einsatz als Kühlelement unter kompressiver Belastung,
since November 2022

Markus Felten, M.Sc.
Experimentelle Untersuchung der dynamischen und quasistatischen mechanischen Materialeigenschaften offenporiger Metallschäume,
since February 2021

Dipl.-Ing. Farshad Daneshpazhoonejad
Thermomechanisch-gekoppelte Simulation selbstfortschreitender Reaktionen in Ni/Al-Multilagen, since June 2020

Francesco Kunz, M.Sc.
Hybridmetallschäume – Untersuchung und Optimierung des elektrochemischen Beschichtungsprozesses, since November 2019

Stefan Bronder, M.Sc.
Modellierung und Optimierung von mechanischen Metamaterialien mittels Neuronaler Netze, since June 2019

Thank you for your attention